FOR FURTHER TRAN/

USARTL-TR-78-22

200007726120

(12)

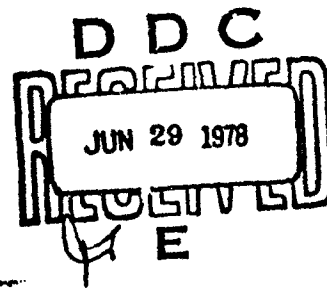# CH-47 CRASH TEST (T-40) STRUCTURAL, CARGO RESTRAINT, AND AIRCREW INFLATABLE RESTRAINT EXPERIMENTS

L. Burrows, R. Lane, J. McElhenney

April 1978

DDC

JUN 29 1978

E

78 06 27 080

REPORT DOCUMENTATION PAGE		READ INSTRUCTIONS BEFORE COMPLETING FORM
1. REPORT NUMBER USARTL-TR-78-22	2. GOVT ACCESSION NO.	3. RECIPIENT'S CATALOG NUMBER
4. TITLE (and Subtitle) CH-47 CRASH TEST (T-40) STRUCTURAL, CARGO RESTRAINT, AND AIRCREW INFLATABLE RESTRAINT EXPERIMENTS.		5. TYPE OF REPORT & PERIOD COVERED Technical Report.
		6. PERFORMING ORG. REPORT NUMBER
7. AUTHOR(s) L. Burrows, R. Lane J. McElhenney		8. CONTRACT OR GRANT NUMBER(s)
9. PERFORMING ORGANIZATION NAME AND ADDRESS Applied Technology Laboratory, U.S. Army Research and Technology Laboratories (AVRADCOM) Fort Eustis, Virginia 23604		10. PROGRAM ELEMENT, PROJECT, TASK AREA & WORK UNIT NUMBERS 1L162209AH76 House Task 76-17
11. CONTROLLING OFFICE NAME AND ADDRESS		12. REPORT DATE April 1978
		13. NUMBER OF PAGES 110 112 p.
14. MONITORING AGENCY NAME & ADDRESS(if different from Controlling Office)		15. SECURITY CLASS. (of this report) Unclassified
		15a. DECLASSIFICATION/DOWNGRADING SCHEDULE

16. DISTRIBUTION STATEMENT (of this Report)

Approved for public release; distribution unlimited.

17. DISTRIBUTION STATEMENT (of the abstract entered in Block 20, if different from Report)

18. SUPPLEMENTARY NOTES

19. KEY WORDS (Continue on reverse side if necessary and identify by block number)
Helicopter, crashworthiness
Helicopter crash test
Helicopter, personnel restraints
Helicopter cargo restraints

20. ABSTRACT (Continue on reverse side if necessary and identify by block number)
A full-scale crash test of a CH-47A troop/cargo helicopter was conducted at the NASA-Langley Research Center Impact Dynamics Research Facility. This joint Army/NASA/Navy test program was performed as part of the Army's continuing research and development program to enhance the crashworthiness of helicopters. This report describes the structural crashworthiness, the load attenuating cargo restraint, and the aircrew inflatable crew restraint experiments that were conducted, and presents the resulting data. The test aircraft crashed with a 9-degree nose down attitude; this impact was representative of the 95th percentile potentially survivable accident crash pulse. Results of the test can be compared with those of a CH-47C crash test (T-39)

DD FORM 1473 EDITION OF 1 NOV 65 IS OBSOLETE

393 742 78 06 27 080

Block 20. Abstract - continued.

conducted in 1975, which impacted at a 10-degree nose-up attitude with approximately the same resultant impact velocity vector.

PREFACE

3

TABLE OF CONTENTS

LIST OF ILLUSTRATIONS

7

LIST OF TABLES

INTRODUCTION

As part of its crashworthiness R&D program, the Applied Technology Laboratory has been involved in 39 full-scale aircraft crash tests during the past 16 years.

On 4 August 1976, the 40th test (termed T-40) was conducted at the NASA-Langley Research Center's Impact Dynamics Research Facility, Hampton, Virginia. The test vehicle was an Army CH-47A troop/cargo helicopter. The objective of the test was to obtain data that would contribute to the development of helicopter crashworthiness features and design criteria, thus enhancing occupant and cargo survivability. This was accomplished by three instrumented on-board experiments:

- Structural

- Cargo Restraint

- Aircrew Inflatable Restraint

The program was a joint Army/NASA/Navy effort. Tests were conducted by personnel from the Applied Technology Laboratory, U. S. Army Research and Technology Laboratories (AVRADCOM); NASA-Langley Research Center; and the Naval Air Development Center. NASA provided the test facility, conducted the test, installed some instrumentation, and reduced the test data in accordance with requirements specified by the Army. The Army was responsible for the experiments, the vehicle readiness, and the overall project management. The Navy installed the inflatable restraint system.

This report documents the test facility, setup, description, and experiment results.

TEST FACILITY

The CH-47A helicopter crash test, hereafter referred to as T-40, was performed at the Langley Impact Dynamics Research Facility shown in Figure 1. The basic structure of the facility is the 420-foot-high by 400-foot-long gantry. It is supported by three sets of inclined legs spread 267 feet apart at the ground level and 67 feet apart at the 218-foot level. A movable bridge spans the gantry at the 218-foot level and traverses the length of the gantry. A control room and an observation room are located in the building at the base of the gantry. Along the center line of the gantry, at ground level, is a strip of reinforced concrete 400 feet long, 30 feet wide, and 0.67 foot thick, which is used as the impact surface.

The apparatus necessary to conduct a helicopter crash test is shown in Figure 2. Swing-cable pivot-point platforms, located at the west end of the gantry, support the winches, sheaves, and pulley systems that control the length of the swing cables. A pullback platform, attached to the underside of the movable carriage, supports the winch, sheave, and pully system that controls the length of the pullback cable. Swing and pullback cables are attached to a specially designed lifting harness, which supports the helicopter from ground lift-off to release position during testing (Figure 3). This harness is attached to special mounting bolts in both the forward and the aft transmissions of the helicopter and to the swing and pullback cables. The harness system cable lengths were designed and assembled with the swing and pullback cables so that the helicopter would have the following impact conditions:

   5° nose-down pitch attitude

   0° roll and yaw

   42 ft/sec vertical velocity

   27.1 ft/sec horizontal velocity

The cable release system for the helicopter is shown in Figure 4. Each harness cable attached to the pullback cable was equipped with pyrotechnic cable cutters. The cutters on the forward pullback harness cables were located adjacent to the rear swing harness cables to prevent cable interference during cable separation. The harness points attached to the swing cables were connected to the helicopter mounting bolts by pyrotechnic release nuts. Pyrotechnic nuts are fired by a lanyard system adjusted to activate the firing circuit at the desired descent height during the test. The lanyard system consists of a contact switch activated by pulling a pin. The 0.0625-inch steel lanyard cable was attached to the pin and extended through a sheave system mounted to the gantry at the 150-foot level. A 5-pound mass was attached to the end of the cable to keep it taut as the helicopter was being raised and lowered. A stop attached to the lanyard was adjusted to contact a block at the sheave-mounting fixture when the helicopter reached the desired height for swing cable separation.

11
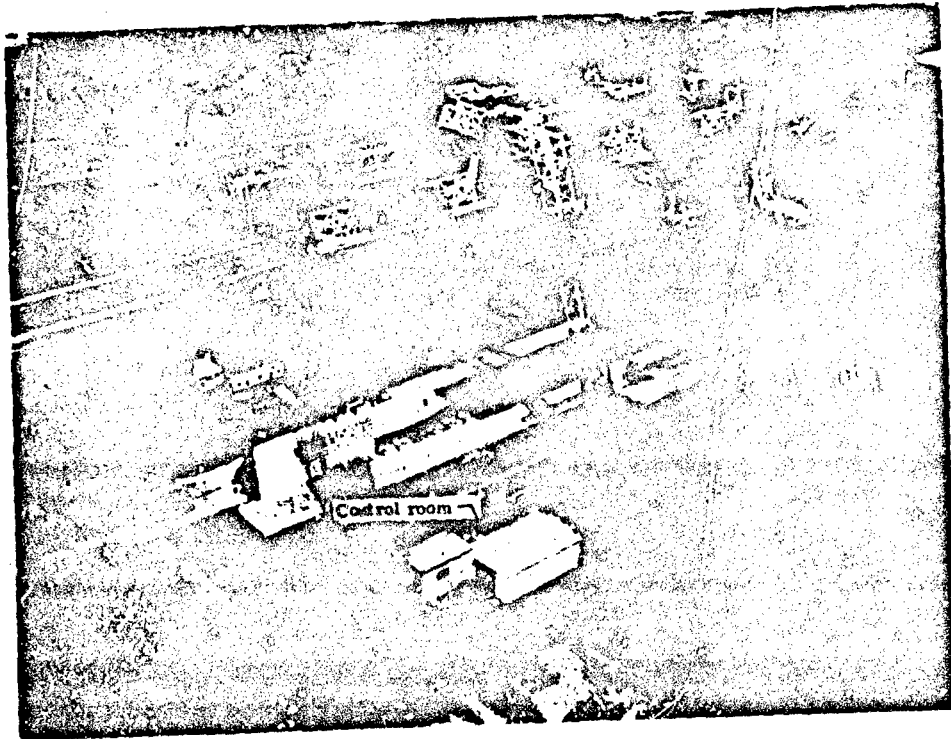
Figure 1. Langley Impact Dynamics Research Facility.
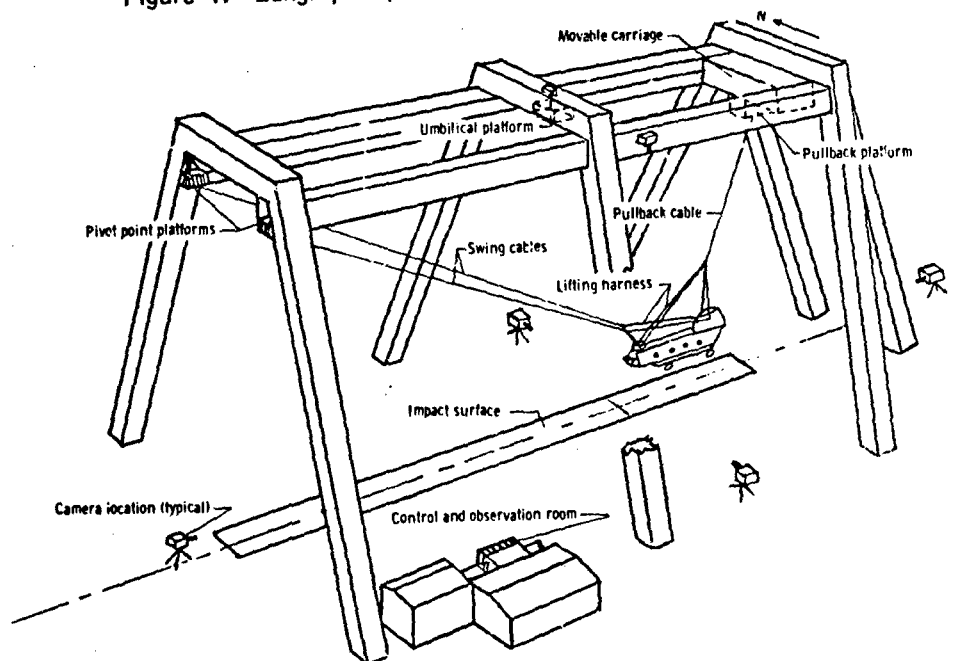
Figure 2. System used in full scale crash simulation test.
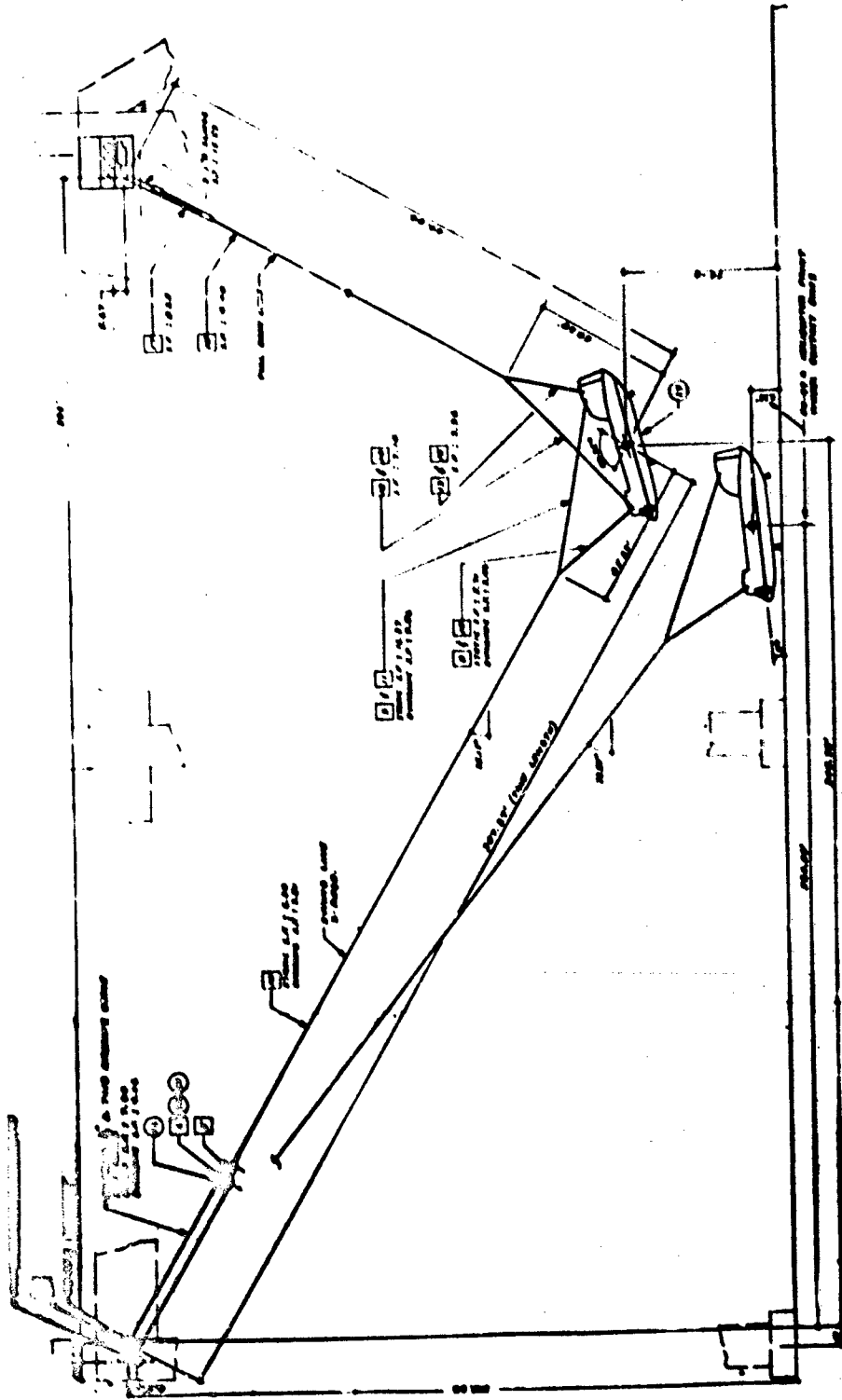
Figure 3.   Lifting harness design assembly.
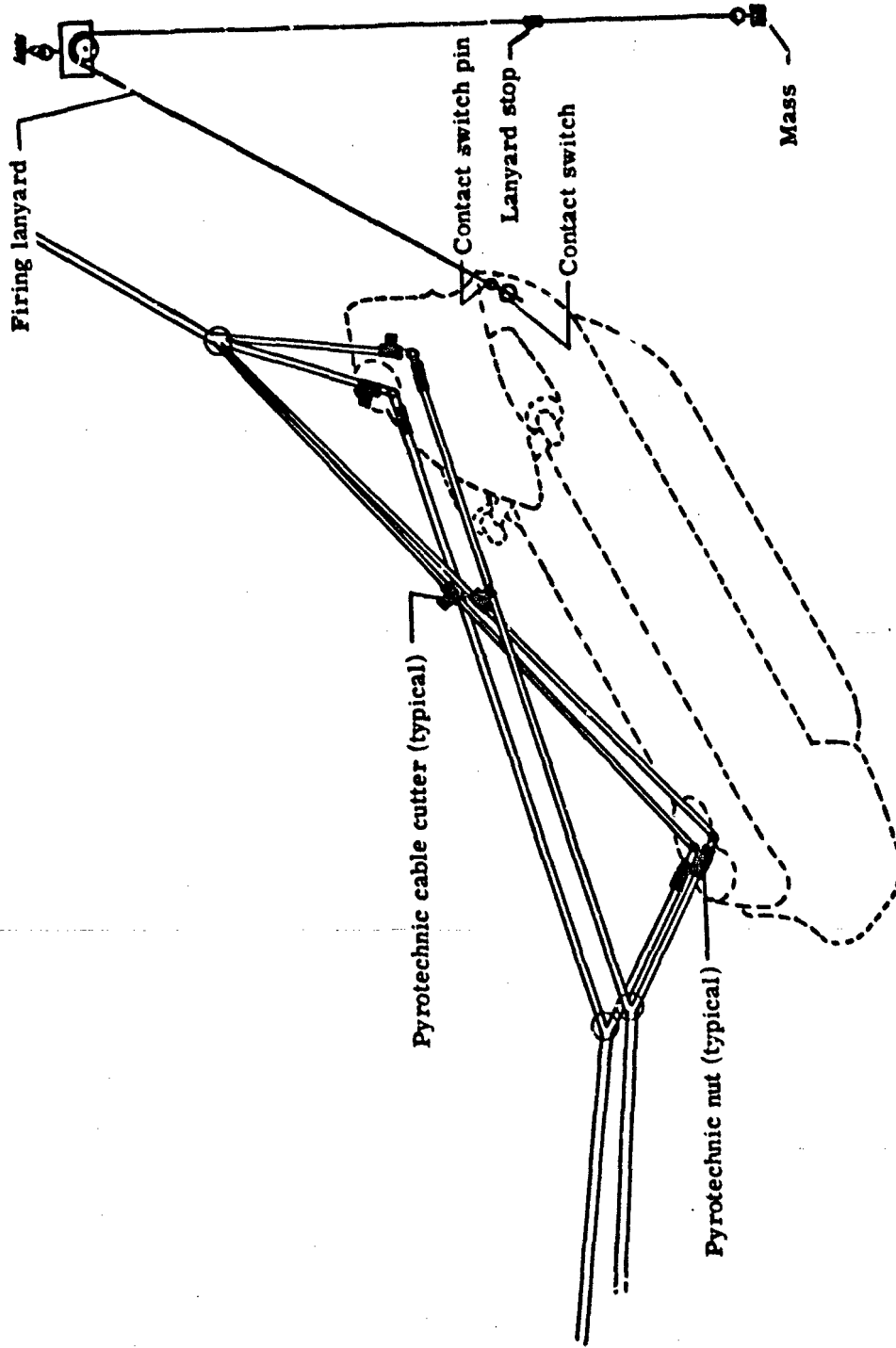
Figure 4. Cable release system.

Firing lanyard

Contact switch pin

Lanyard stop

Contact switch

Mass

Pyrotechnic cable cutter (typical)

Pyrotechnic nut (typical)

14

TEST SETUP

AIRCRAFT

The test specimen was a CH-47A helicopter, S/N 61-2418B, which had been retired from service. It was equipped with both engines, all transmissions, and stub blades. The aircraft was initially prepared for testing at the Applied Technology Laboratory (ATL), Fort Eustis. This preparation included cleaning, interior stripping, installation of new fuel cells, plexiglass removal, interior and exterior painting, and preliminary weight and balance calculations.

Mounts and fixtures for the on-board cameras and flashbulbs were designed and fabricated by ATL personnel, as were the pallets, trailer loads, instrumentation mounts, deflection tubes, and many other items supporting the experiments.

The interior was painted white and the exterior yellow with black lines, indicating the location of bulkheads and longerons of interest. An exterior view of the test specimen is shown in Figure 5. The test aircraft was transported from Fort Eustis to the Langley test site, where an ATL team, assisted by NASA and Naval Air Development Center (NADC) personnel, installed the experiment hardware, instrumentation, cameras, lights, and fixtures aboard the helicopter. Standard rotor blades could not be used as they were not compatible with the hoist rigging concept. Stub blades were installed to provide some representation of the rotor mass effects on the main transmissions.

Figure 5. Test specimen.

A final weight and balance calculation yielded a C.G. position at station 323.7 and an aircraft gross weight of 25,010 pounds, which is close to the normal design gross weight of 25,500 pounds for a CH-47A helicopter. A summary of the weight components is given in Table 1. The fuel cells were filled with water to the weight consistent with a full load. Ballast was placed in the closets at station 107.5 to aid in obtaining a C.G. that was within an inch of that stated in the CH-47A model specification as the normal C.G. location.

TABLE 1. WEIGHT AND BALANCE COMPONENTS

Item	Weight (lb)	Station	Moment
Basic aircraft	13,488	354.5	4,781,496
Fuel cells	60	316.8	19,008
Water in fuel cells	3,811	316.8	1,207,325
Dummies (two)	390	75.1	29,289
Aft trailer and restraints	1,426	369	526,194
Forward trailer and restraints	1,378	165	227,370
Aft pallet and restraints	834	462	385,308
Forward pallet and restraints	814	280	227,960
Baseline cargo package	179	326	58,354
Batteries and mounts	152	300	45,600
Forward stub blades	384	86.7	33,293
Aft stub blades	384	553.7	212,621
Cameras and fixtures: No. 3 & 5	134	370	49,580
2 & 6	119	196	23,324
4	55	390	21,450
1	72	133	9,576
Ballast:			
Right-hand heater closet	517	107.5	55,578
Left-hand closet	517	107.5	55,578
Miscellaneous Fixtures	296	428.5	126,833
TOTAL	25,010	323.7	8,095,737

Final test preparation activities included completion of instrumentation installation and connection to umbilical cables, check of each data channel on an oscilloscope, loading the cameras, and installation of the pyrotechnics.

INSTRUMENTATION

One hundred twenty-eight instruments were used to record data during the test. These consisted of 64 accelerometers; 42 strain gages; 10 load cells; 3 pressure transducers; Doppler radar; and 8 deflection tubes, two of which were rigged for manual measurement of the maximum structural deflection of the cabin ceiling. Figure 6 shows the general

16

Figure 6. CH-47 T-40 transducer locations.

LEGEND

⊗	DEFLECTION TUBE
▲	ACCELEROMETER
▭	LOAD CELL
⊕	STRAIN GAGE
▣	DISPLACEMENT ST. GAGE
◆	PRESSURE

location and the type of each on-board instrument and its recorded channel number designation.

Appendix A provides a detailed description of the instrumentation used in this test, and describes the instrumentation mounting, calibration, cabling, circuitry, and and recording procedures. Because of the importance of obtaining valid crash acceleration data in the vertical direction, redundant accelerometers for this axis were installed at many locations.

Each experiment section of this report addresses instrumentation supporting that specific experiment. There was a concerted effort to place instrumentation such that the data would be applicable to more than one experiment.

PHOTOGRAPHIC COVERAGE

Color motion picture coverage was provided for each of the on-board experiments. Nine Photosonic high-speed 16mm motion picture cameras were installed in the test aircraft, as shown in Figure 7. These cameras were cho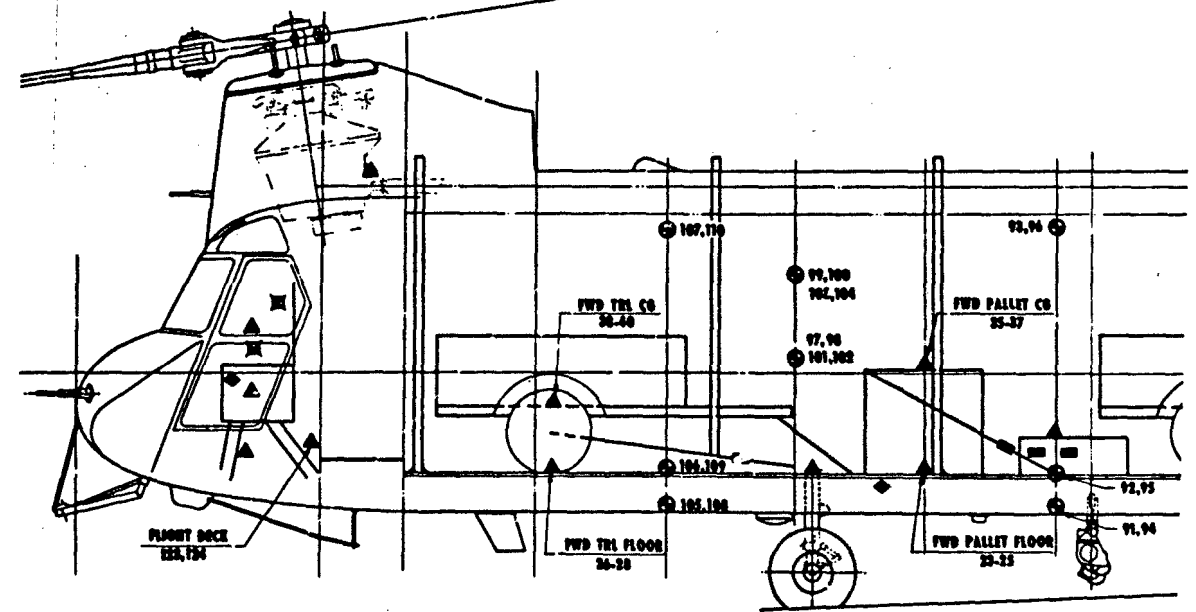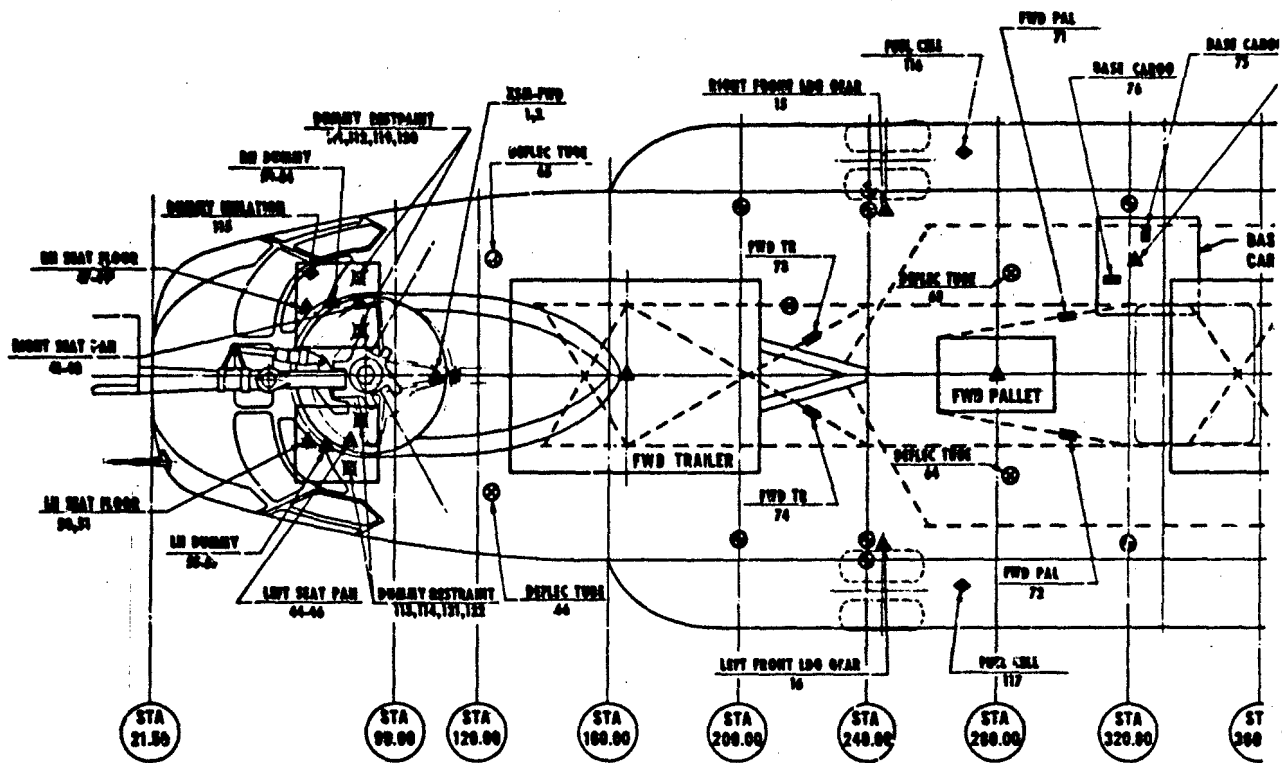sen because they are compact, lightweight, and have the ability to withstand high impact shocks. Seven cameras were placed in the cargo compartment and two were mounted in the cockpit. A protective covering made from heavy gauge aluminum was constructed and used to enclose each camera. They were then mounted on a specially designed shock-absorbing mounting plate to reduce camera motion and impact shock. Due to limited camera placement locations inside the aircraft, a 13mm wide-angle lens was used for its wide field of view and its ability to obtain visual data at close quarters. Experiment observation requirements dictated that as much of the tie-downs and cargo be photographed as possible.

A 28 VDC aircraft-type NICAD battery placed on-board was used to power the cameras and their control circuitry. The camera control system was activated by an aircraft release signal from the drop control room, which allowed camera turn-on and a "run-up" of approximately 1.25 seconds before the light intensity became sufficient for adequate exposure. All cameras, once on, continued to run through their total film supply and then automatically shut off at approximately 14 seconds after release. The cockpit cameras were attached to ceiling structural members to minimize camera movement during the impact sequence.

Because of the high impact forces to be encountered, Sylvania FF-33 special-purpose flash lamps were selected for interior lighting. Previous impact tests had proven that these lamps were suitable for this type of application. The lamps were installed in 7-inch polished reflectors with a wire retaining screen and located as shown in Figure 7. The interior of the aircraft was painted white so that reflected light would increase the light level inside the aircraft. A second NICAD battery was installed to power both banks of flash bulbs. Bank 1 consisted of 12 flash lamps, while Bank 2 contained 14. The control system was activated by a rear-mounted aircraft lanyard switch that was tripped upon aircraft release and subsequent movement. Light Bank 1 was designed to activate approximately 1 second after aircraft release and Bank 2 approximately 1.5 seconds after release.

19

The exterior photography was provided by NASA. Coverage included eight high-speed ground cameras, two of which were on the gantry overhead, and four 70mm still sequence ground cameras stationed to cover the right, left, fore, and aft views of the test helicopter. In addition, NASA provided video tape coverage for immediate post-test replay.

Figure 7. CH-47 T-40 camera and light locations.

2

TEST DESCRIPTION

PROCEDURE

The test specimen was lifted by the two swing cables and pullback cable winches until the longitudinal and vertical center of gravity was located in the proper impact position, as shown in Figure 5. The swing cables were locked in this position, and the test specimen was raised by the pullback cable until the center of gravity of the test specimen was at the desired height of 54.14 feet (Figure 3). This height was calculated to provide a flight path that would result in the planned impact conditions given in Table 2. The pendulum method of impact testing was used because a combined horizontal and vertical velocity resultant impact vector was desired and crash impact condition predictability was important.

TABLE 2. CRASH TEST IMPACT PARAMETERS

	Planned	Actual
Pitch angle, deg	-5	-8.7
Yaw angle, deg	0	0
Roll angle, deg	0	0
Vertical velocity, ft/sec	42	43.5
Horizontal velocity, ft/sec	27.1	28.3
Resultant velocity, ft/sec	50	51.9

The planned crash conditions for T-40 were selected because they would cause a large plastic deformation of the primary airframe structure and would permit an assessment of the airframe failure modes in a severe but survivable crash impact. The nose-down crash attitude was selected because the previous CH-47 crash test (T-39) had a 10-degree nose-up attitude impact, and the attainment of data for this range of impact conditions would enhance its usage and empirical correlation potential, especially in the development of the structural crash simulation computer model, KRASH.

A 50-ft/sec resultant impact velocity vector was selected for both T-39 and T-40. This is representative of the 95th percentile potentially survivable crash pulse as defined in MIL-STD-1290(AV) and given in Table 3.

TABLE 3. 95TH PERCENTILE POTENTIALLY SURVIVABLE
ACCIDENT DESIGN PULSES

Direction along aircraft axis	Velocity change (ft/sec)
Vertical (downward)	42
Lateral Type I aircraft	25
Type II aircraft	30
Longitudinal (forward)	
Cockpit	50
Passenger compartment	50
Resultant vector*	50

*The downward, sideward, and forward velocity components
of the resultant velocity vector do not exceed 42, 30, and
50 ft/sec respectively.

The crash test sequence began when the instrumentation recording equipment was
started, approximately 30 seconds prior to releasing the test helicopter. The release
of the helicopter was initiated in the control room by a push switch that closed relays
and sent signals from the pyrotechnic power supply to the guillotine cable cutters in
the pullback harness. A second and third relay initiated external and internal camera
coverage. A lanyard system for the internal flight programmer initiated the light
sequence after approximately 1 second of free-fall time. When the helicopter had
dropped to where the landing gear was approximately 1 foot above the impact surface,
the lanyard was pulled to fire the swing cable harness pyrotechnics, which in turn
separated all harness cables from the test specimen and permitted free flight to time
of impact.

IMPACT

T-40 took place on 4 August 1976 with release at 1430:0.0381. Impact occurred at
1430:1.9243. After initial impact, the test helicopter slid approximately 10 feet on
the facility's concrete apron.

Actual impact parameters differed from the planned conditions, as shown in Table 2.
Nevertheless, the resultant impact velocity is representative of the 95th percentile
potentially survivable crash pulse.

Actual impact parameters were determined by analysis of the still sequence and motion
pictures and by the Doppler radar data. Analysis of the pictures permitted determina-
tion of the aircraft's pitch attitude at impact, its flight path, and its vertical velocity.
The horizontal velocity of the helicopter at impact was obtained using data from a
Doppler radar unit that was located on the impact surface approximately 200 feet in
front of the impact point. Radar data was continuously recorded.

The drop sequence, as obtained from the 70mm ground cameras, is shown in Figures
8 and 9 for the right-side and left-side views of the aircraft respectively. Figures 10
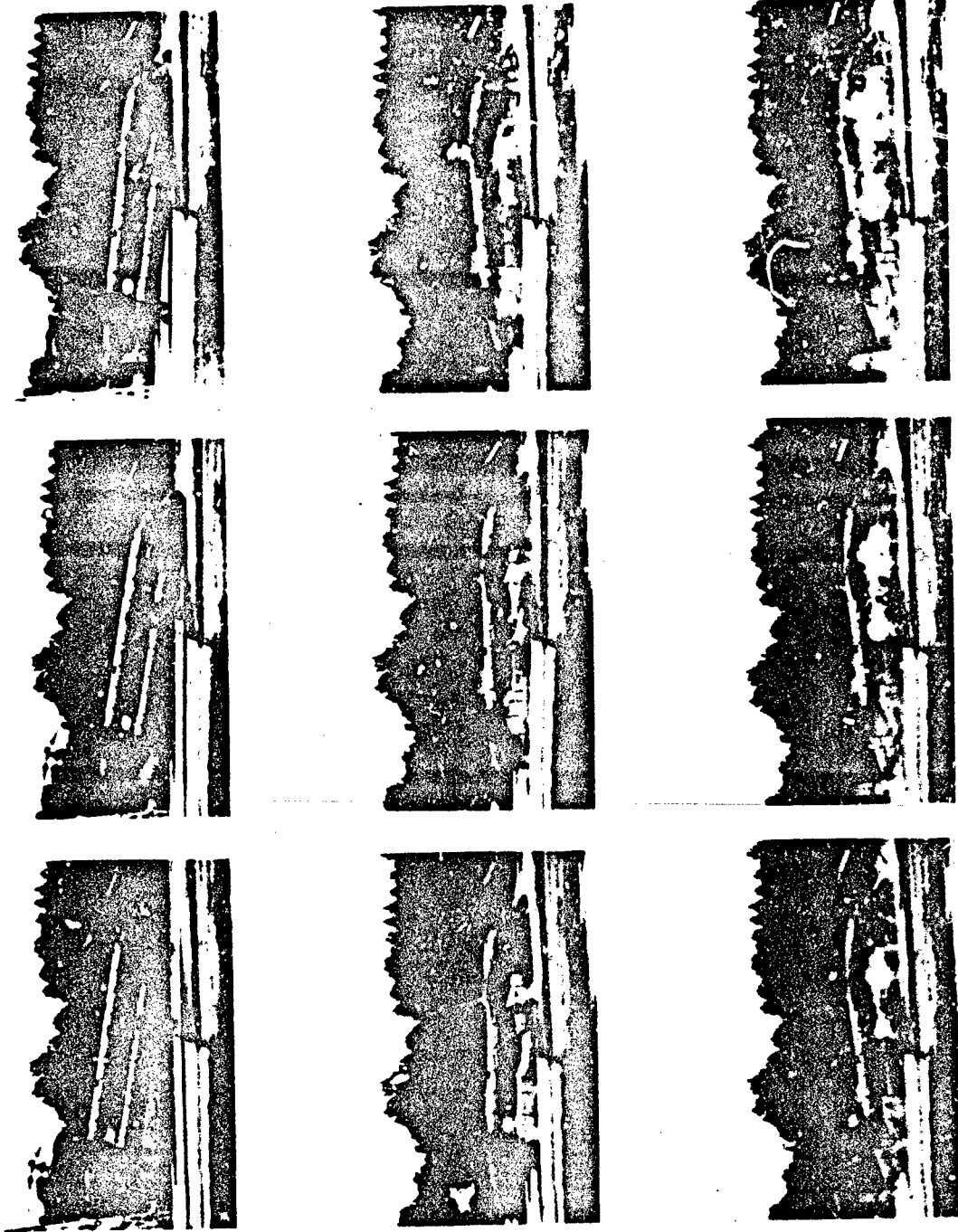and 11 illustrate the crash impact severity.

24

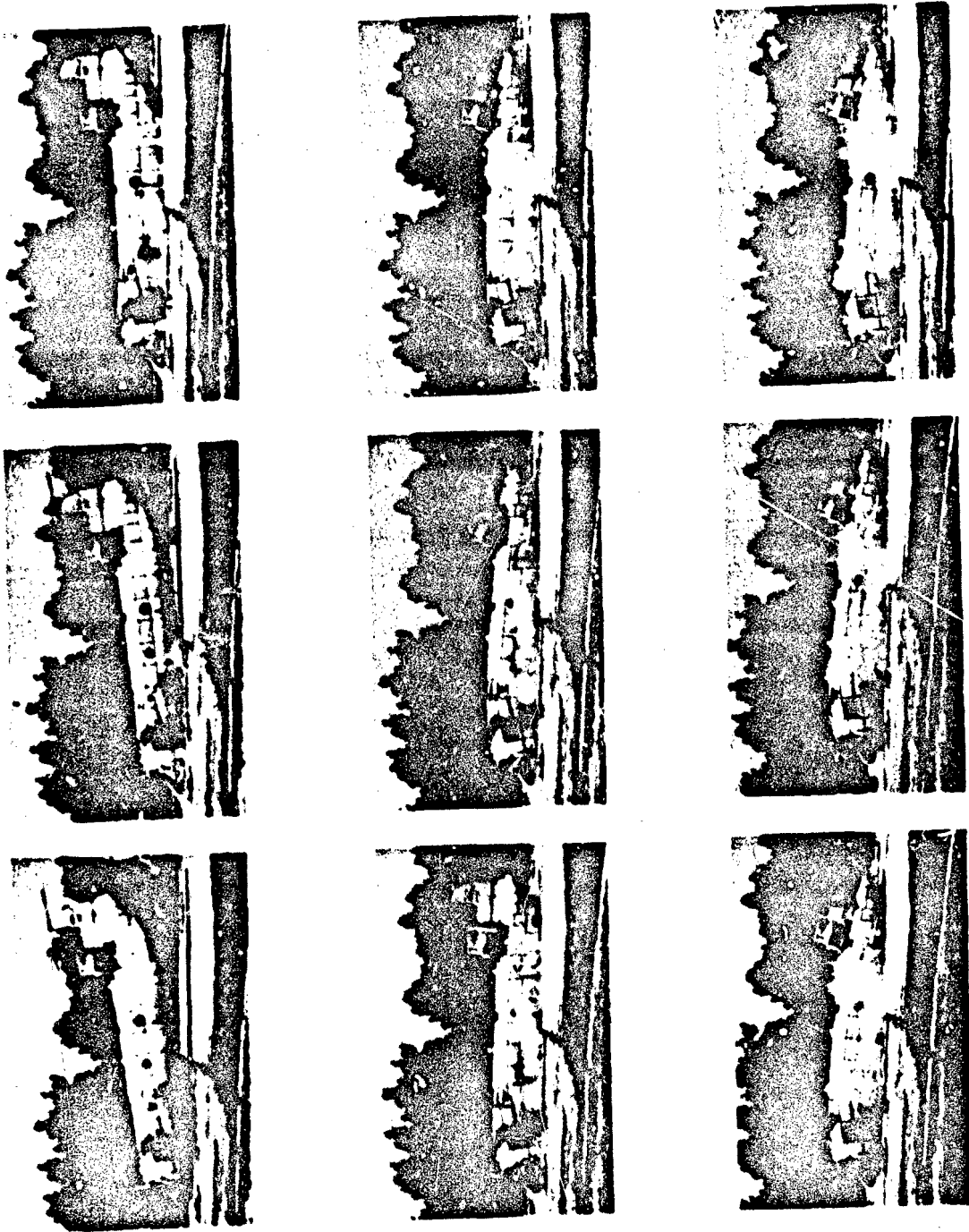Figure 8. Impact sequence - right-side view.

25

Figure 9. Impact sequence - left-side view.

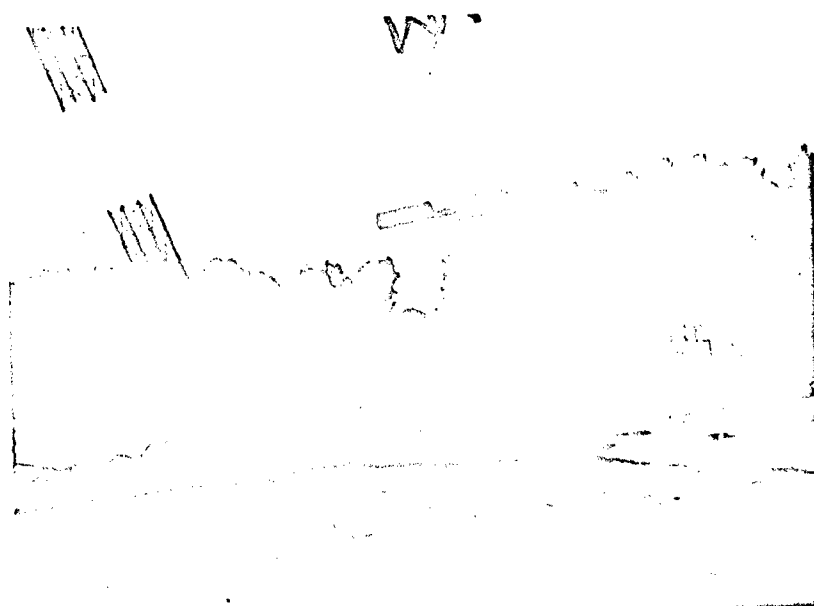Figure 10. Post-crash view - right front.

Figure 11. Post-crash view - left rear.

DATA ACQUISITION

The impact severity and aircraft breakup resulted in 19 channels of data being lost during the impact. Of these, twelve were lost due to cables being severed by fuselage and component breakup, five were lost due to separation from their mounting pads, and the two fuel cell pressure sensors were lost when the forward landing gear impacted the fuel cell end plate.

All interior cameras functioned as planned; however, after the crash it was discovered that three camera lenses were damaged. This damage was caused by the extreme shocks sustained by those cameras located over the landing gear structure. The impact drove the landing gear upward into the aircraft and into the camera mounts. Some of the flash lamps were separated from their base sockets upon impact, but the magnesium filament continued to burn and provide adequate light.

DATA REDUCTION AND PRESENTATION

The test data were recorded on FM magnetic tape and processed by NASA/LRC. After the analog-to-digital conversion using a sample rate of 4000 samples per second, the data were filtered using a 100-Hz low-pass digital filter. The 100-Hz low-pass filter is similar to the class 60 filter described in the Society of Automotive Engineers Recommended Practice SAE J2119 for full-scale vehicle impact test data reduction. All accelerometer data were numerically integrated twice, using the trapezoidal rule integration method with a 0.00025-second time step. The resultant time histories were then plotted to provide the following information:

1. Unfiltered accelerometer, deflection tube, strain gage, restraint displacement, pressure transducer, Doppler radar, and load cell data.

2. 100-Hz filtered accelerometer, load cell, and deflection tube data.

3. Velocities and displacements obtained from integration of deceleration data.

Zero time for all plots was 1430:1.800, or 1.7619 seconds after the time of aircraft release; the data were plotted for a duration of 0.600 second.

In the following structural and restraint experiment discussions, only a portion of the data that was acquired from T-40 is presented. Plots of data acquired from all 126 channels are available for review at the Applied Technology Laboratory, U. S. Army Research and Technology Laboratories (AVRADCOM), Fort Eustis, Virginia.

EXPERIMENTS

STRUCTURAL

Purpose

The purpose of the structural crashworthiness experiment was to obtain data for use in the development of analytical techniques that can be used to predict helicopter structural behavior over a range of crash impact conditions, and for use in the establishment of design criteria for crashworthy structures that will minimize crash forces transmitted to occupied areas and thereby reduce occupant injuries. Also, the effect of structural breakup on fuel cell integrity was sought.

Background

Analysis methods, such as KRASH, for improving crashworthiness of helicopter structures are in their infancy, but the correlation of these methods with testing is beginning to lend credence to their effectiveness. Previous efforts to develop the KRASH model have been directed primarily to the utility helicopter. Analysis of a structure as complex as that of the CH-47 cargo helicopter presents a more difficult challenge. Accordingly, the Boeing Vertol Company was awarded Contract DAAJ02-76-C-0015 (Reference 1). The objectives of that contract were: (1) to simulate the dynamic response of a CH-47A helicopter for a crash impact as defined in Table 2, using computer program KRASH; (2) to correlate the predictions of KRASH with the data obtained from this test (T-40); and (3) to formulate and recommend improvements to KRASH. To ensure adequate correlation of the test results with predictions, Boeing Vertol specified the types and the locations of the structurally related instrumentation that was to be installed in the test helicopter.

Description

To provide adequate data for correlation with the structural behavior predictions obtained from KRASH, 34 strain gages were discretely mounted in the test helicopter. Also, floor- and component-mounted accelerometers and deflection tubes were installed for correlation purposes. The deflection tubes provide a time history of the vertical displacement of the fuselage crown with respect to the cabin floor at six locations in the cabin. Two other deflection tubes were rigged for post-test measurement only.

The test aircraft was equipped with two new standard (noncrashworthy) fuel cells. All connectors had been removed and connecting points securely sealed. Each cell contained 1905.5 pounds of water. This weight is equivalent to that of 300 gallons of JP-4 fuel, which is the design capacity for the CH-47A fuel cell. To measure the

---

[1] BadriNath, *Math Model (KRASH) - CH-47A Crashworthiness*, Boeing Vertol Co., USARTL-TR-78-24, Applied Technology Laboratory, US Army Research and Technology Laboratories (AVRADCOM), Fort Eustis, Virginia, to be published.

hydraulic ram at impact, a pressure transducer was located at the forward bottom connector mount of each fuel cell end plate. The water was dyed red and green in the left and right side cells respectively.

Results

A detailed discussion of the structural experiment results is contained in Reference 1. For this reason, only a limited presentation of results is provided in this report.

The nose-down crash attitude resulted in the forward landing gear making initial ground contact. As the impact progressed, the gear rotated aft, impacting and displacing the end plates of both fuel cells. This reaction, coupled with pod and fuselage material failures and resultant jagged metal punctures, resulted in a massive rupture of the fuel cells and immediate dissipation of their contents. This effect is depicted in Figures 12 and 13.
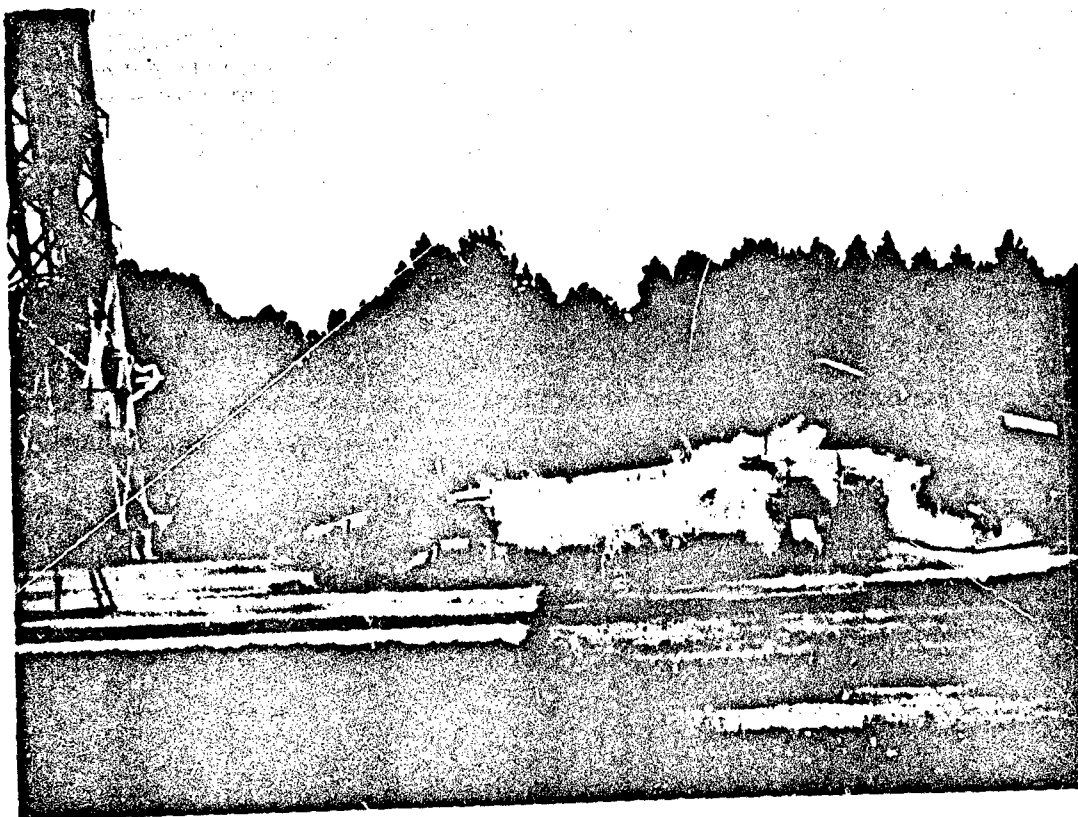
Figure 12. Fuel cell rupture and water dissipation.

Figure 13. Post-crash view of fuel pod and cell.

The pressure transducers were destroyed by the impact of the landing gear on the end plate, but pulses were recorded for approximately 0.080 second after touchdown. These data show hydraulic ram peaks of 200 psi for the right-side cell and 170 psi for the left-side cell.

The very rigid attachment of the landing gear to the box beam structure at station 240 caused this structure to follow the gear rotation, breaking the aircraft at this location. This sequence is shown in Figures 8, 9, and 14. The interior floor deformation resulting from this structural failure was severe, as shown in Figure 15.

The transmission and engine mounts adequately retained these components, preventing their penetration into the helicopter's occupiable interior. As an example, a failed rear engine mount is shown in Figure 16.

Figure 14. Structural failure at station 240.
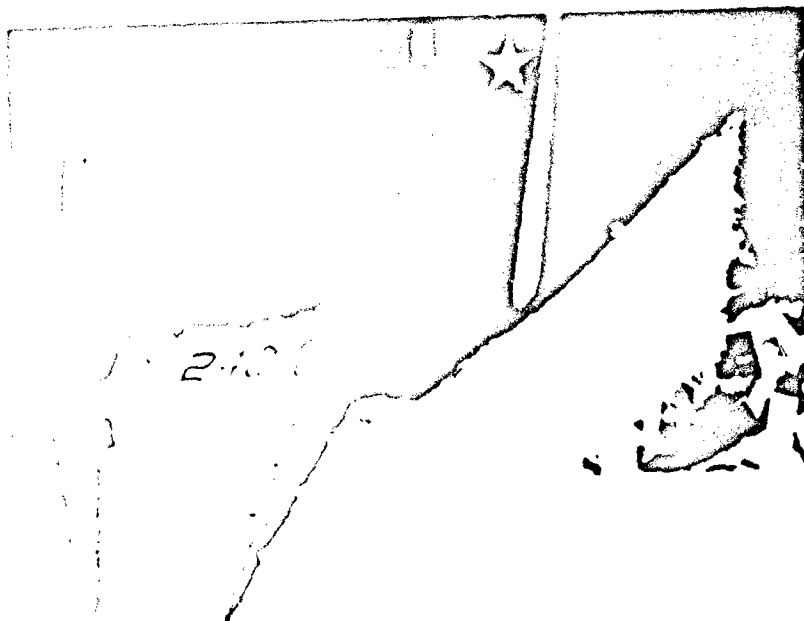
Figure 15. Interior floor deformation at station 240.
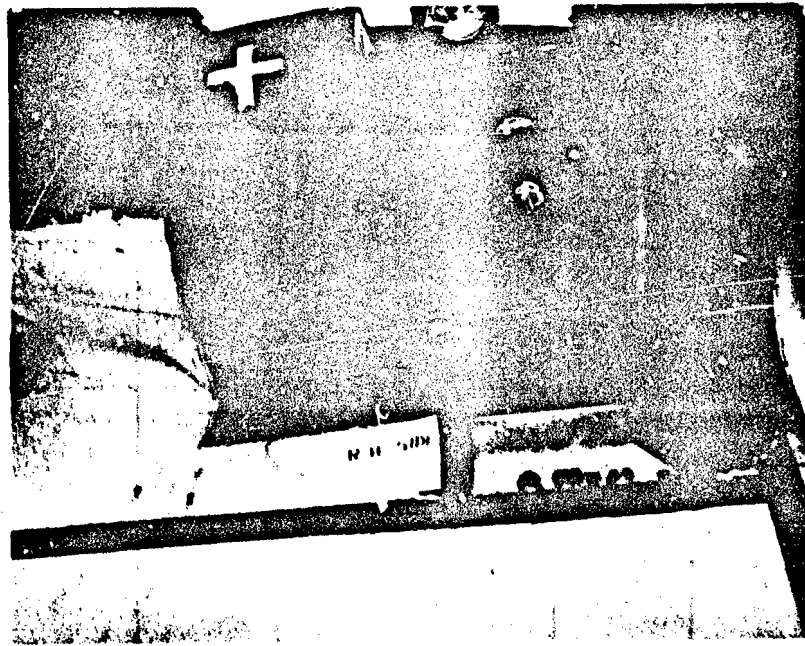
Figure 16. Rear engine mount failure.

Standard CH-47A seats were installed in the test specimen. As shown in Figure 17, both seat pans broke as a result of the crash impact. While the failure of the copilot inertia reel allowed the dummy to pitch forward, the pilot inertia reel engaged, causing the restraint to tear the back of the seat. This is also shown in Figure 17.
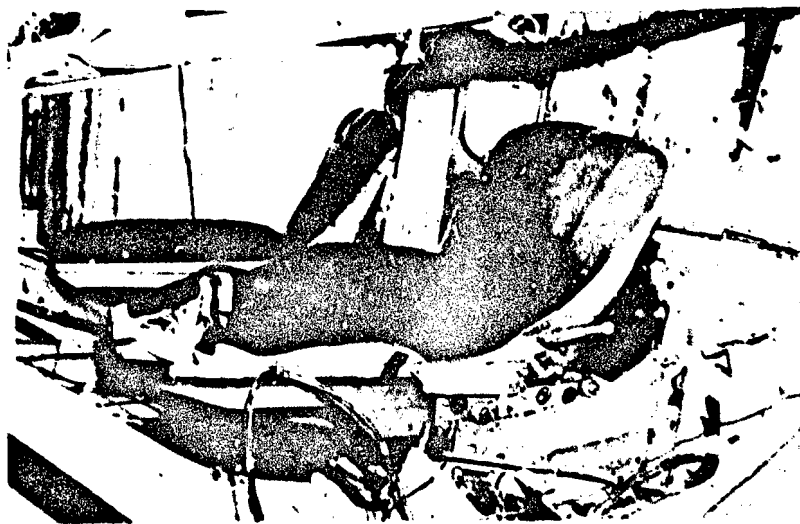
Figure 17. Seat pan failure.

33

Figure 18 shows the variation of the 100-Hz filtered peak decelerations (measured along the cabin floor centerline) and the cabin height reduction with the aircraft station.
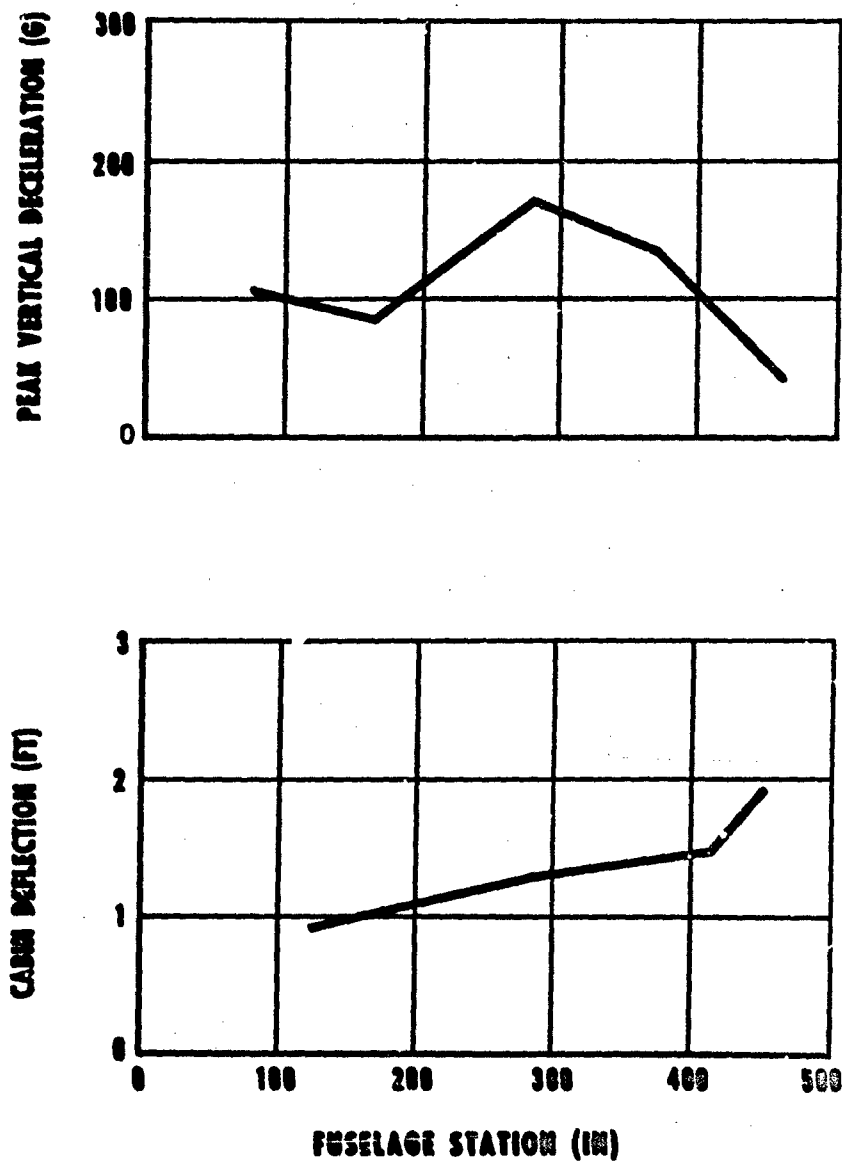
Figure 18. Variation in peak decelerations and cabin height reduction with aircraft station.

In Figures 19 through 28, the ordinate specifies the tape recorder/recorded channel and the unit of measurement. (For example: A02-G indicates this is a plot of measured acceleration (G) recorded on Channel "2" of recorder "A".) The abscissa depicts the time history beginning at 1430:1.800. The impact sequence began 0.1243 second later, when the forward gear contacted with the facility concrete apron. Each data plot has a label that describes the instrumentation and provides other information as depicted by the following example:

a	b	c	d	e	f
CH-7	Engine-Right	LO	R-496	5	N

a.   Designated data channel number (1 to 126)

b.   Transducer location, description, or purpose

c.   Instrumentation type and/or function:

   V - Accelerometer, vertical direction
   LO - Accelerometer, longitudinal direction
   LA - Accelerometer, lateral direction
   DTP - Deflection tube
   LC - Loal cell
   SG - Strain gage
   SGI - Strain gage, inner
   SGO - Strain gage, outer
   PT - Pressure transducer
   PTN - Navy pressure transducer
   SGN - Navy extensiometer

d.   Aircraft location [center (C), left (L), or right (R)] and fuselage station

e.   Transducer sensitivity $\times 10^{-2}$ G

f.   Recorder: Army (A), NASA (N)

The deceleration time history during impact for the engines and transmissions is presented in Figures 19 and 20 respectively. Comparison of these data with Figure 21, which gives the cabin floor and landing gear attachment deceleration time history, illustrates the energy-absorption capability of the deforming structure. For instance, deceleration readings in the vertical direction range from 210.5 G at the rear right landing gear at station 482, to 59.8 G at the floor centerline at station 460, to 9.2 G at the rear transmission at station 540.

Figures 21, 22, 23, and 24 deal with the deceleration time history of the cabin floor and reflect the extent of the data reduction accomplished. This includes:

- Raw and 100-Hz filtered data.

- Expanded scale filtered data.

- First integration of data for velocity.

- Second integration of data for displacement.

Figure 25 gives the time history recording of cabin height reduction measured by the deflection tubes. Figure 26 presents the longitudinal deceleration time history at the cabin floor centerline for various stations. Also shown is the fuel cell hydraulic ram pressure at impact. These pressure transducers were destroyed just after impact.

Crash force attenuation from cockpit floor to seat to occupant is shown in Figures 27 and 28 for the pilot and copilot stations respectively.

CONCLUSIONS

1. The data acquired from T-40 provided a sound basis for empirical correlation with the computer model KRASH predictions and subsequent improvement of the model.

2. The rigid forward landing gear attachment caused aircraft breakup at station 240 in both T-39 and T-40. This structural deficiency poses a crash safety hazard to cabin occupants, which could be eliminated by designing the attachment to fail at a load lesser than that necessary for structural member failure.

3. Seat pan failures at both the pilot and the copilot stations are indicative of the severe tailward decelerations experienced by occupants in a 95th percentile potentially survivable impact. Had this been a manned helicopter, it is most probable that the pilot and copilot would have sustained incapacitating injuries.

4. The interaction of the forward landing gear with the fuel cell end plate for the nose-down crash attitude poses a potential CH-47 post-crash fire hazard with or without crashworthy fuel systems installed.
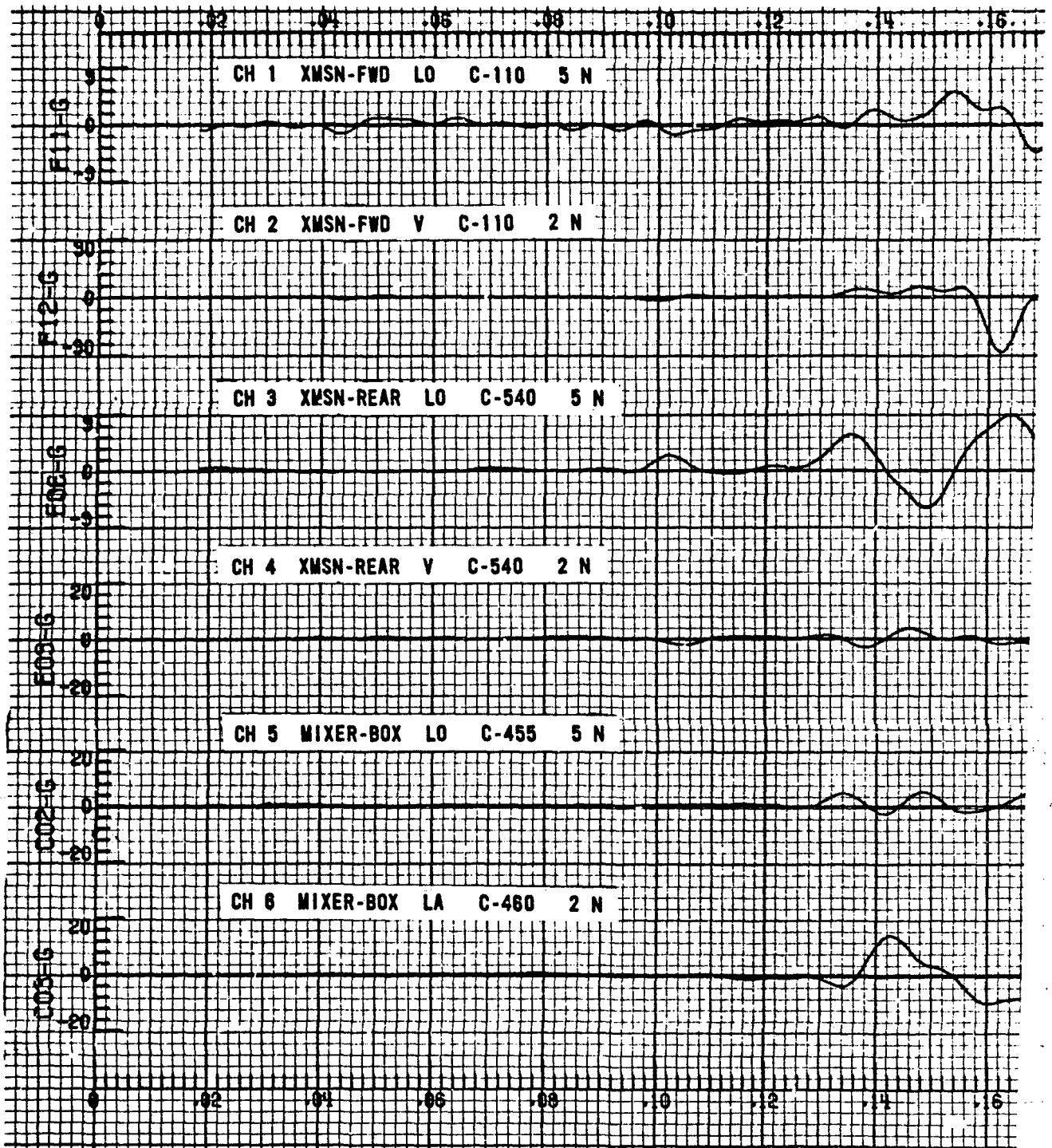
Figure 19. Gearbox decelerations.

37

TIME (SEC)

.0   .32   .34   .36   .38   .40   .42   .44   .46   .48

.0   .2   .4   .6   .8   .40   .42   .44   .46   .48
TIME (SEC)
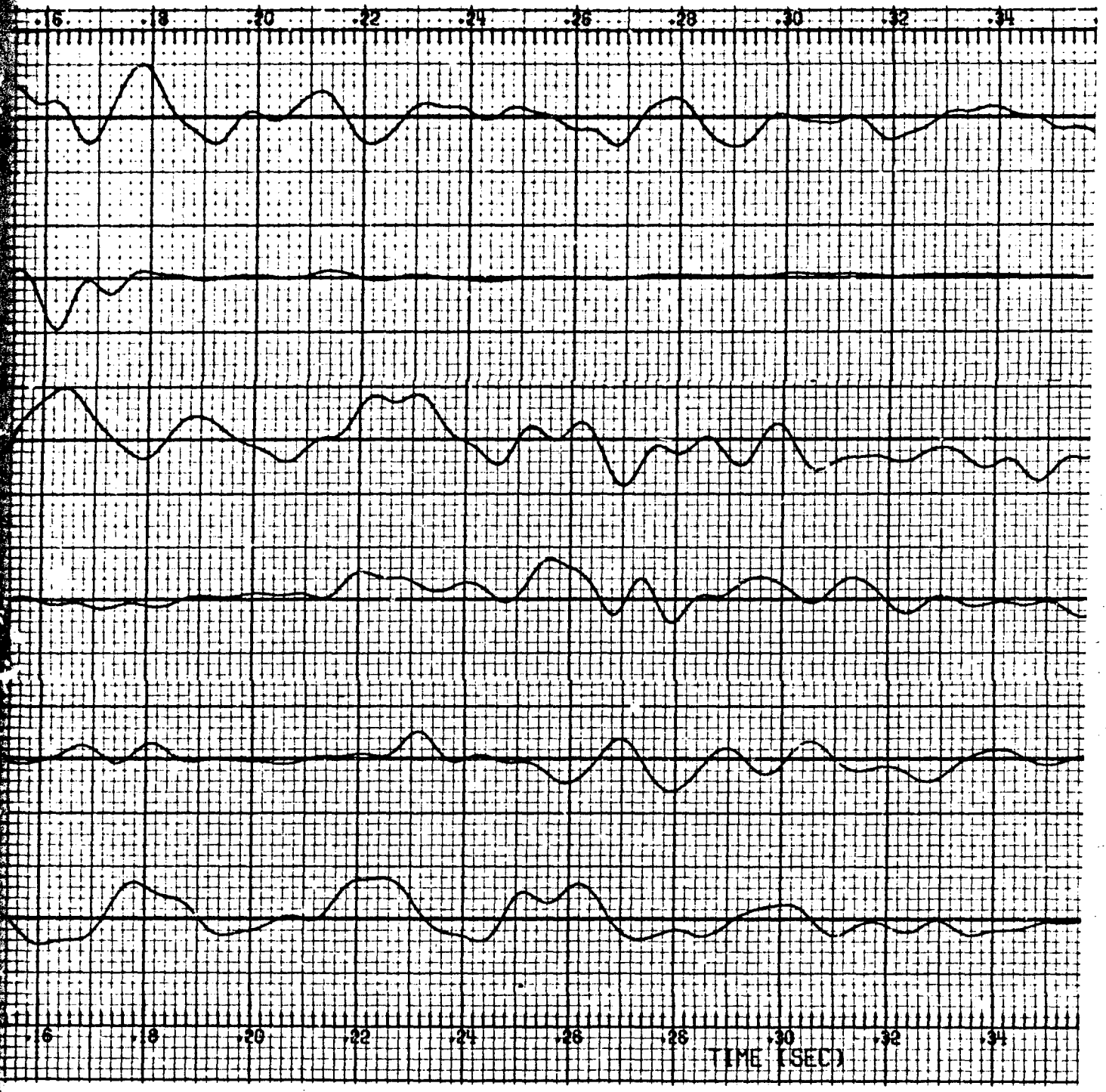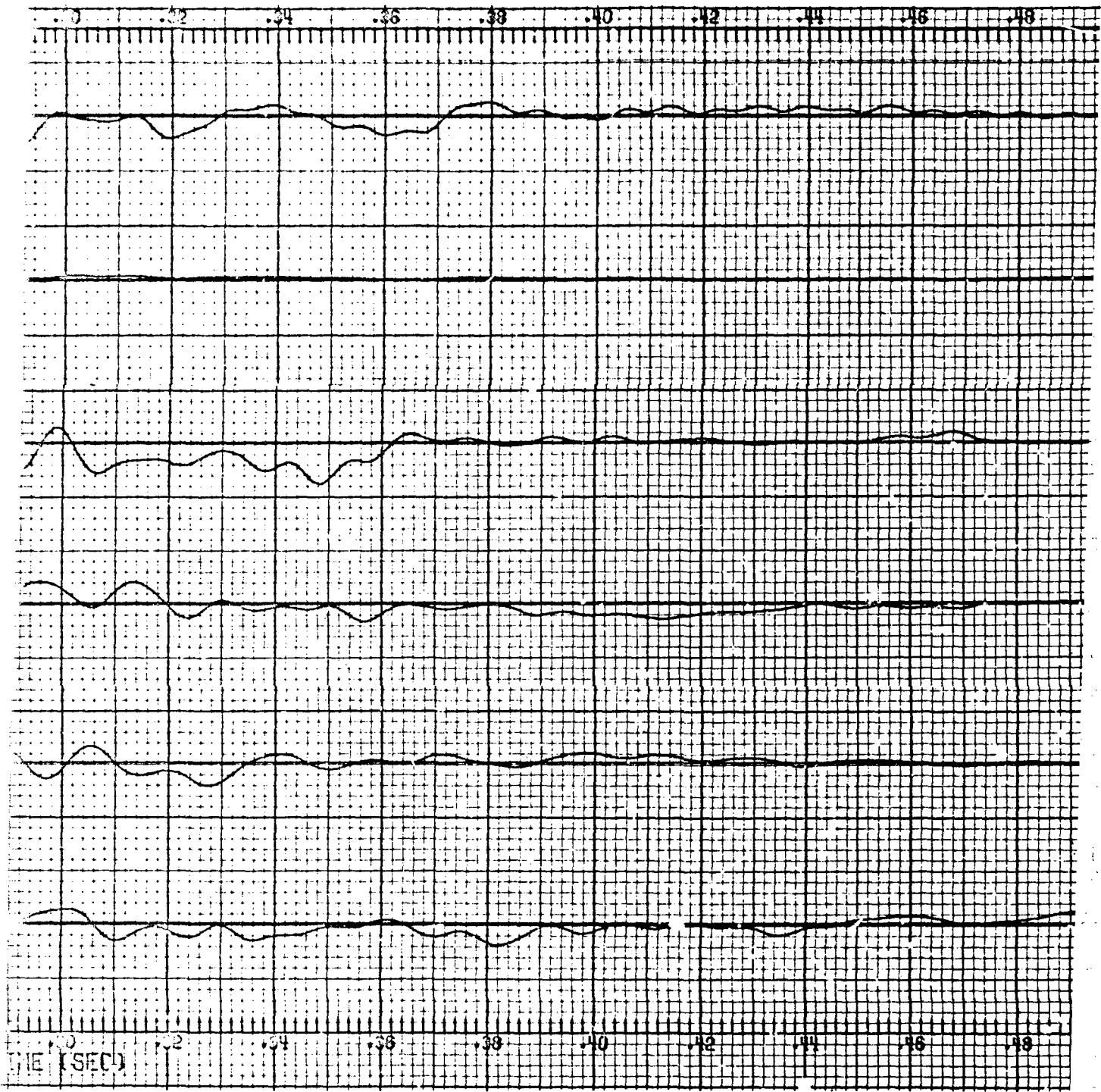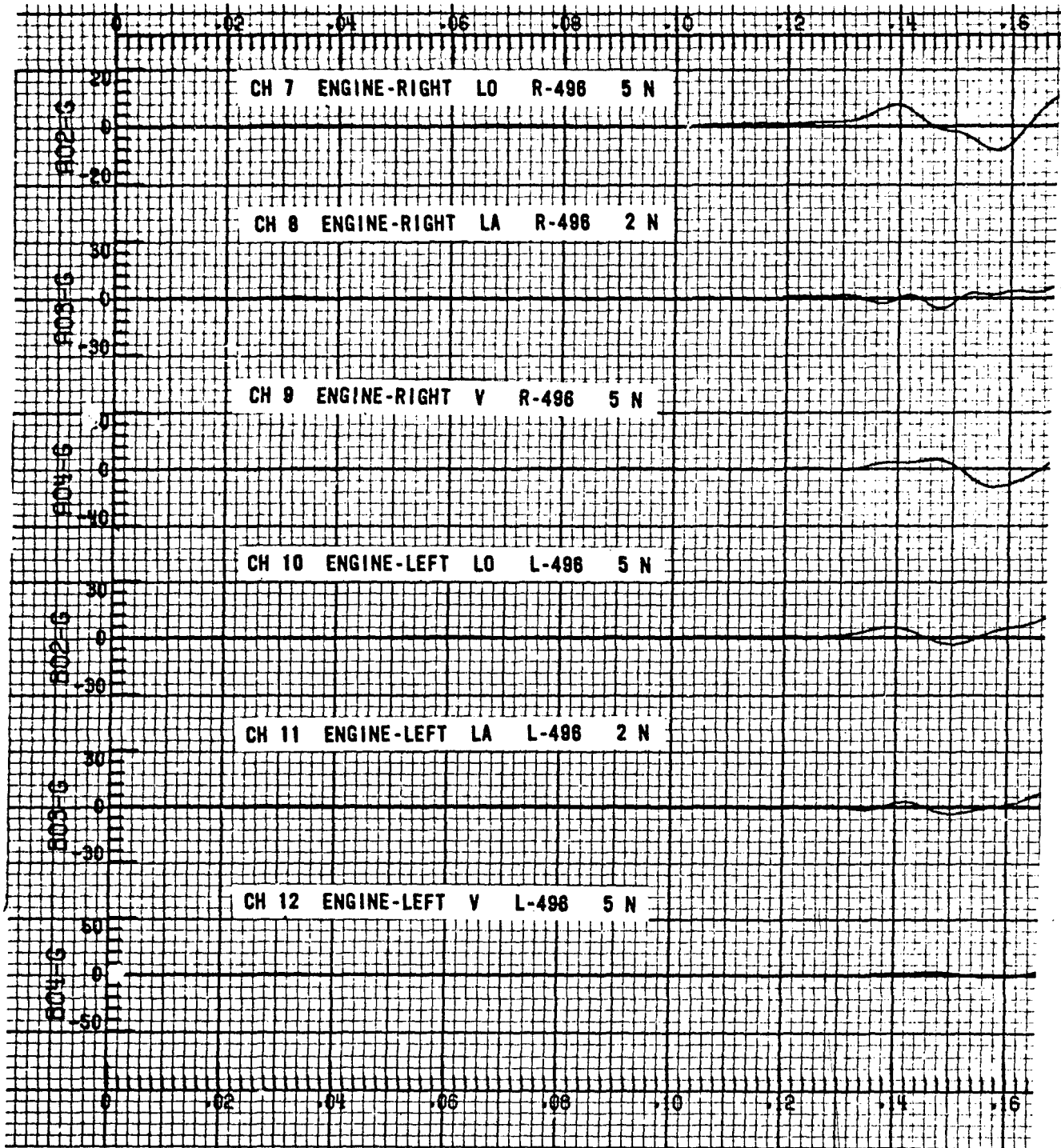
Figure 20. Engine decelerations.

39

TIME (SEC)
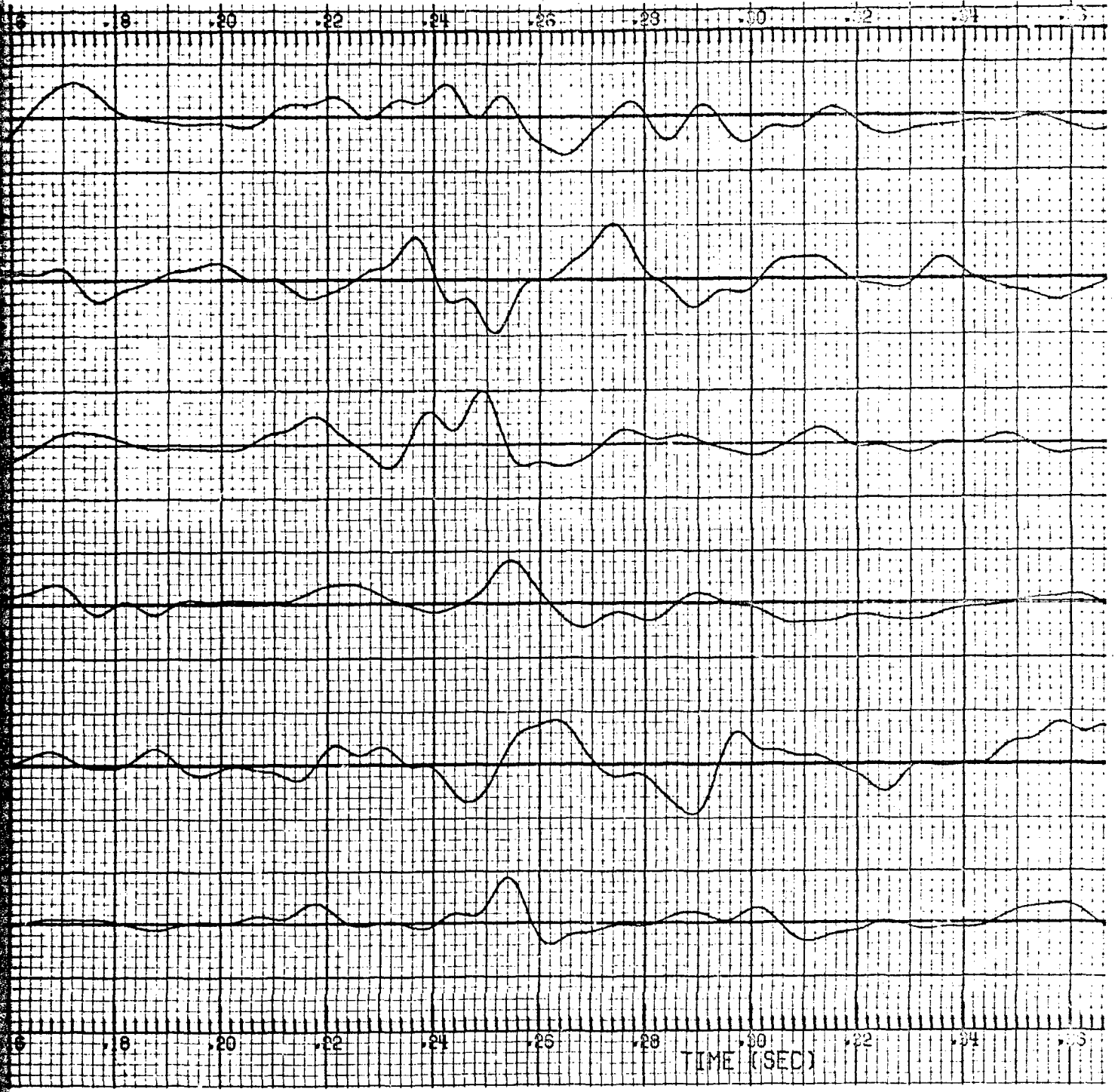
3
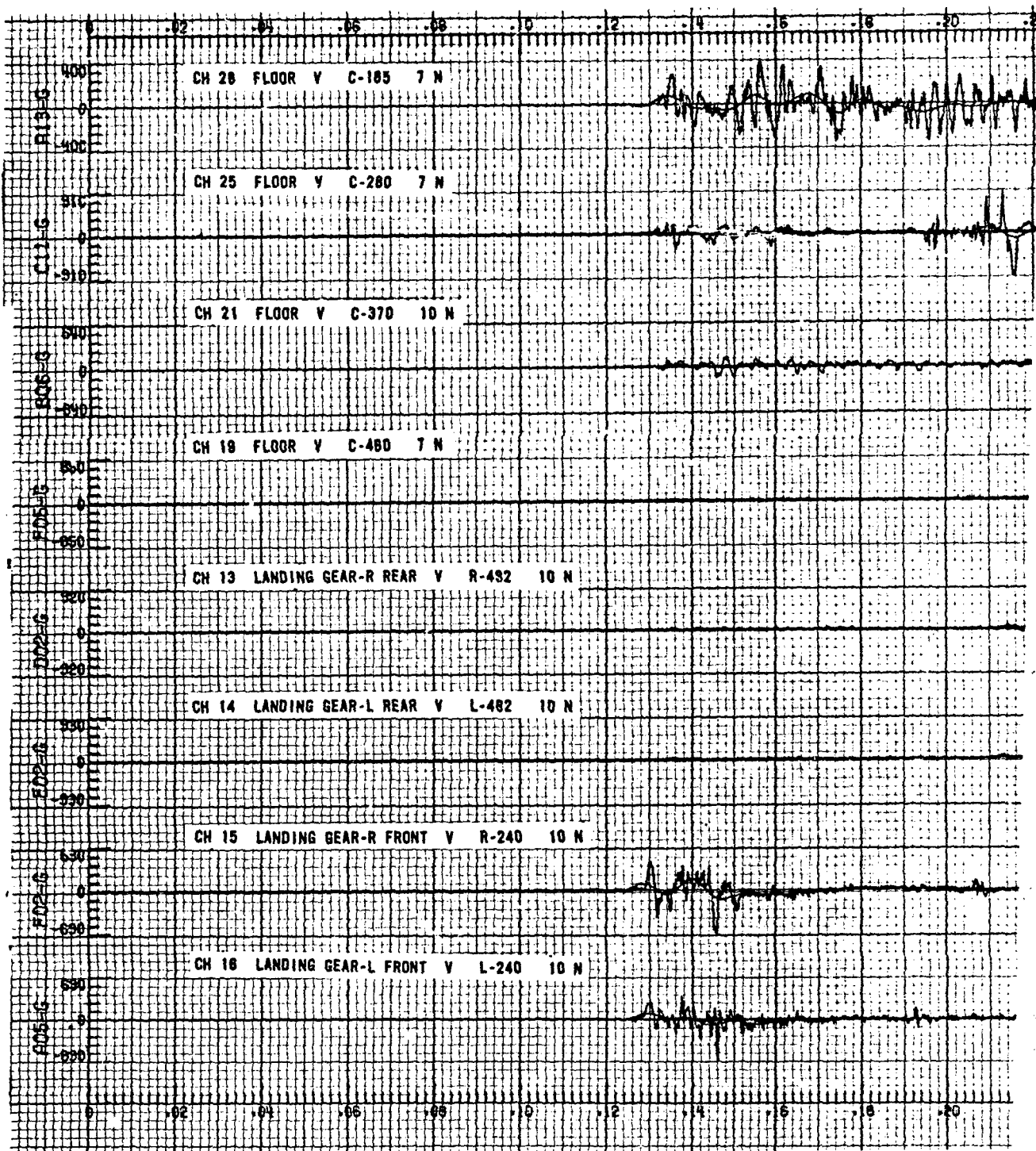
Figure 21. Cabin floor and landing gear attachment vertical decelerations (raw and 100 Hz filtered).

41
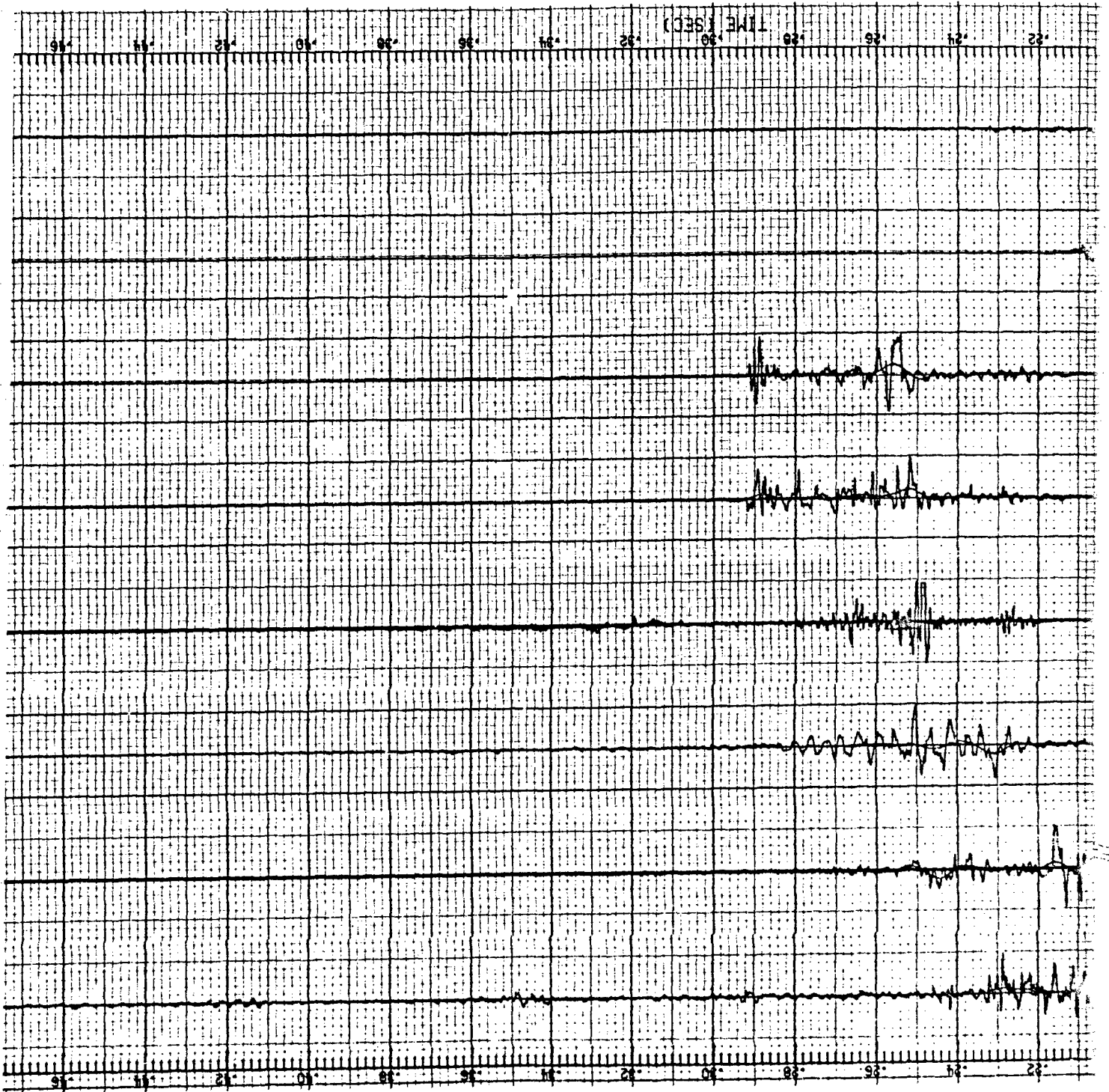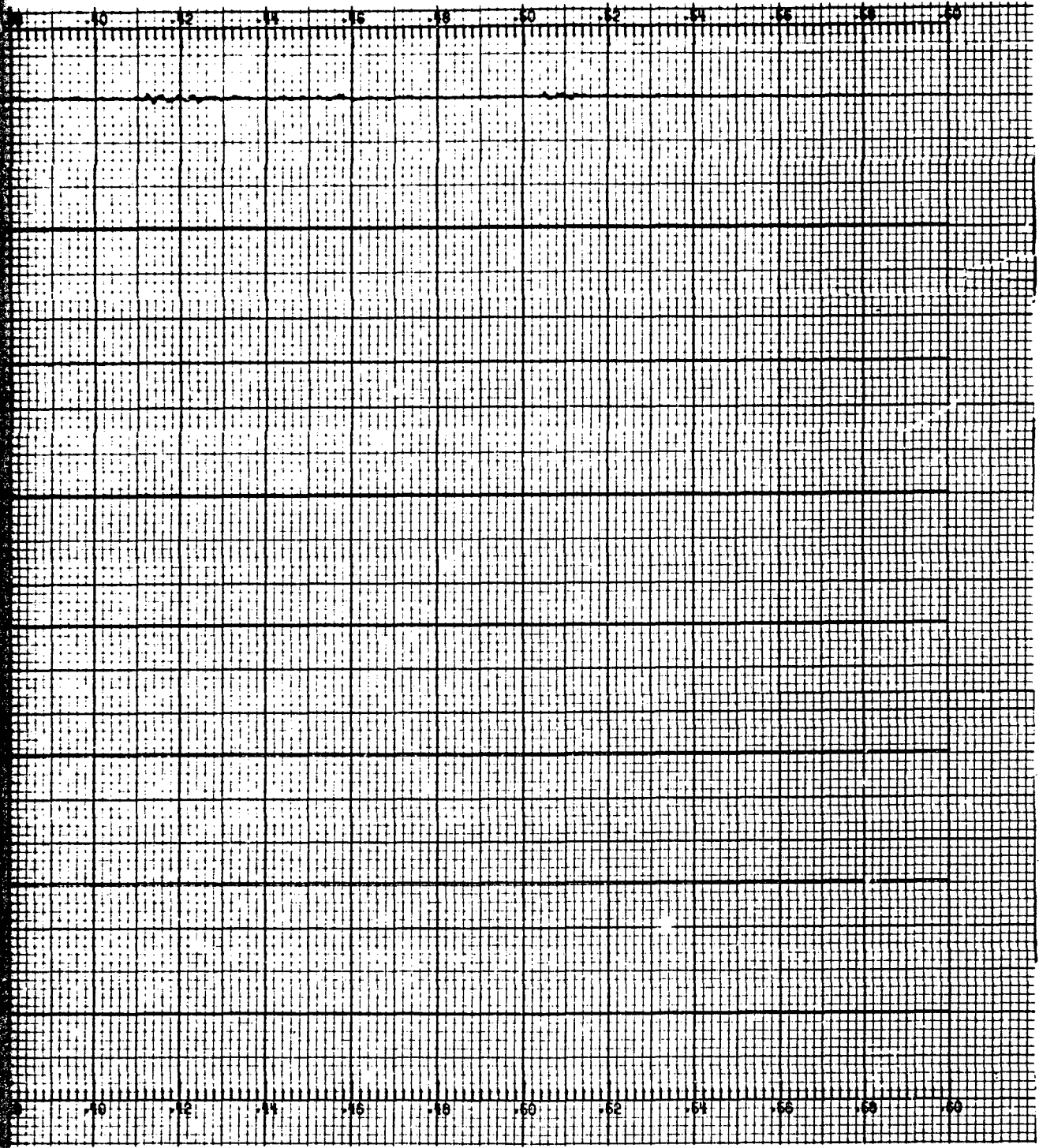
3
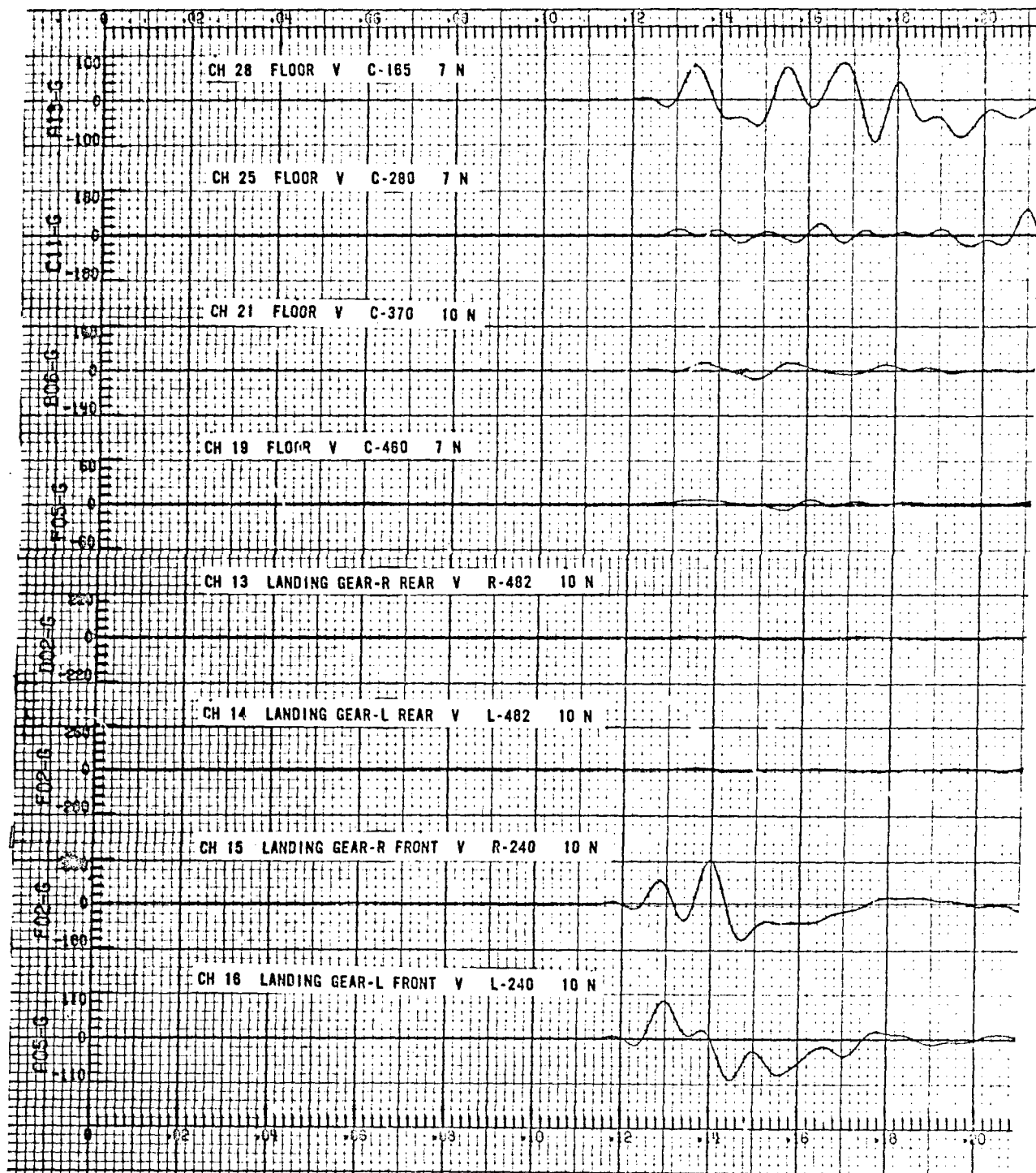
Figure 22. Cabin floor and landing gear attachment vertical decelerations (100 Hz filtered).

43

TIME (SEC)

2

.40 .42 .44 .46 .48 .50 .52 .54 .56 .58 .60

.38 .40 .42 .44 .46 .48 .50 .52 .54 .56 .58 .60
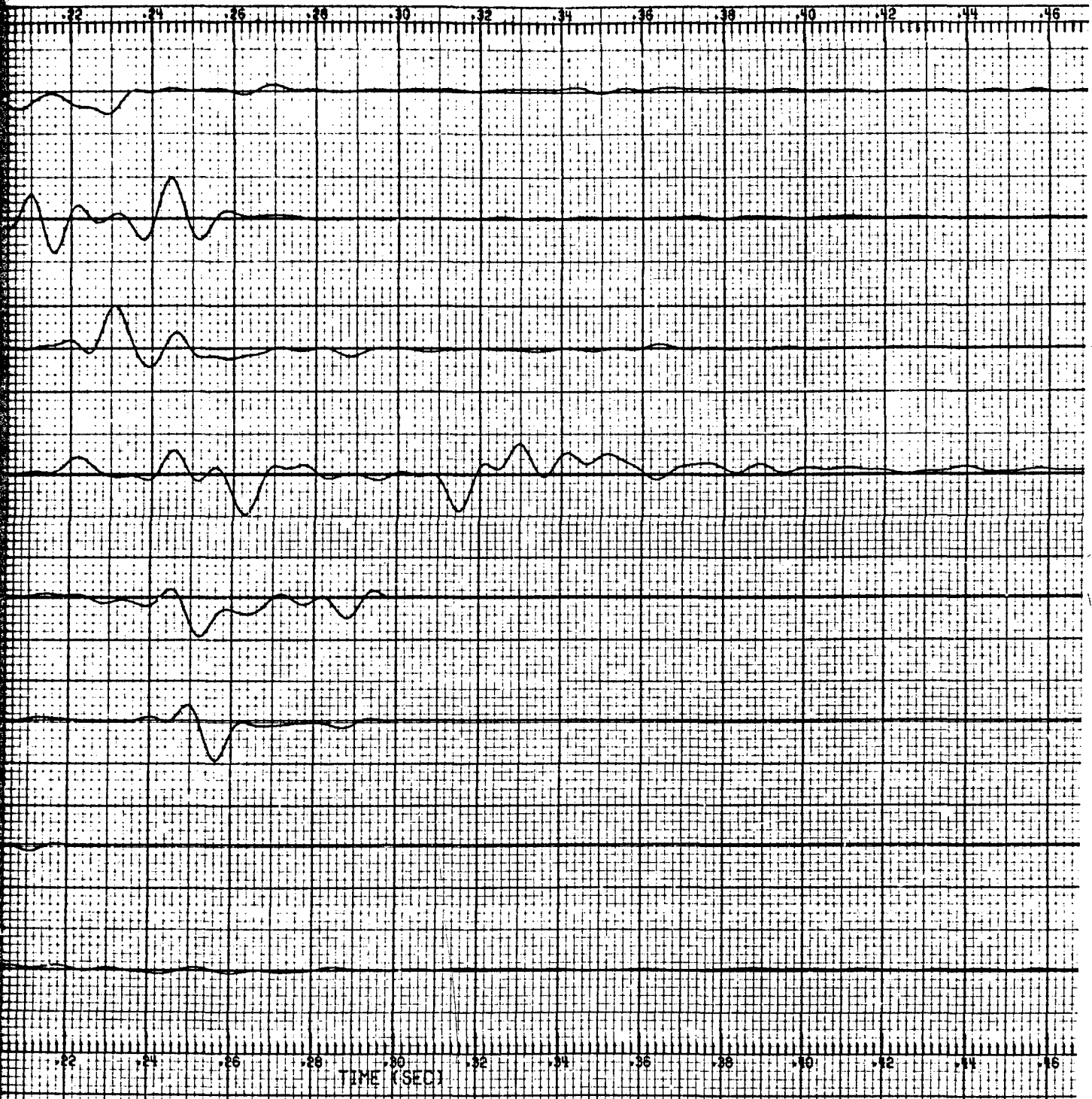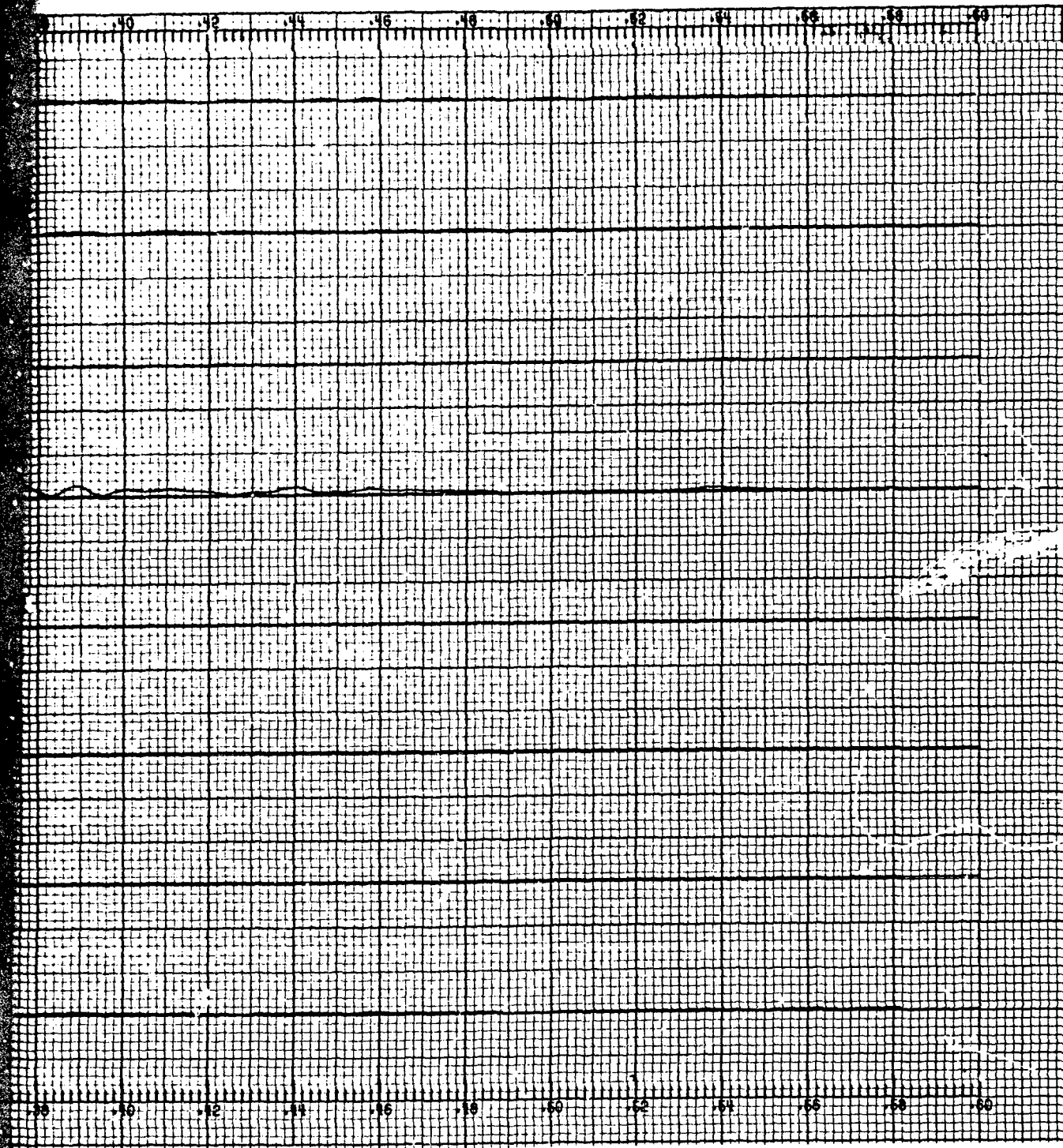
3
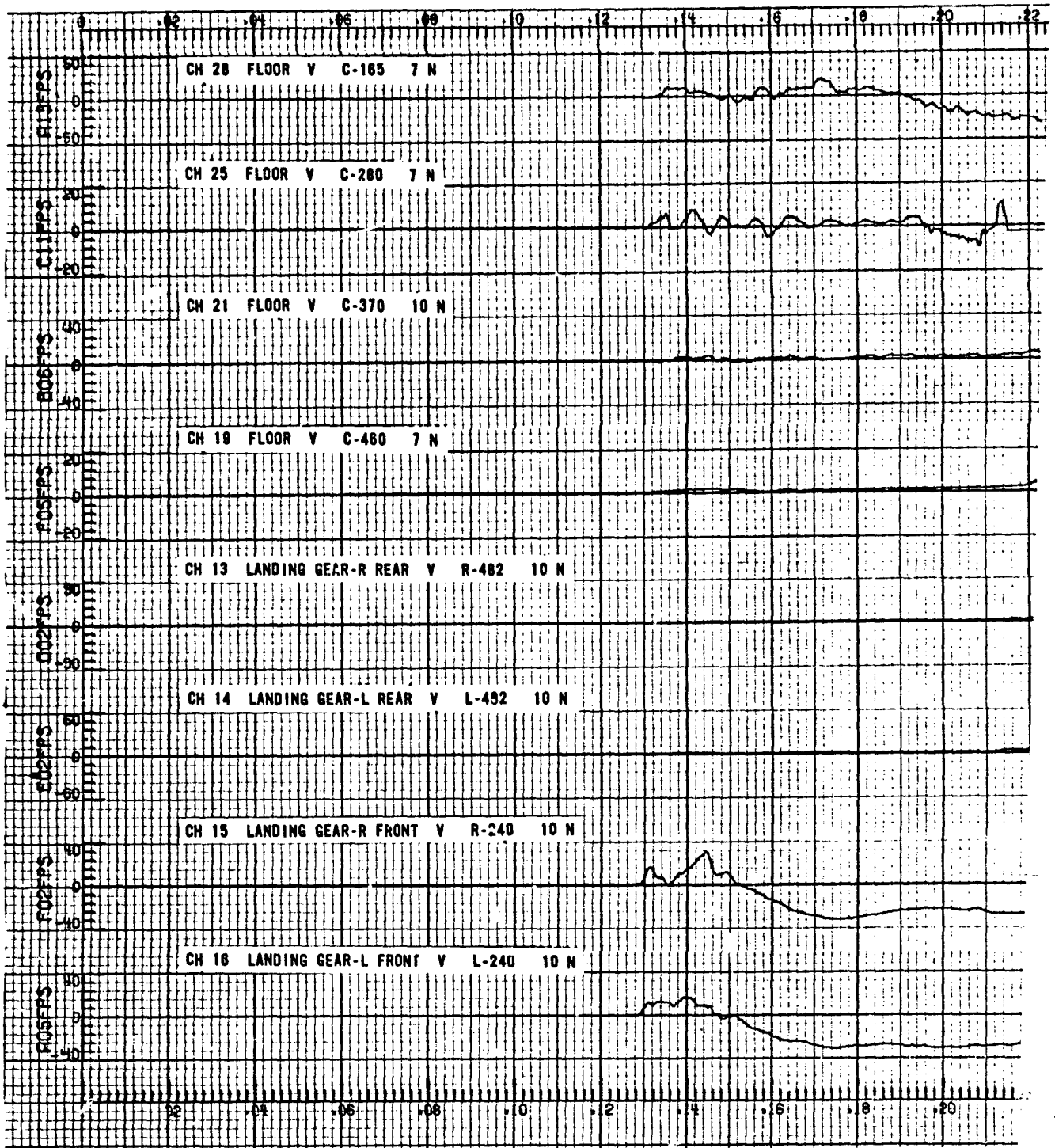
Figure 23. Cabin floor and landing gear attachment vertical decelerations (velocity integration).

45

TIME (SEC)
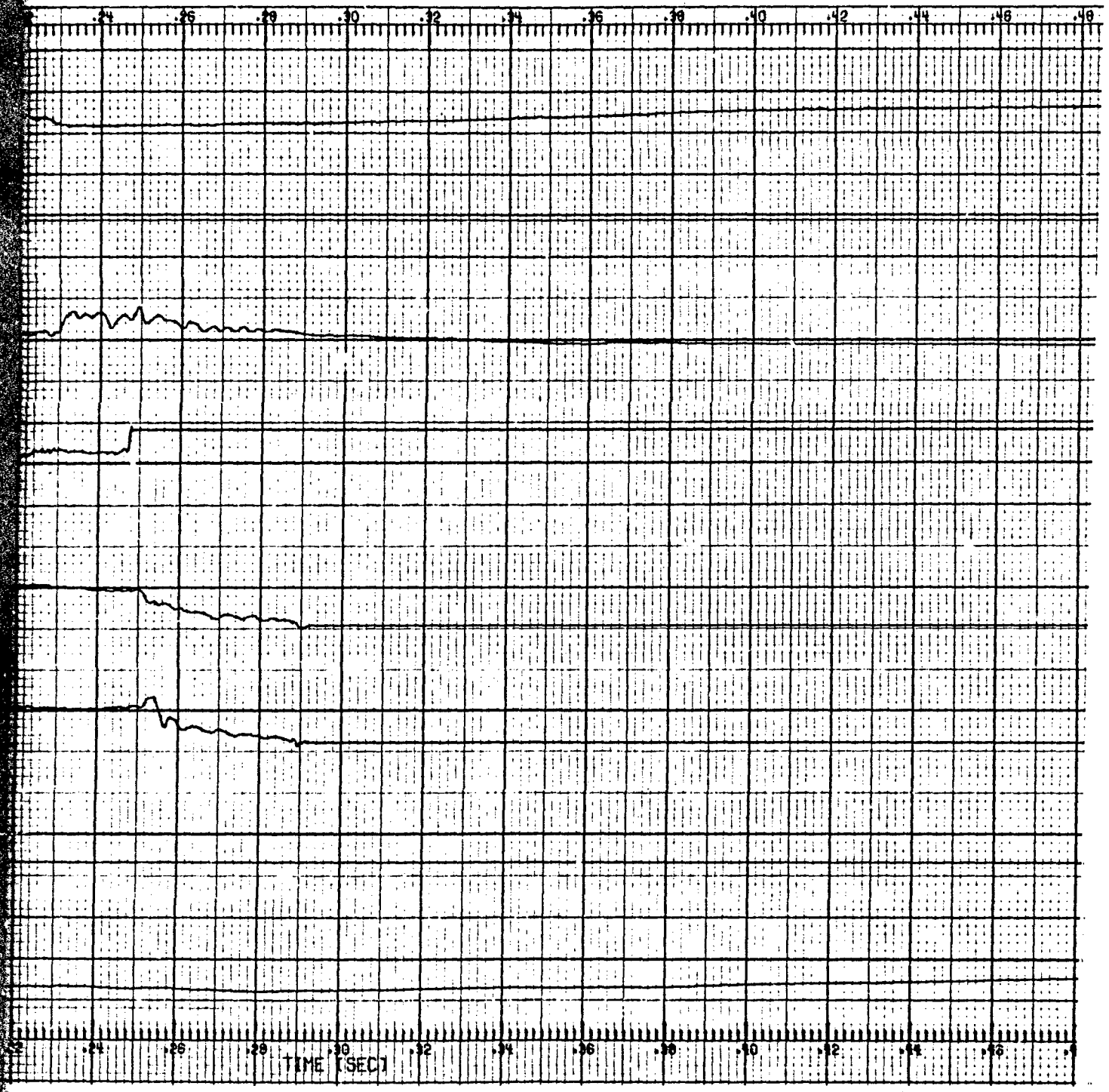
2
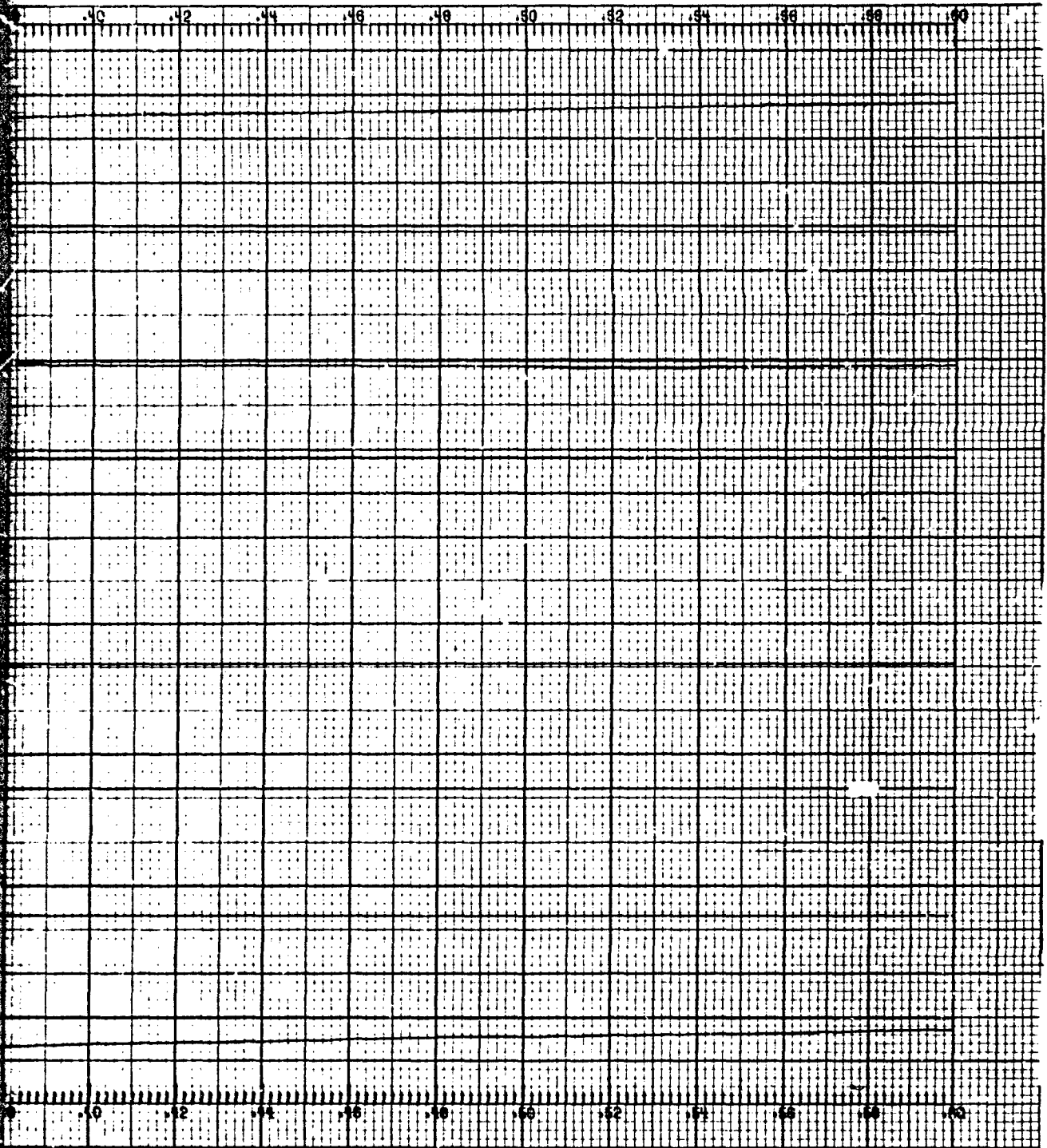
3
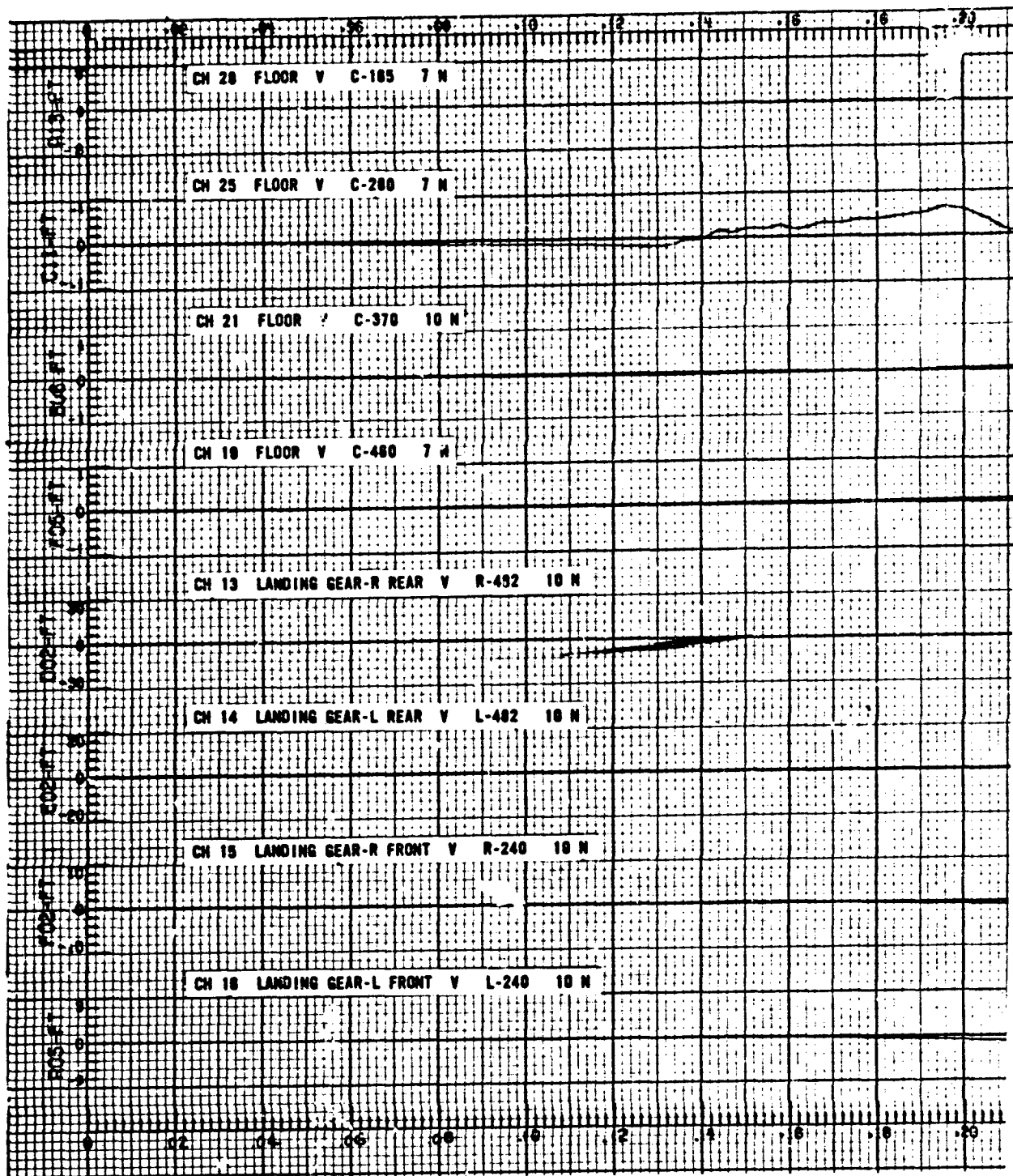
Figure 24. Cabin floor and landing gear attachment vertical decelerations
(displacement integration).

47

TIME (SEC)
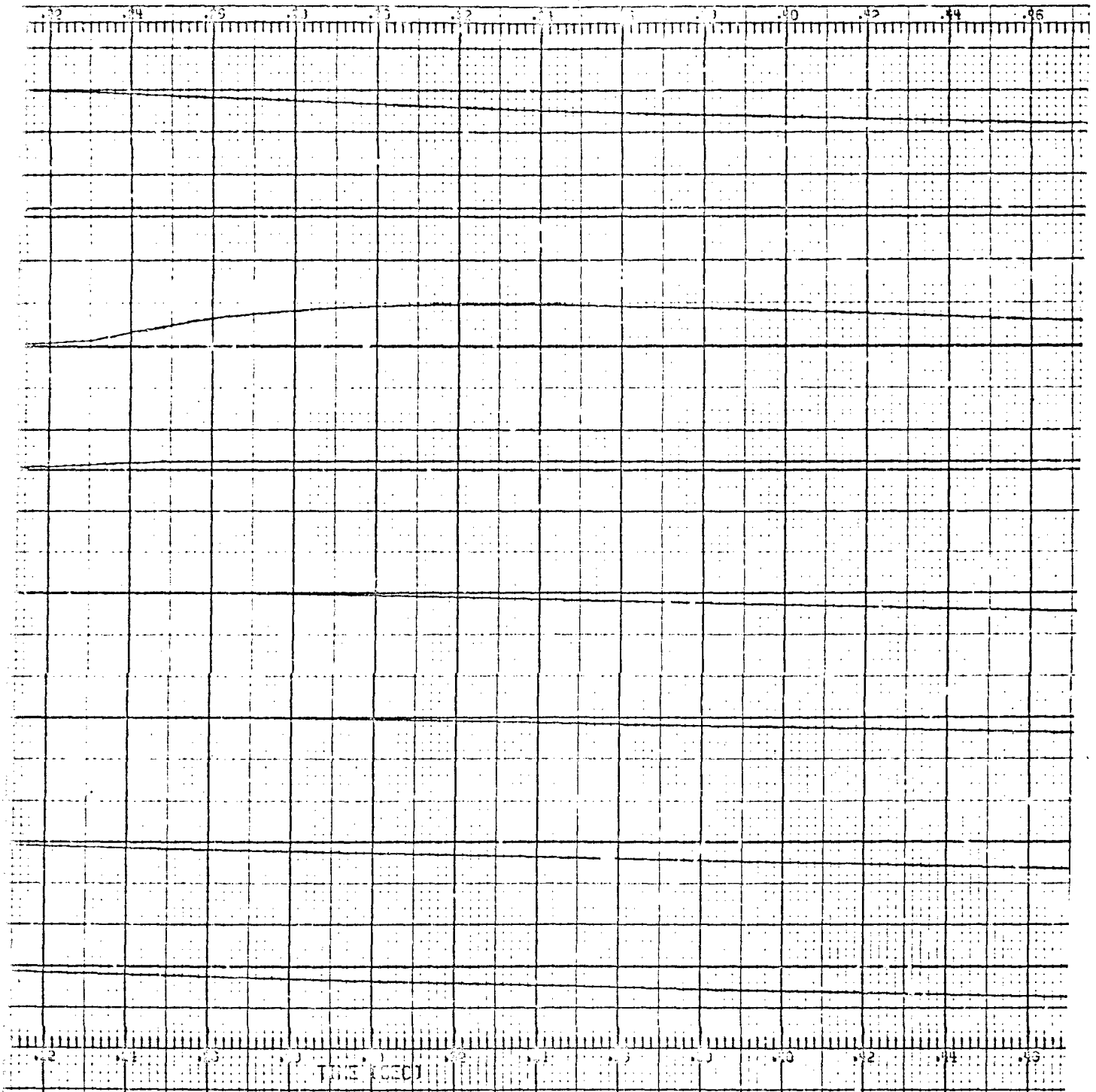
2
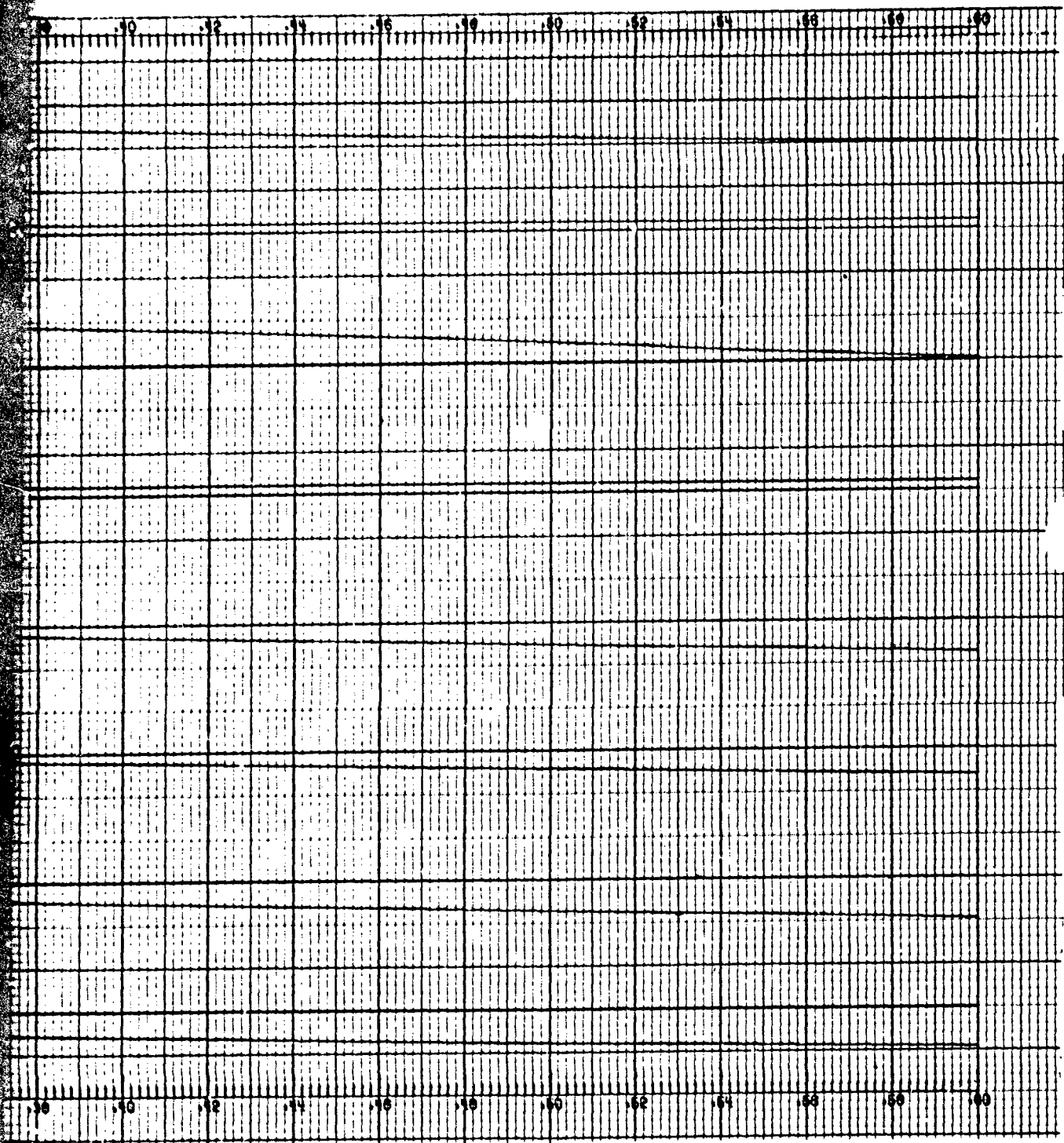
3
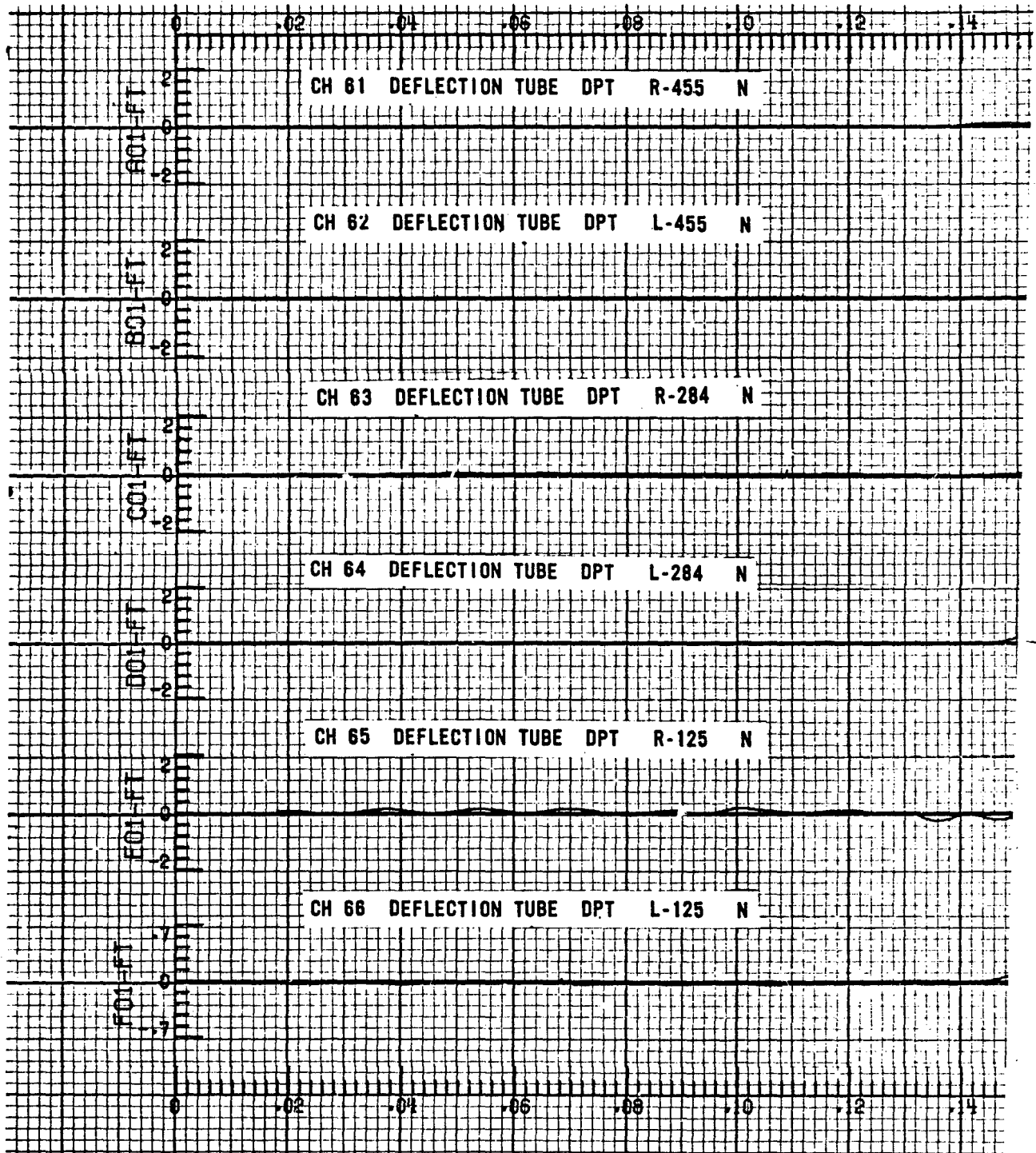
Figure 25. Cabin height reduction.

49

TIME (SEC)

2

TIME (SEC)
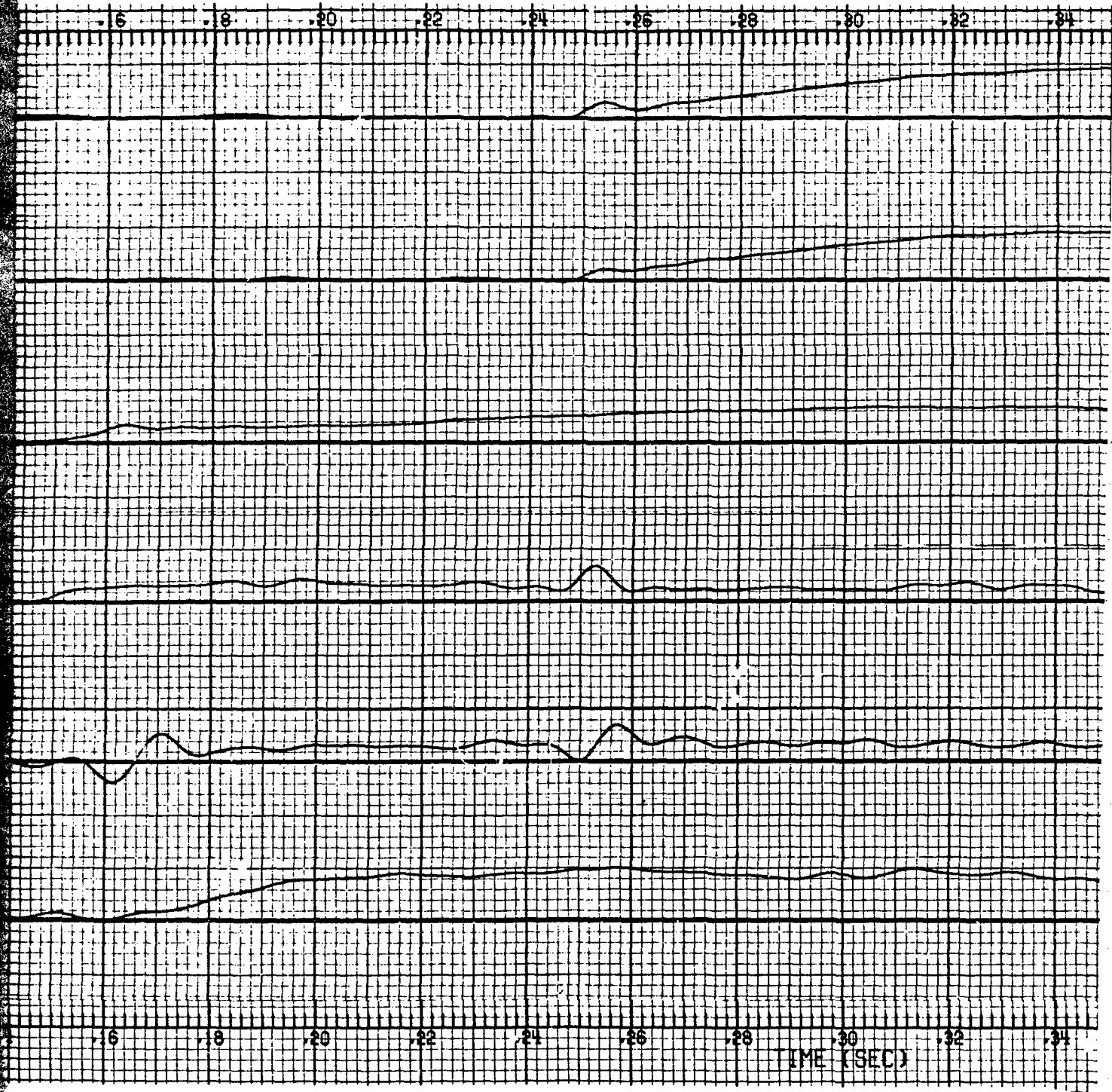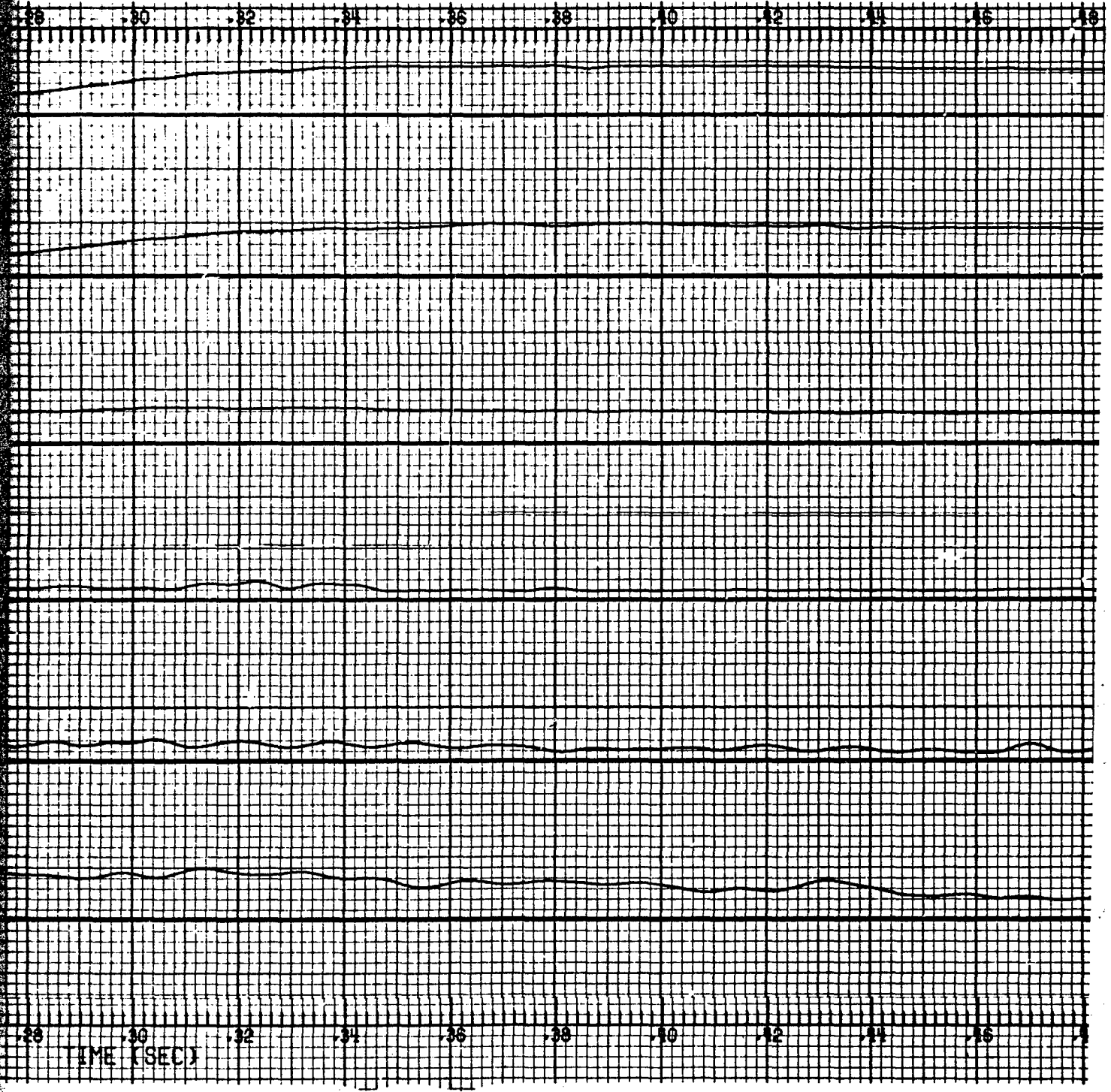
3
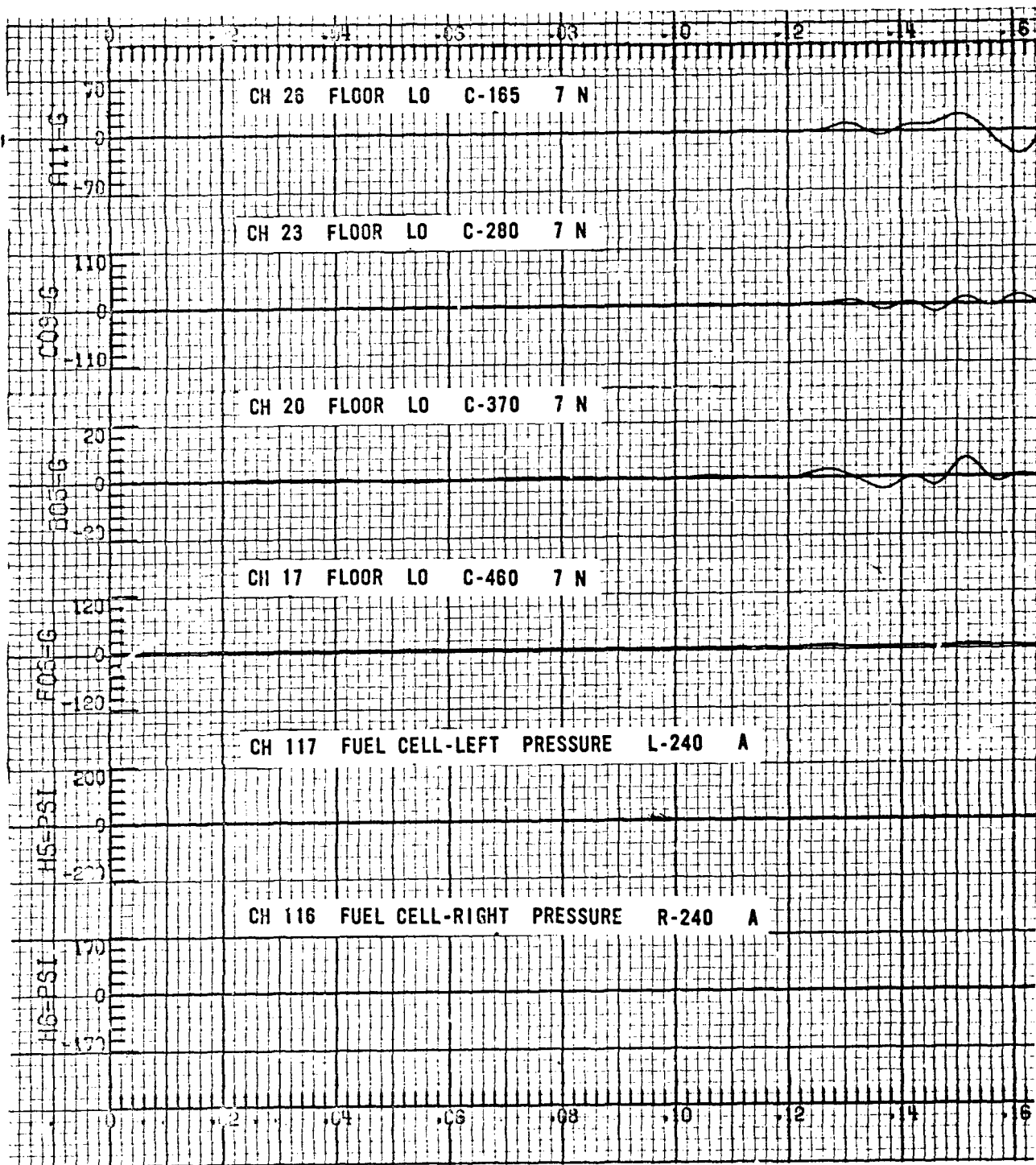
Figure 26. Cabin floor longitudinal decelerations and fuel cell pressure.

TIME (SEC)

2

TIME (SEC)

.30   .32   .34   .36   .38   .40   .42   .44   .46
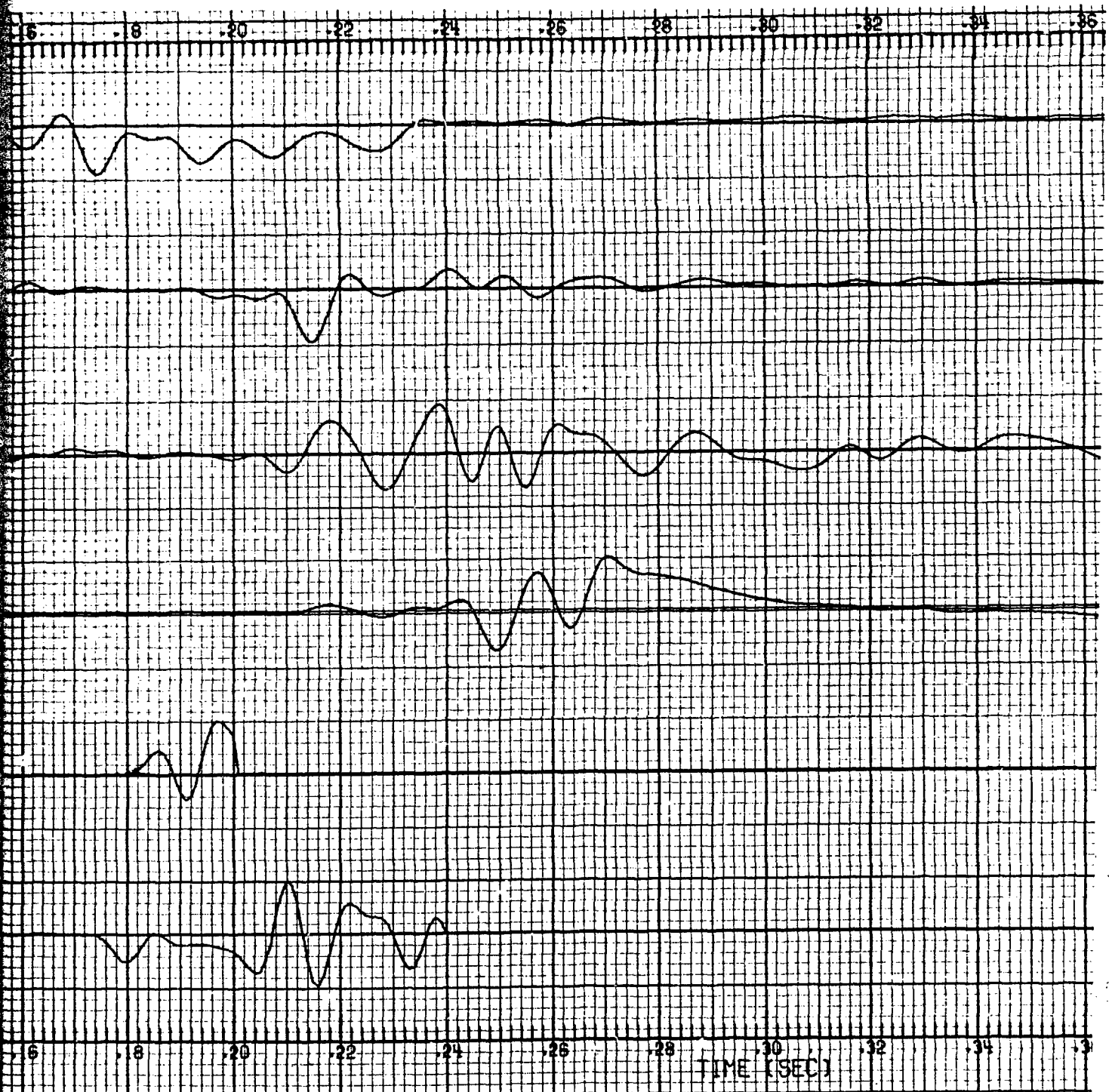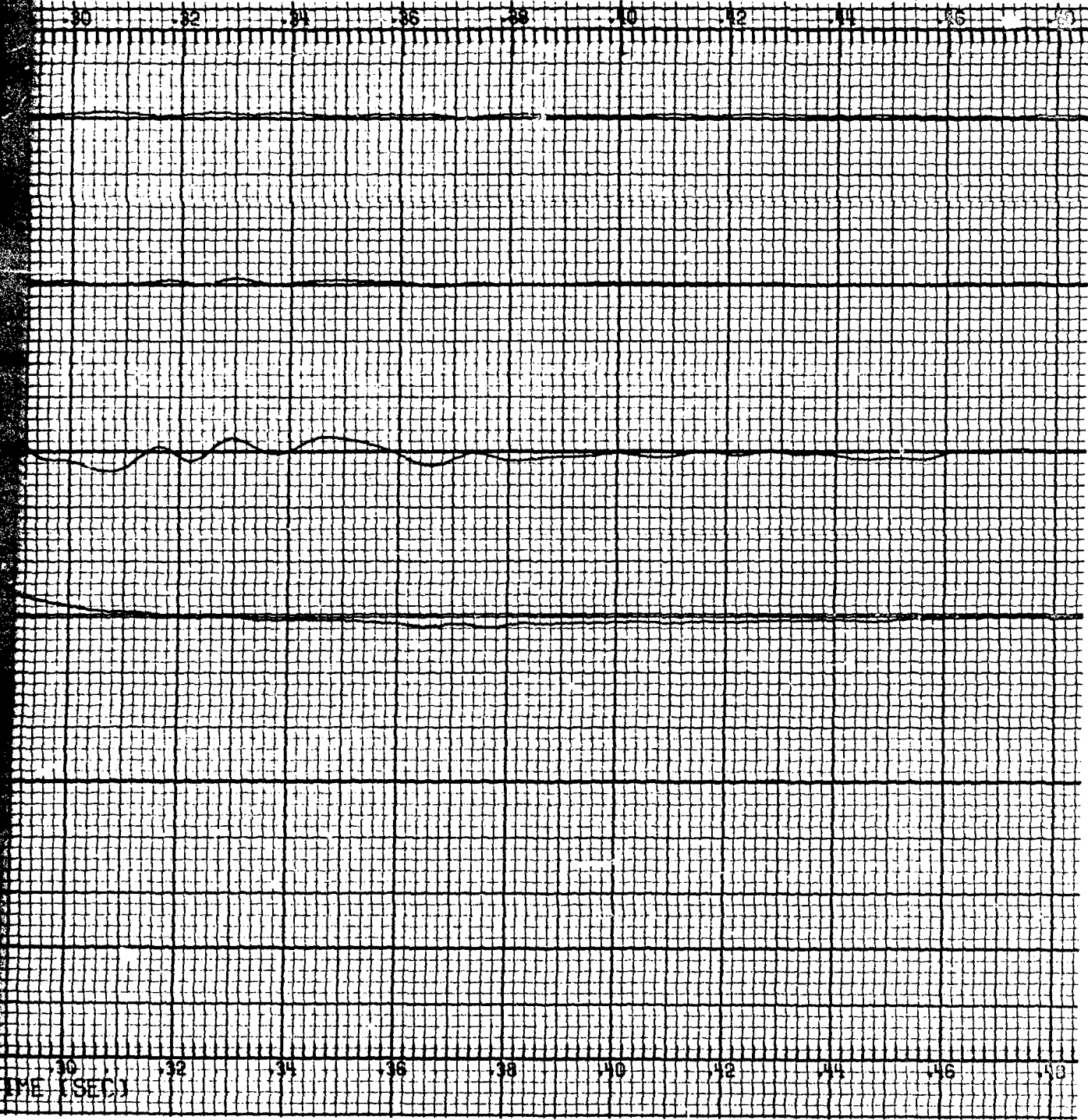
3.
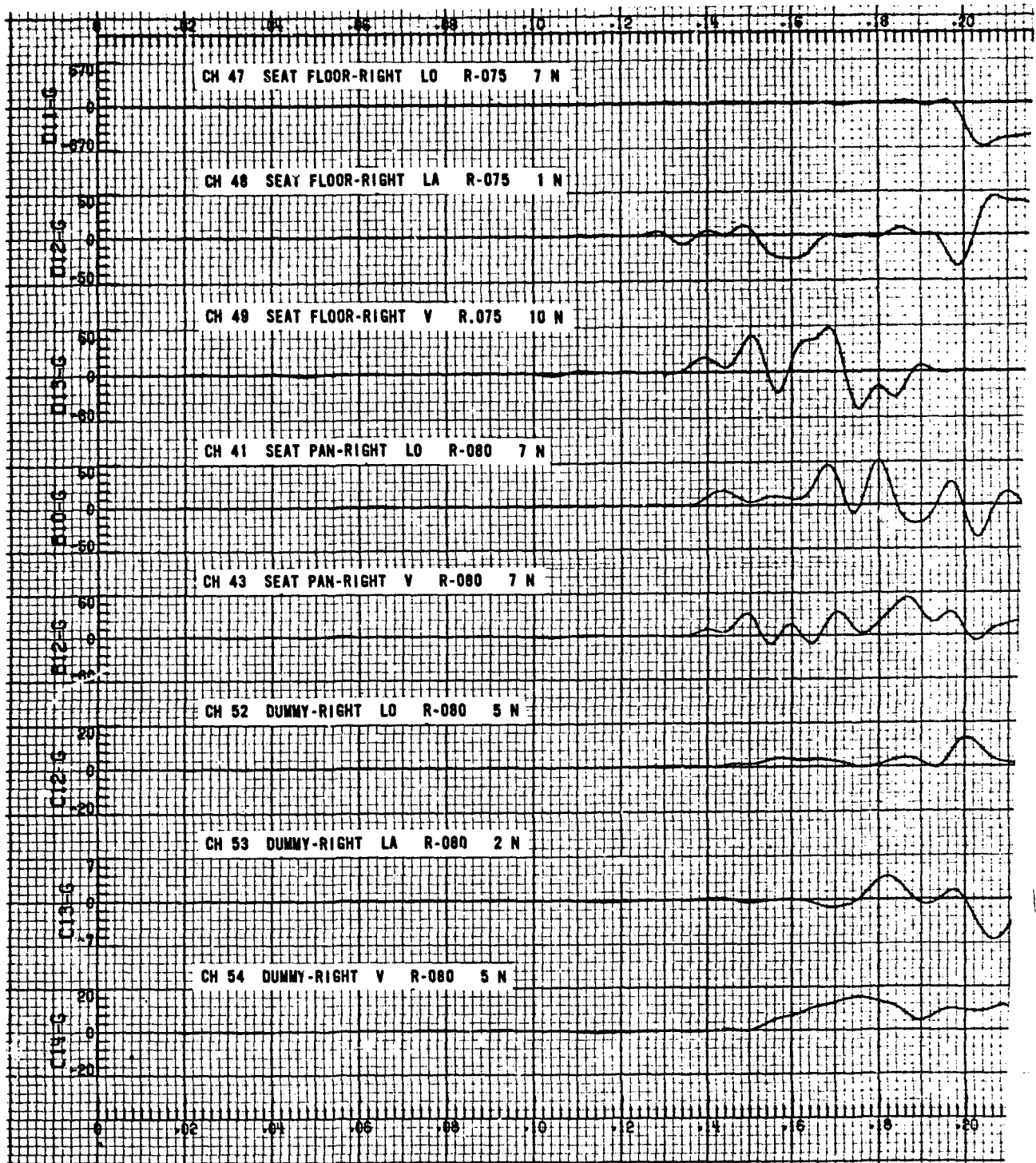
Figure 27. Pilot station decelerations.

53
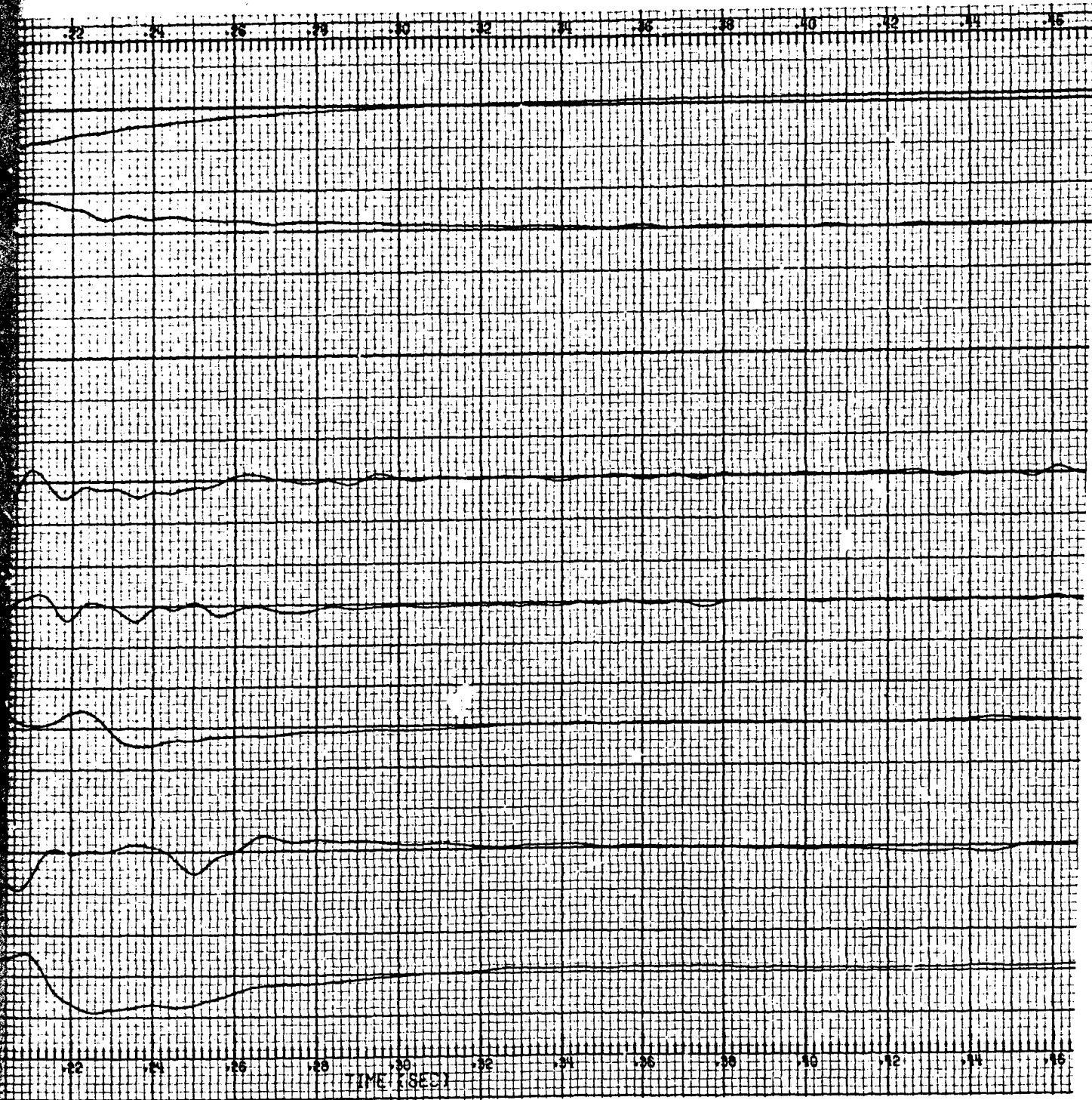
2
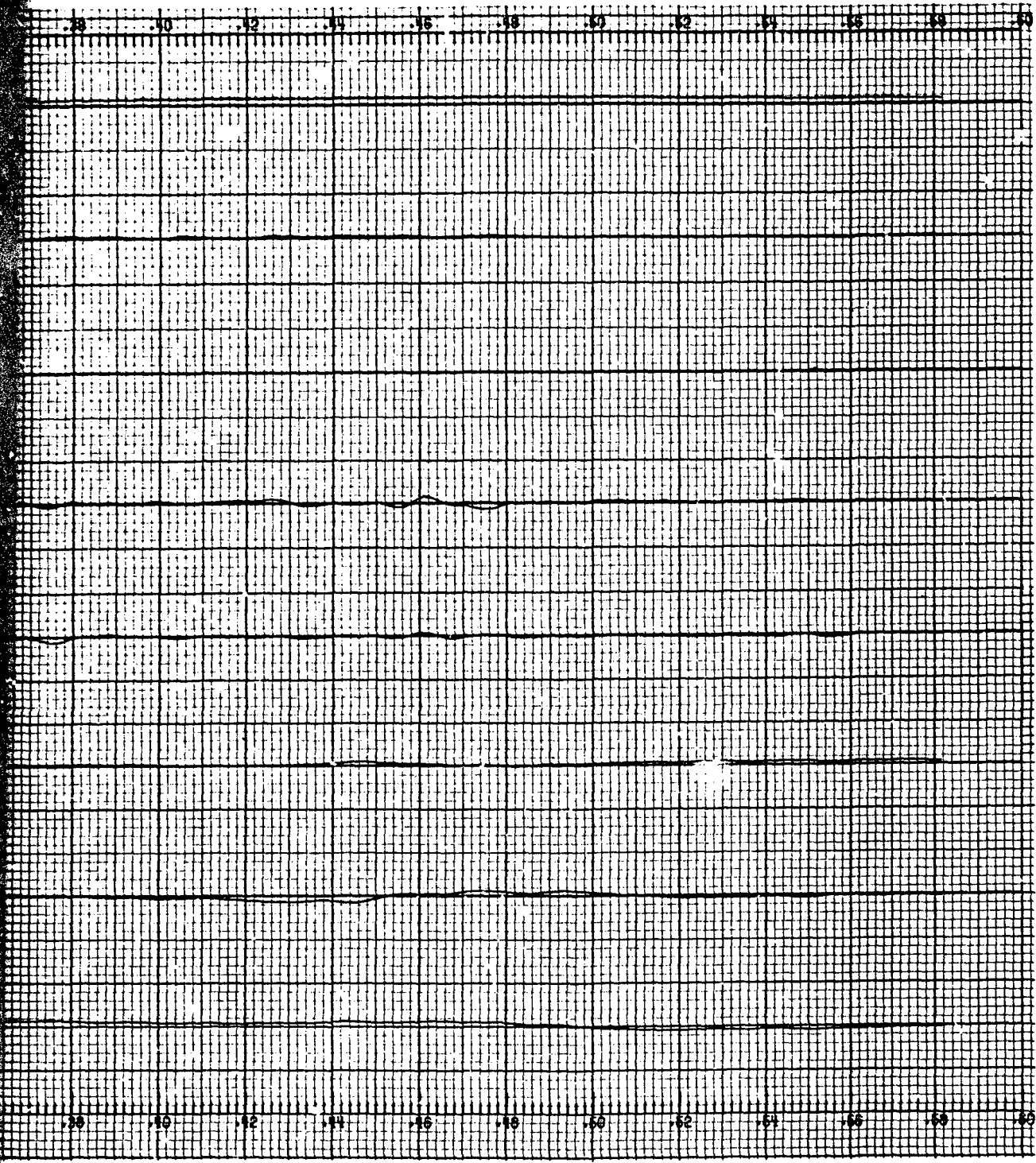
3
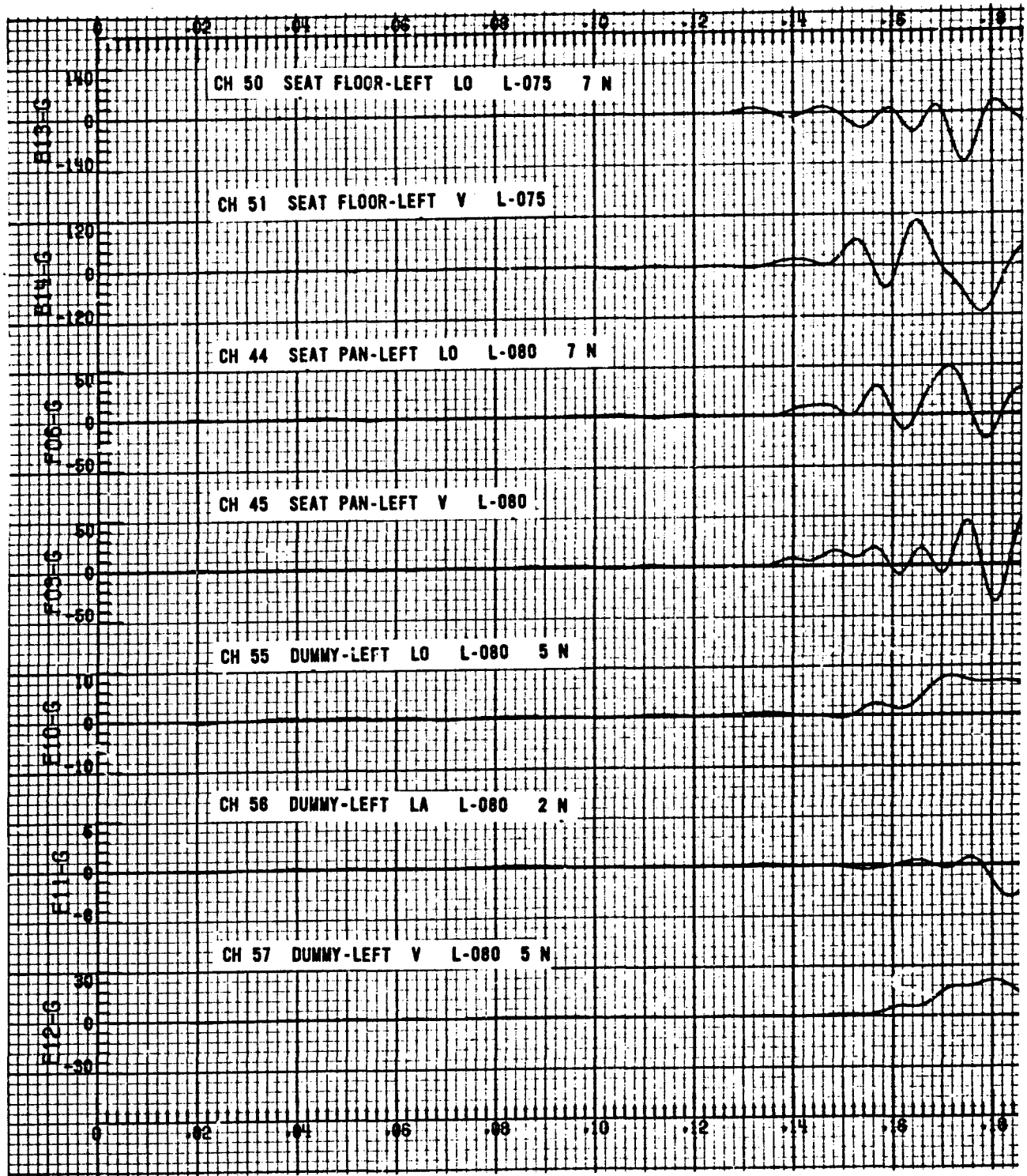
Figure 28. Copilot station decelerations.
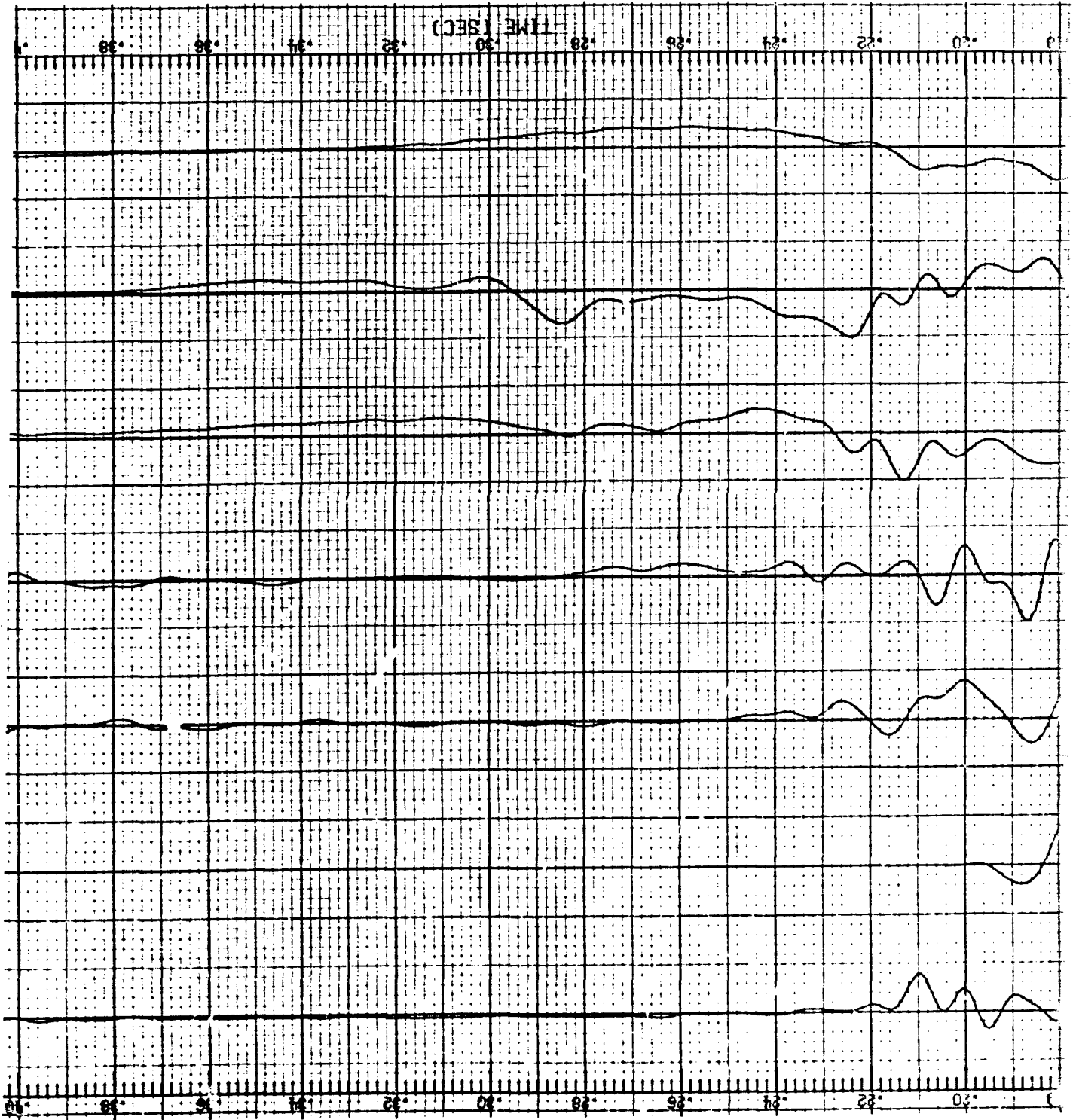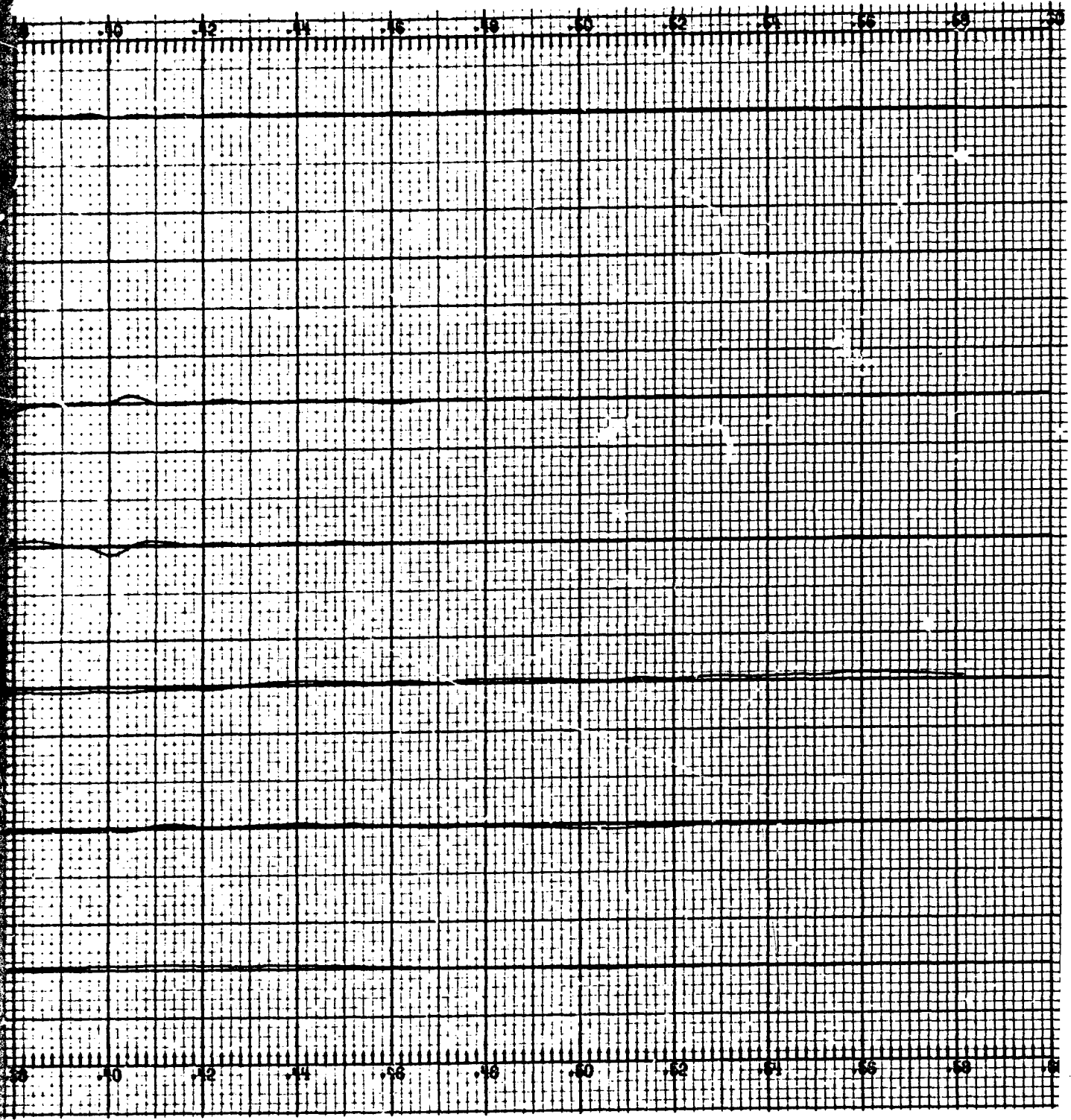
3

CARGO RESTRAINT

The load attenuator or energy-absorber concept looks promising as a means by which internal helicopter cargo loads may be restrained with a minimum of individual tie-down devices. By reducing the number of required tie-down devices over that normally required, the downtime necessary for a helicopter to be loaded or unloaded under combat conditions may be significantly reduced, thus reducing the exposure time of the helicopter and crew to enemy ground fire. The load attenuators, fabricated especially for this test, were demonstrated under actual crash conditions for the first time during this test.

Purpose

The purpose of the cargo restraint experiment was to demonstrate the effectiveness and the performance of the wire-platten-type load attenuating device when it is installed in series with conventional cargo restraints in an actual crash environment.

Description

Five individual experiments were conducted aboard the CH-47 test helicopter: two M-100 ¼-ton trailers with simulated cargo, each with a nominal weight of 1,315 pounds; two pallet loads of simulated 155mm howitzer projectiles weighing approximately 800 pounds each; and a cargo package for baseline crash data acquisition, which was rigidly mounted to the floor at the aircraft longitudinal CG.

All items of cargo were positioned and restrained according to TM 55-450-18, CH-47 Internal and External Loads Manual, by experienced personnel from the Fort Eustis Transportation School using the standard MB-1, 10,000-pound-capacity chains and the CGU-1/B 5,000-pound-capacity nylon straps. The final configuration of the cargo and restraints is shown in Figure 6.

The baseline crash data package consisted of a free mass attached to two load cells that sensed forces in the lateral and longitudinal planes. In addition, accelerations in all three planes were measured by accelerometers. The package that was located on the starboard side of the cargo compartment is shown in Figure 6.

In the forward section of the cargo compartment, one trailer was restrained in the conventional manner with six MB-1, 10,000-pound-capacity chain restraint devices, and one pallet load was restrained with four CGU 5,000-pound-capacity nylon strap devices. The remaining trailer and pallet loads were restrained in a similar manner in the aft section of the cargo compartment with the load attenuators connected in series with the normal restraints (Figure 29).

The load attenuators used in this test were the wire bending/extrusion type (Figure 30), whose dynamic characteristics can be controlled during the manufacturing process by varying the diameter and metallurgical properties of the wire and the distance between the extrusion rollers. The energy-absorbing devices that were used in series with the cargo restraints were designed with an initial extension force (breakout force) of 4,940 pounds, which is just under the maximum strength of the aircraft floor fittings.
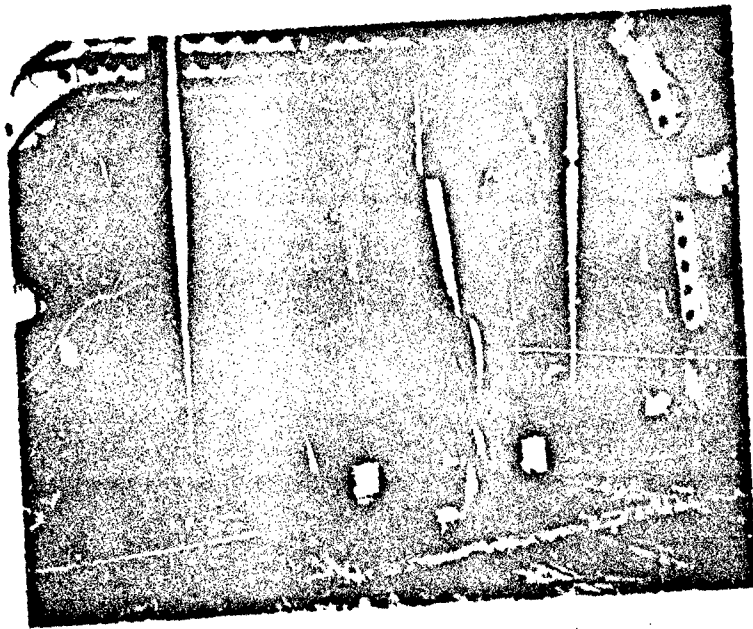
Figure 29. Rear pallet load looking forward, after impact.
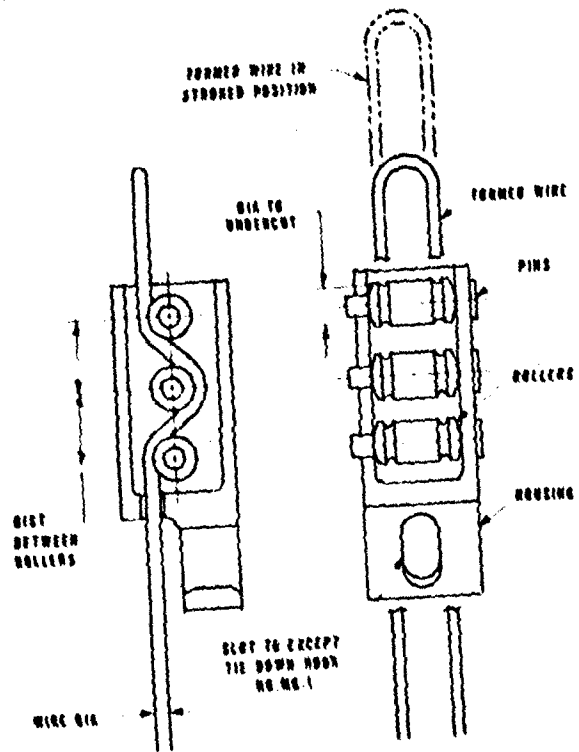
Figure 30. Cargo load attenuator.

Load cells were placed in series with the forward restraints on all cargo. Triaxial accelerometers were mounted on each load and on the floor beneath each load. Rapid sequence cameras were mounted at various points in the cargo compartment and focused on loads, restraints, and floor fittings to record the impact dynamics.

Results

After the CH-47 came to rest, all items of cargo were generally in their original positions, although some of the restraints had become detached by the end of the impact sequence. There was also some evidence that the forward trailer impacted the bulkhead at the head of the cargo compartment (Figure 36).

Of the four items of cargo in the helicopter, the aft trailer equipped with load attenuators in series witn the restraints was the only item to sustain major damage.

The aft trailer experienced high vertical G loads as evidenced by the 130 G peak measured on the floor beneath the trailer. These high vertical forces compressed the trailer springs, causing the shackles to penetrate the floor and to severely distort the axle, the wheel rims, and the chassis (Figures 31 and 32). The trailer rebounded from this position and induced loads of sufficient magnitude simultaneously in all restraints to stroke the attenuators on both the forward and lateral restraints and to fail the two aft restraint floor fittings. The reason that the attenuators in series with the aft restraints did not stroke and prevent failure of the floor fittings is not clearly understood. The nonstandard attachment of the starboard floor fitting to the base of the crash data package may have contributed to its failure.

The port floor fitting (ST-340) was subjected to tensile loads severe enough to cause its mounting bolts to tear aftward through the floor for a distance of 7/8 inch without stroking the load attenuator (Figures 33 and 34). In this case the integrity of the load attenuator was questioned. Unfortunately, load cells were not available for direct load monitoring of the aft restraints. The forward trailer also experienced a bent axle from vertical G loads of 80 G peak measured on the floor beneath the trailer, although it was still serviceable after impact, as was most of the cargo. However, the crushed and distorted fuselage of the helicopter prevented the immediate removal of the cargo without special equipment.

The right-hand forward trailer restraint, terminating at ST-240, sustained a nearly constant tensile load of 5,255 pounds for a period of .032 second before failure of the floor fitting due to buckling of the floor (Figure 35).
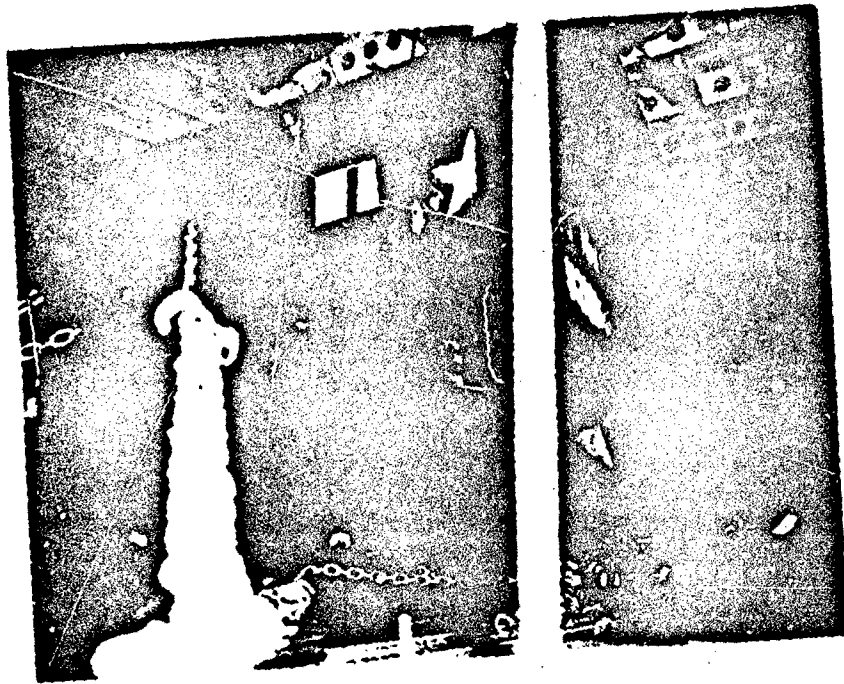
Figure 31. Rear trailer looking forward from starboard side, after impact.
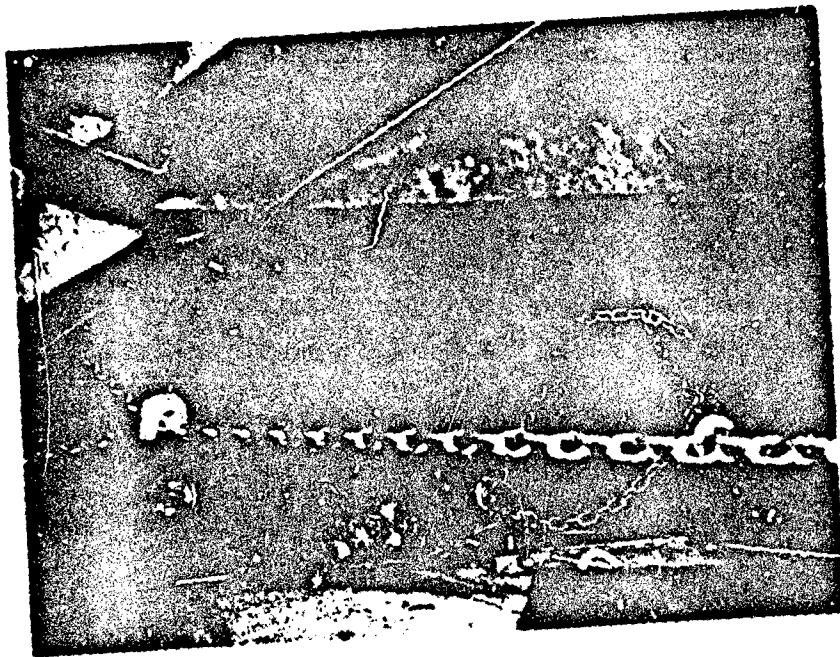
Figure 32. Rear trailer looking forward, after impact.
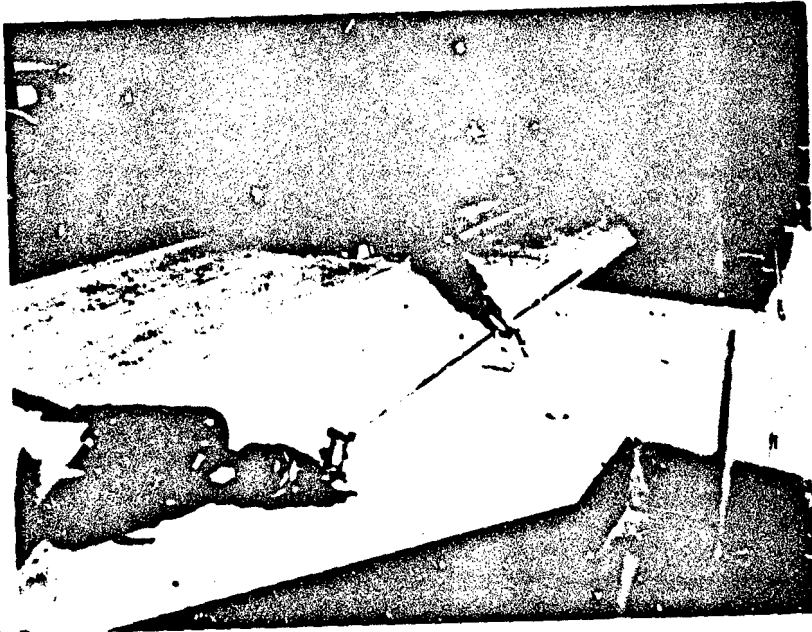
Figure 33. Rear trailer, aft restraints with energy absorbers, before impact (station 340).
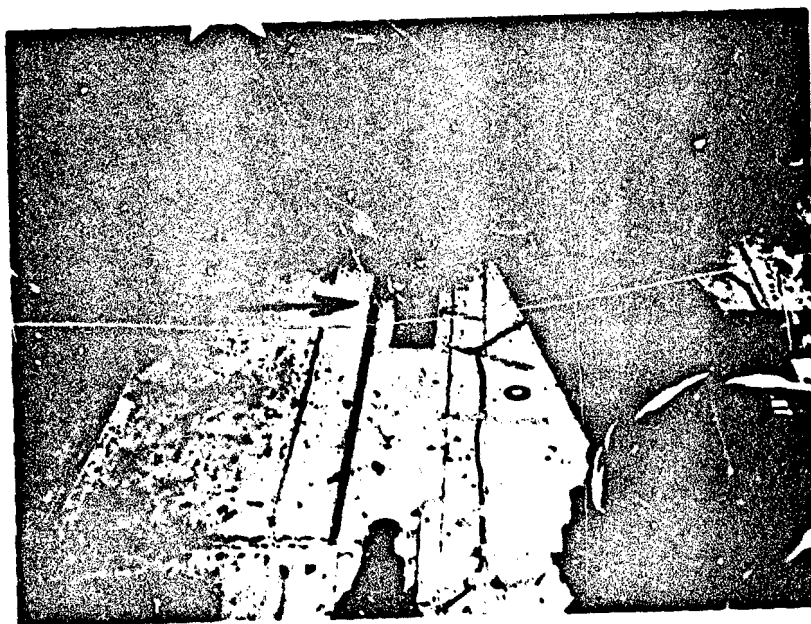
Figure 34. Rear trailer, aft restraints, after impact (station 340).

Figure 35. Forward trailer, forward and lateral restraints, after impact (station 240).
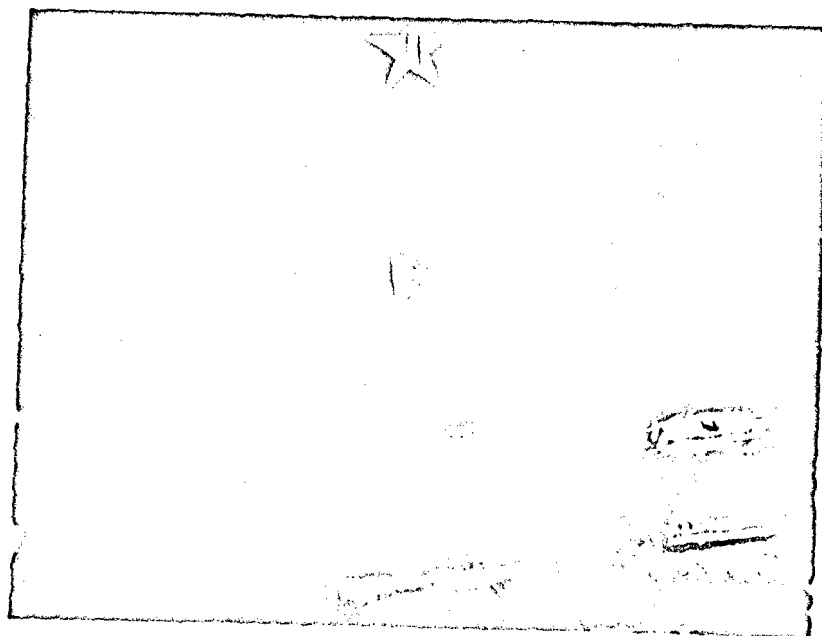
Figure 36. Forward trailer just aft of bulkhead.

Post-Crash Laboratory Test

A laboratory test was conducted at ATL in an attempt to learn why the floor fittings at ST-340 failed without extension of the load attenuators. The objective of the laboratory test was to determine the exact load at which the two unextended attenuators, which were attached to the floor fittings at ST-340, would break out and begin to stroke. With this information, it could be assumed that the tie-down fittings were subjected to loads just short of this amount. A third unused load attenuator was stroked completely in 141 milliseconds to simulate a crash pulse.

Both of the questionable attenuators were stroked at a rate of 4 inches per minute, duplicating the manufacturer's performance qualification tests.

Under test conditions, both attenuators achieved peak loads of 5,200 and 5,300 pounds (breakout force) and stroked at level loads of 4,800 and 5,000 pounds, which was above their design performance of 4,940 pounds peak load and 4,600 pounds stroking load (Figure 37).

The results of these tests suggest that both floor fittings at ST-340 could have been subjected to loads up to approximately 4,600 pounds, since some indication of attenuator platten wire deformation would have been evident at loads above this level. CH-47 helicopter floor fittings have failed under static test loads of 5,050 to 5,150 pounds in the past; however, the age, corrosion, and general deterioration of this particular CH-47 fuselage probably contributed to early failure of these fittings.

The third test produced surprisingly similar results with a breakout force of 4,818 pounds, only 122 pounds less than the design value, which reinforces the validity of the manufacturer's low rate method of testing.

Conclusions

In T-40, loads were developed in the cargo restraints which exceeded the ultimate strength of some of the floor tie-down fittings in the test helicopter. Energy-absorbing devices were effective in attenuating peak loads in cargo restraints during the helicopter crash, as evidenced by the extension of both the forward and the lateral load attenuators on the aft trailer.

Noting the two failed floor fittings (ST-340), the results of this test suggest that the designed attenuator breakout force should be substantially lower to allow more energy dissipation and earlier stroking to avoid any chance of excessive peak load buildup. The load attenuators used in this test were designed with a breakout force of 4,940 pounds, which now appears to be too high for maximum system energy dissipation in this case, and perhaps too close to the ultimate strength of the floor fittings in the CH-47 helicopter.

In the final design of a load attenuator of this type, accuracies greater than ±400 pounds would be difficult and expensive to achieve, considering practical manufacturing tolerances and the variances of metallurgical characteristics of available materials.

63

CURVE			RATE Oʏ APPL. OF LOAD
(1) ATTENUATOR	ST-340	RH	4''/MINUTE
(2) ATTENUATOR	ST-340	LH	4''/MINUTE
(3) ATTENUATOR			8''/141 SEC.
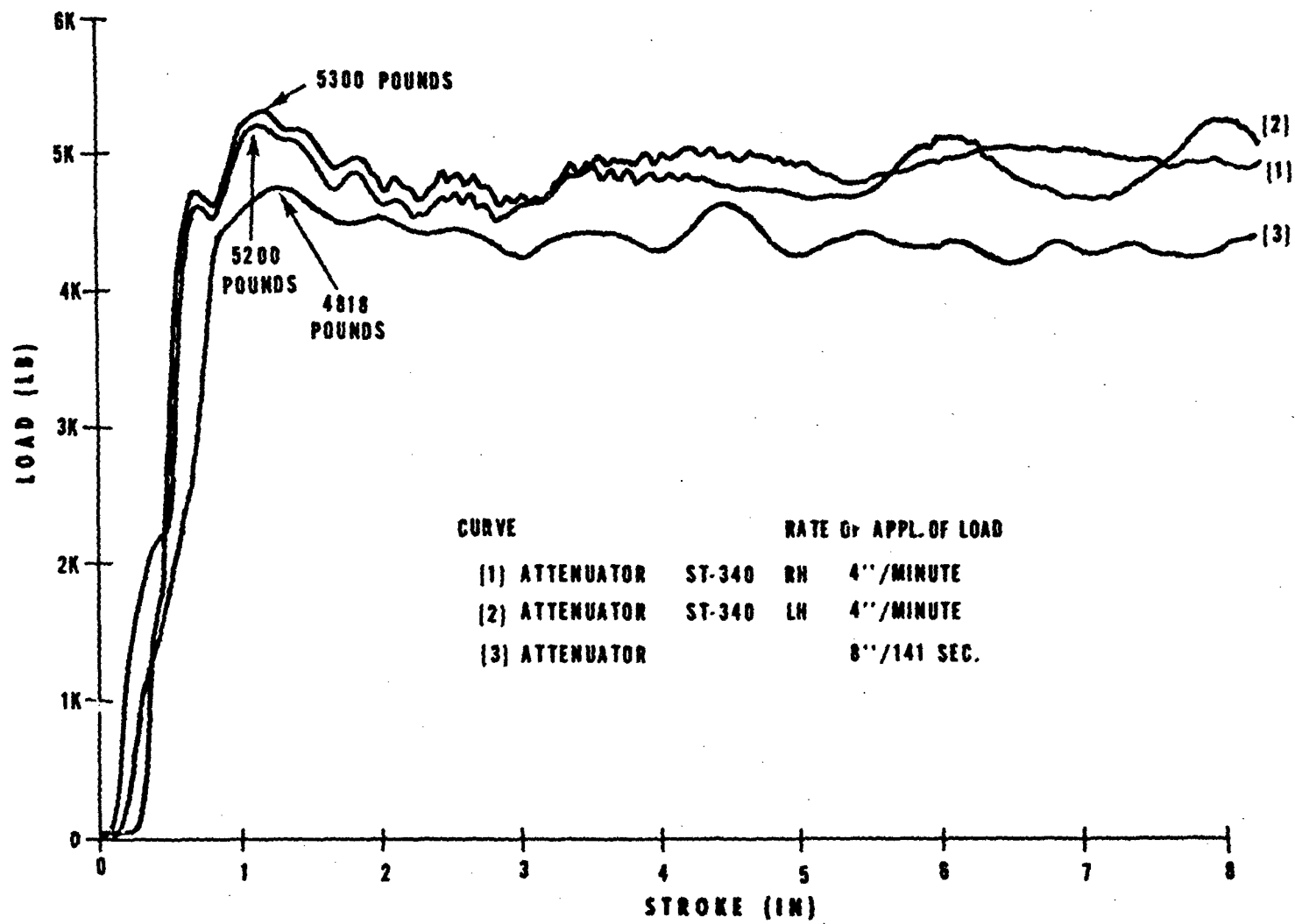
Figure 37. Post-crash load attenuator laboratory tests.

In selecting attenuators for cargo restraint, a much greater margin should be allowed between the ultimate strength of critical components and the limit load value than was allowed in this cargo restraint experiment.

The load attenuators used in this experiment were designed to fit in series with the MB-1 chain, or the CGU strap restraint devices; however, several operational problems were experienced that will require future hardware modifications. One of the hooks on the CGU strap restraints did not fit the attenuator body and a shackle was required. The long sections of wire extending out from the attenuator body interfered with operation of the MB-1 latch and the tensioning device and should be repositioned in the final operational hardware (Figure 38).

The results of this experiment have provided some valuable design data for future cargo restraint systems, although the test impact conditions were less than ideal for an internal cargo restraint experiment. Impact conditions having a higher longitudinal velocity component would produce a more challenging environment for evaluating cargo restraint components.

The use of load attenuators in series with conventional cargo restraints improves the survivability aspects of a helicopter crash and reduces the number of individual restraints required. As more emphasis is being placed on transporting cargo internally, maximization of the total load on each flight is essential to increase productivity of the helicopter.

The plan view of the test CH-47 cargo compartment (Figure 6) illustrates how the placement of conventional cargo restraints, radiating outward from each load to the floor tie-down fittings to achieve the most advantageous restraint angle, limits the cubic capacity of the cargo compartment.

Development of an energy-absorbing system to facilitate quick restraint of large quantities of internal cargo in one operation would promote optimum utilization of the total cargo space.
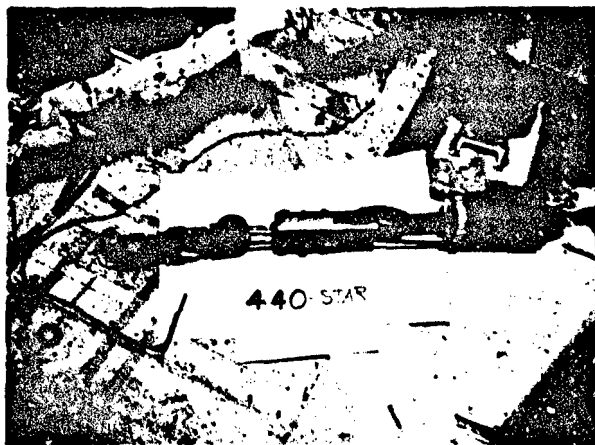
Figure 38. Partially extended energy attenuator showing interference of platten wire with tension adjustment wheel on MB-1 chain restraint.

65

AIRCREW INFLATABLE RESTRAINT

Purpose

The purposes of this experiment were: to demonstrate that an aircrew inflatable restraint system is capable of functioning under "real world" conditions; to provide comparative data between an inflatable and a conventional restraint under identical conditions; and to obtain the "crash signature," i.e., the magnitude and duration of the crash pulse, to aid in further development of the crash sensor.

Background

The Naval Air Development Center is developing an inflatable restraint system for helicopter crewmen, which provides greater crash protection to the wearer than the standard lap belt/shoulder harness system now used. The inflatable restraint provides automatic pretensioning, which removes any slack in the system and forces the occupant back in his seat, thereby reducing dynamic overshoot. Strap loading on the wearer is reduced when the inflated restraint is compressed during crash loading. The concentration of the strap loads on the body is reduced because of the increased bearing surface provided when the restraint is inflated. In addition, an inflated appendage of the restraint that fits under the wearer's chin will reduce the head motion and the whiplash induced trauma which occurs during a crash. Submarining by the seat occupant is prevented by the use of a crotch strap.

The inflatable restraint system was designed using the air bag concept of enveloping the seated occupant with a gas-filled inflatable device to prevent fatalities and to reduce occupant injuries during a potentially survivable crash. Unlike the automotive air bag, which is a passive device remotely located from the occupant, the inflatable restraint is worn in a fashion similar to the present-day crewman harness. The inflatable restraint has been configured essentially the same as the harness currently being used in helicopters and other nonejection-seat aircraft. These harnesses usually consist of 1-3/4-inch-wide shoulder straps and 3-inch-wide lap belt straps joined at a central fitting. Both shoulder straps are joined directly behind the occupant's neck and terminate in an inertia reel mounted onto the seat back. The ends of the lap belt are anchored to the lower rear portion of the seat bucket.

The restraint system (Figure 39) is comprised of three m ~r subsystems: (1) the inflatable bladder/restraint, (2) the inflator, and (3) the crash sensor. The system has been designed so that in its stowed position it appears somewhat like the conventional harness. When unfurled, the bladder/restraint is revealed as shown in Figure 40.

The inflator is a cylindrical pyrotechnic gas-generated inflator manufactured by the Thiokol Chemical Corporation for this system (Figure 41). It is located within the bladder.
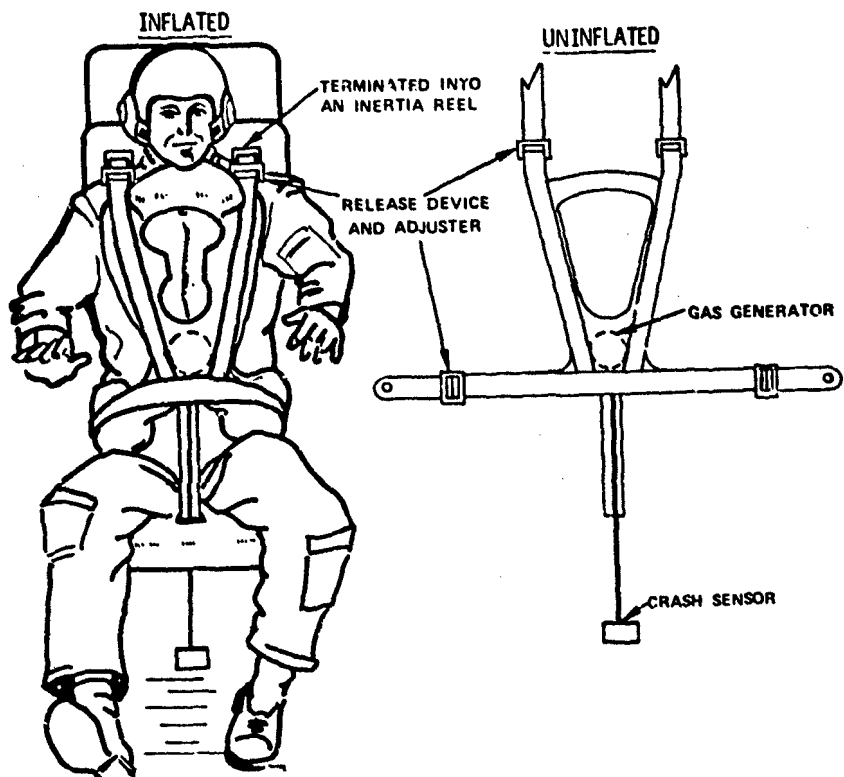
Figure 39.   The inflatable restraint system.
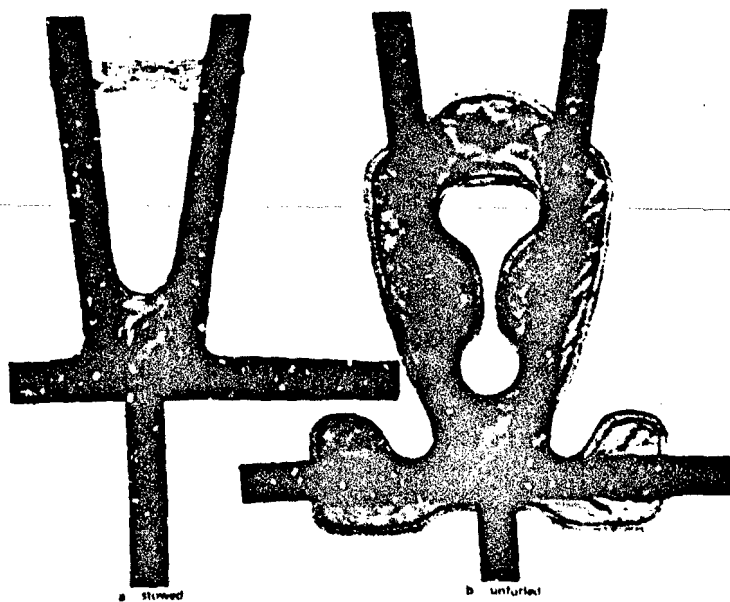
Figure 40.   Comparison of inflatable restraint in stowed position and unfurled.
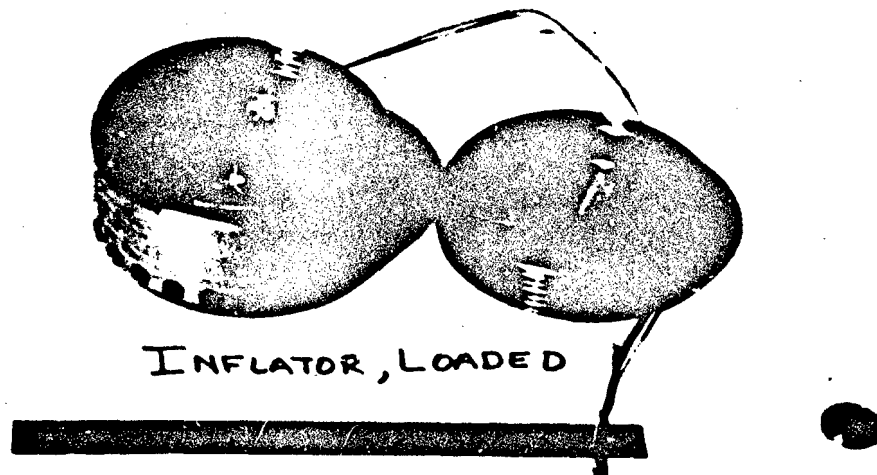
Figure 41. Thiokol Chemical Corporation's pyrotechnic inflator.

A nontoxic gas, mainly composed of nitrogen, fills each of the restraint bladders to a pressure of 3 psi in less than 20 msec after initiation. The inflator ignition system is initiated by an electrical pulse from a crash sensor located on the floor of the aicraft. The crash sensor is an acceleration switch selected because of its ability to act as an integrator of acceleration time. The sensor is set to close at an energy level of 5 G for 11 msec. Inflation of the restraint occurs within the initial 30 msec after the sensor closes. As the occupant's body moves into the bladders, the bladders' pressure increases while they are being squeezed by the torso against the outer straps, offering further resistance to the occupant's movement into the restraint. The material, being semipermeable, then allows the gas to escape so that in less than 0.1 second after initiation the pressure has decreased to its original 3 psi, and the bladder continues to deflate with time. Should a secondary impact occur, the uninflated restraint is still positioned around the occupant, offering protection against further decelerative forces.

Description

To obtain the comparative data, two 95th percentile dummies were restrained in the pilot and copilot seats by an inflatable system and a conventional restraint system, respectively. Each dummy was clothed in white thermal underwear and wore a Naval aviator's helmet. No slack was allowed in either restraint. Standard CH-47 seats and cushions were used, and no attempt was made to improve the strength of the seat or its support structure.

Each dummy had a triaxial accelerometer mounted in the chest cavity, and each restraint had force transducers mounted on the webbing to measure loads on the lap belt and shoulder harness. In addition, a pressure transducer was used to measure the internal gas pressure of the inflatable system. The cockpit was photographically covered by two high-speed motion picture cameras equipped with wide angle lenses. The crash sensor was mounted on the floor in the rear cockpit area between the seats. An initiation wire ran from the gas generator located inside the bladder of the restraint through the crash sensor to a battery pack in the cockpit. A triaxial accelerometer was mounted near the crash sensor to record the acceleration levels of the crash.

Results

A review of the motion pictures revealed that the inflatable restraint system functioned properly during the crash. Although the seats were considerably deformed by the crash forces, the inflatable restraint was able to constrain the dummy in the pilot seat (Figures 42 and 43). Unfortunately, the inertia reel on the copilot's seat failed, releasing the shoulder straps and allowing the dummy to pitch forward in the seat. This unforeseen failure eliminated all chance for a meaningful comparison of the data collected from transducers on both dummies.

Drop test data are presented in Table 4. Time response plots of the data summarized in this table are shown in Figures 44 through 52. All data shown in these plots were filtered at 100 Hz.

Analysis of the data showed that the pressure developed in the inflatable restraint reached a maximum of 9.6 psi. This is considerably less than was experienced during horizontal sled tests, but it is explainable since peak pressure results from the compression of the bladder as the occupant's torso loads the straps. For T-40 impact conditions, the motion is directed predominately downward into the seat bucket. The severe deformation of the seat absorbed a portion of the energy, resulting in reduced strap loads and lower internal pressure. Figure 43 shows the failure of the seat pan and the tearing of the seat back due to the strap loading; it also reveals the inflatable restraint in a partially inflated condition because of its semiporous nature. This feature permits a quick removal of the restraint by the wearer and a rapid egress from the aircraft.
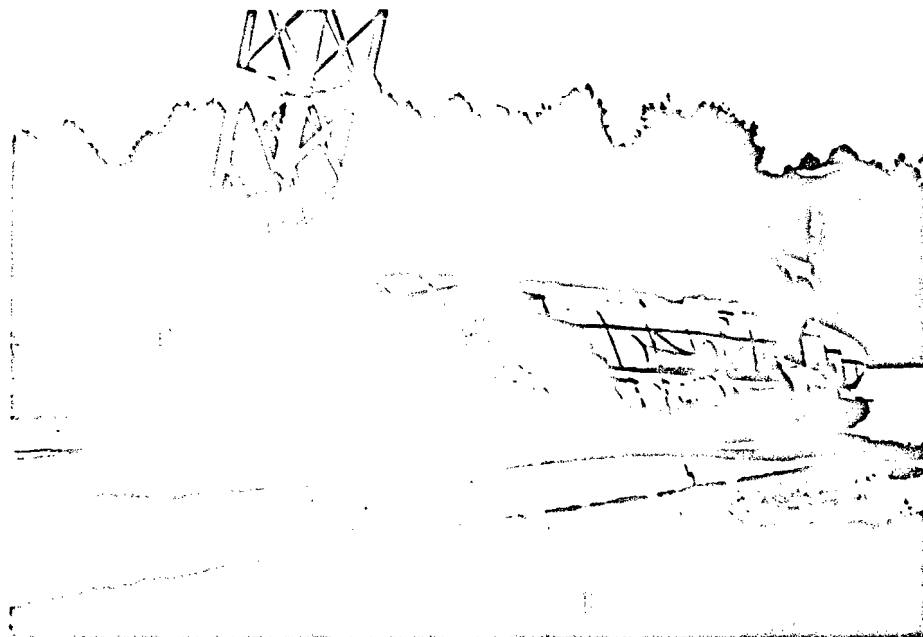
Figure 42. CH-47A test vehicle (post-test).

69

Figure 43. Post-test cockpit showing crash damage and dummy position.

TABLE 4. SUMMARY OF DROP TEST DATA

| Parameter | Peak Load | | | Time |
	Psi	G	Lb	(msec)
Internal Pressure	9.6			105
Floor, Gx		19.0		68
Floor, Gz		158.0		58
Pilot Chest, Gx		12.6		81
Pilot Chest, Gy		3.7		62
Pilot Chest, Gz		15.9		55
Pilot Chest Resultant, Gr		19.2		106
Copilot Chest, Gx		9.6		94
Copilot Chest, Gy		6.0		105
Copilot Chest, Gz		21.7		61
Copilot Chest Resultant, Gr		22.7		61
Pilot Left Shoulder			535	73
Pilot Right Shoulder			666	103
Pilot Left Hip			385	115
Pilot Right Hip			247	176
Copilot Left Shoulder			158	156
Copilot Right Shoulder			135	62
Copilot Left Hip			379	188
Copilot Right Hip			394	180

70
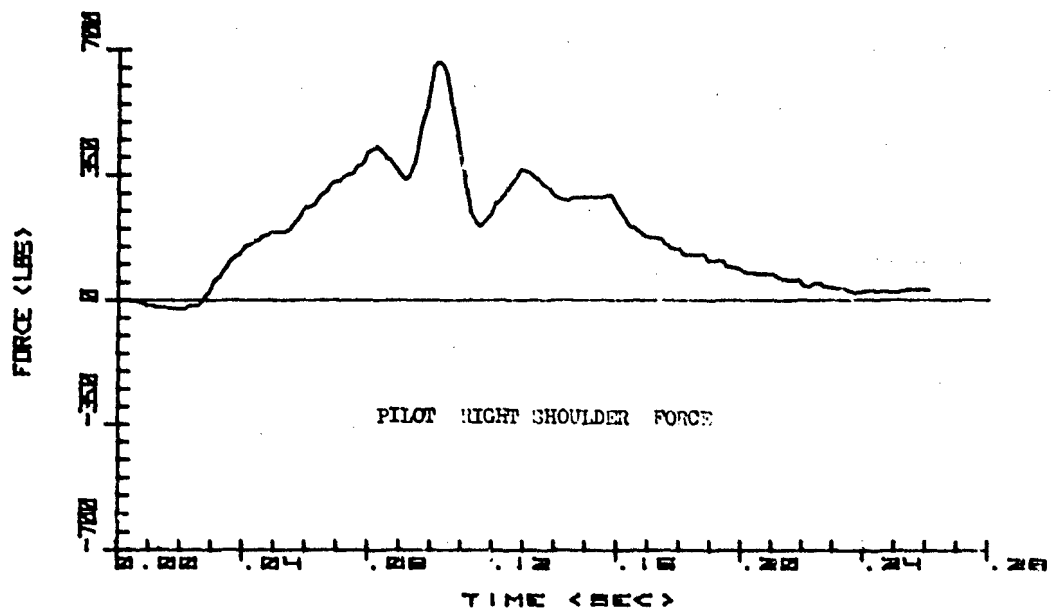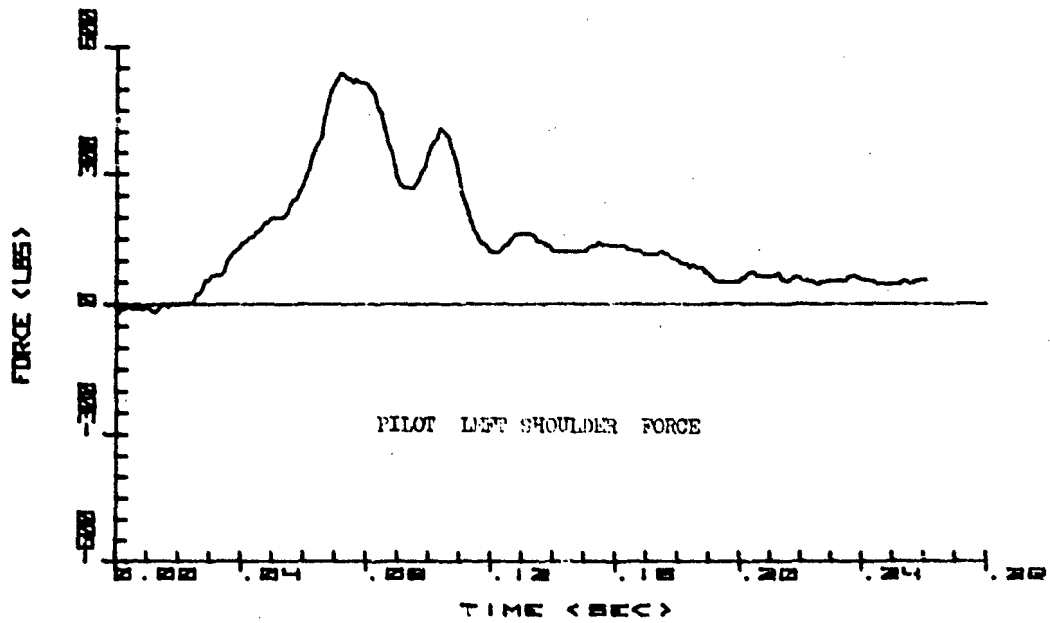
Figure 44. Pilot restraint shoulder loads versus time.

71
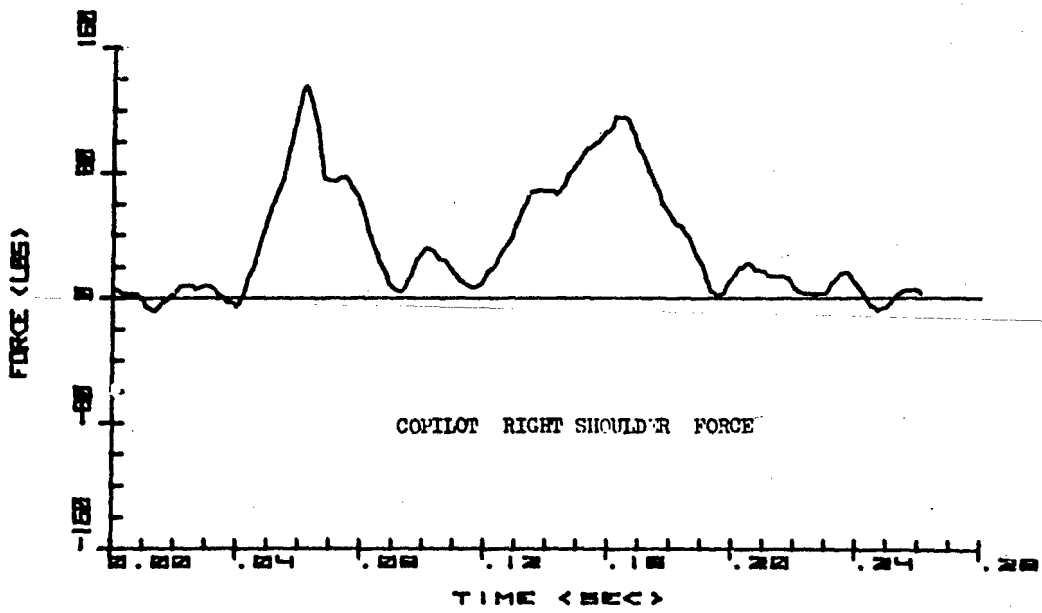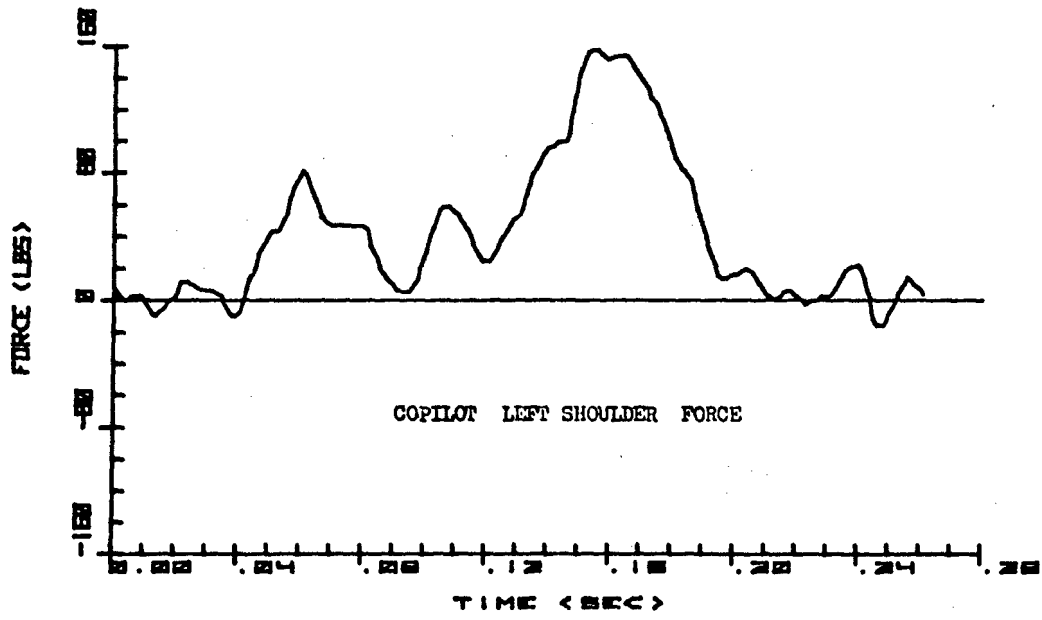
Figure 45. Copilot restraint shoulder loads versus time.

72
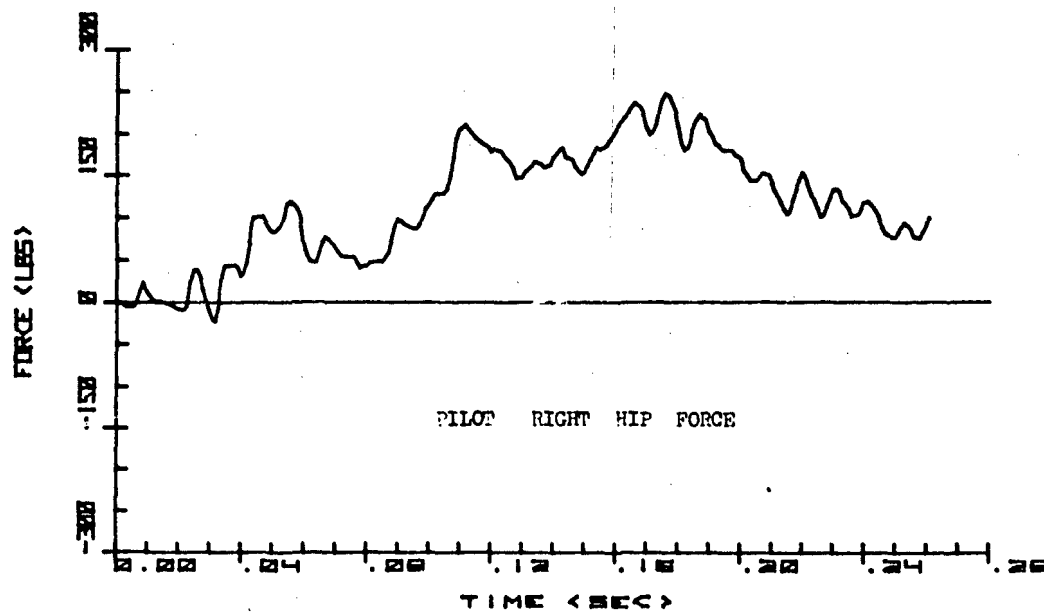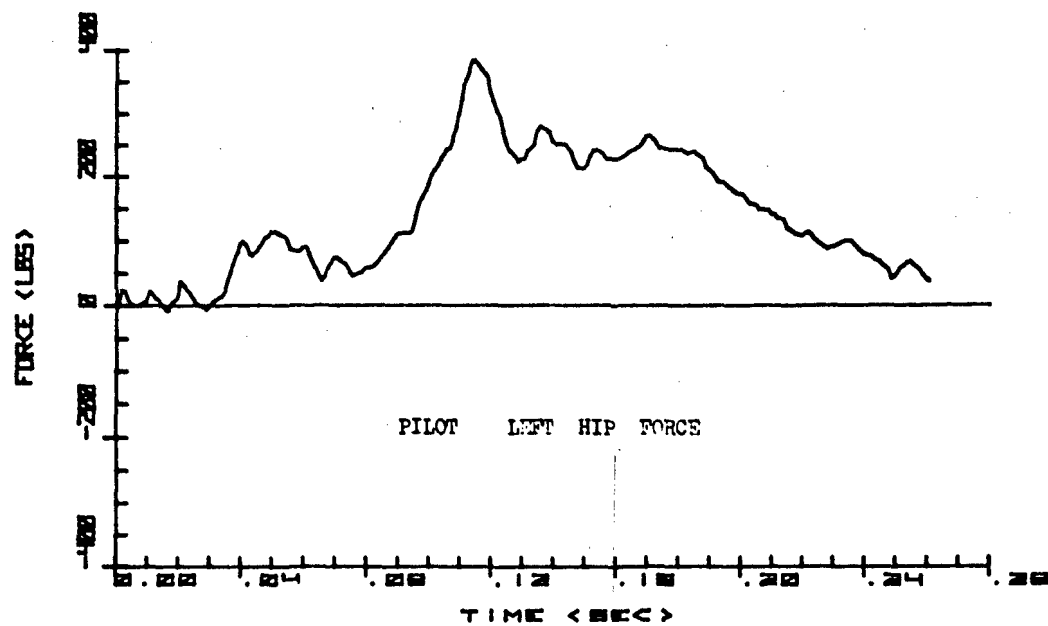
Figure 46. Pilot restraint hip loads versus time.
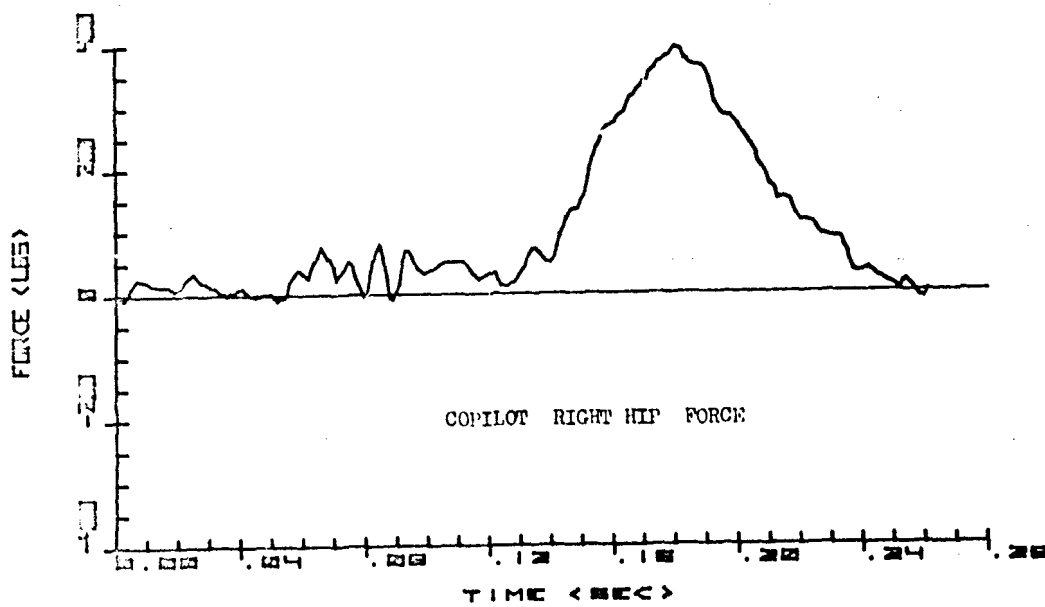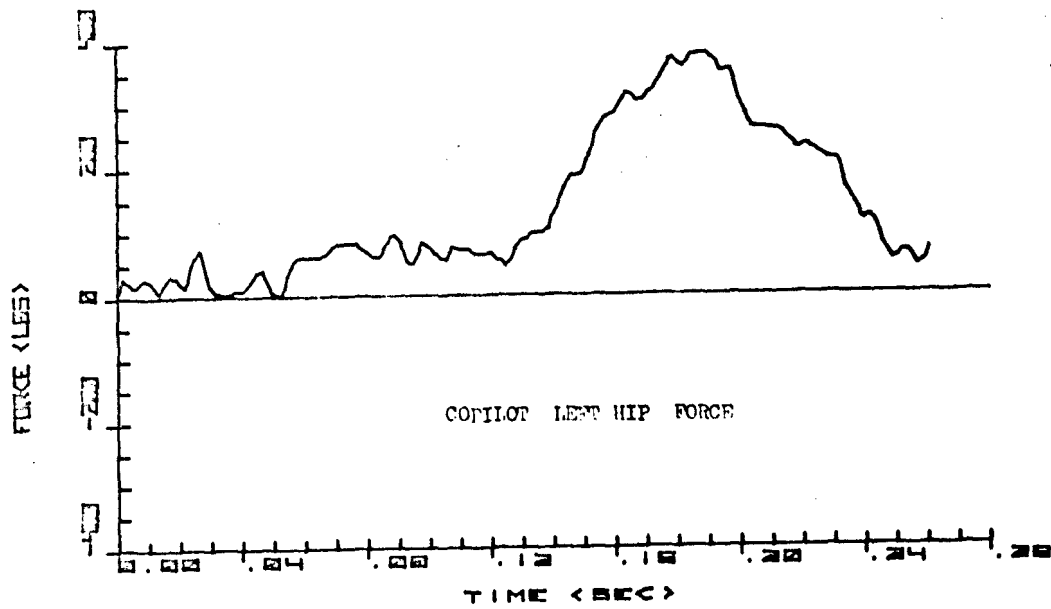
Figure 47. Copilot restraint hip loads versus time.
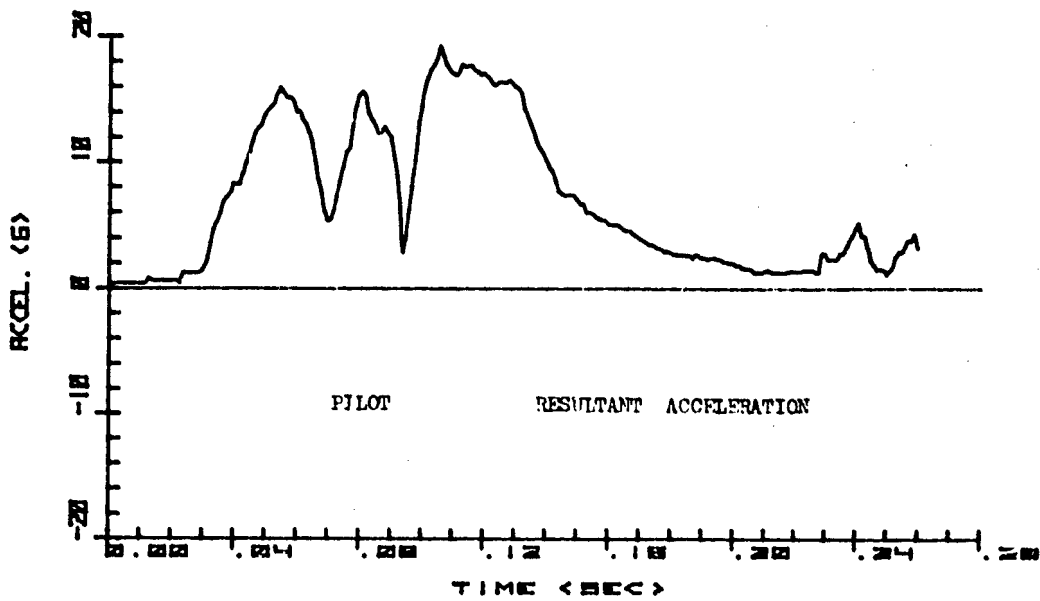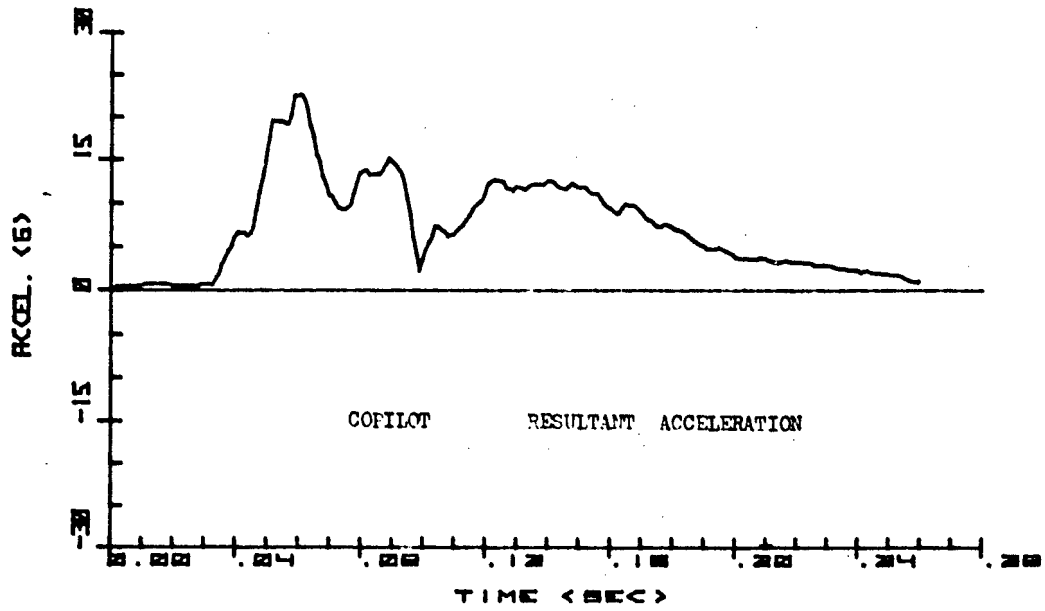
Figure 48. Pilot and copilot resultant chest acceleration versus time.
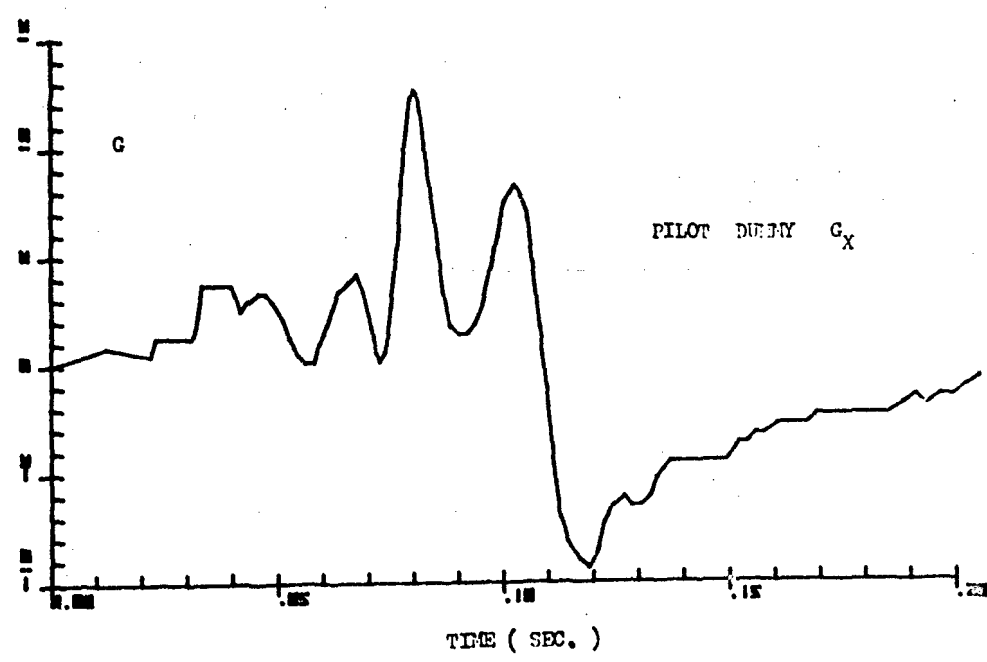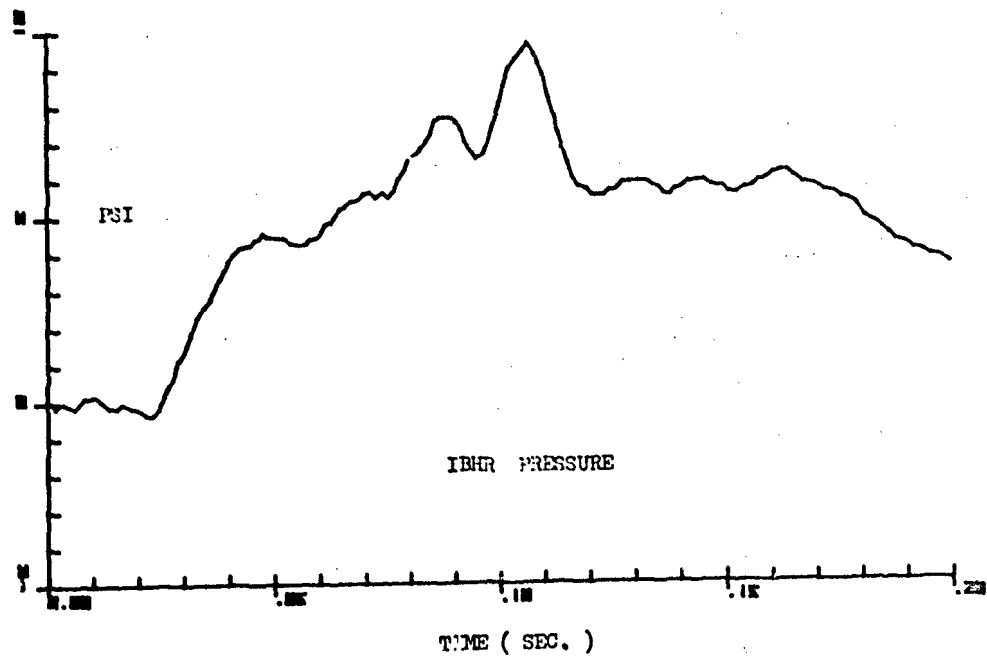
Figure 49. Pilot horizontal chest acceleration and bladder pressure versus time.

76

PSI

INNER PRESSURE

TIME (SEC.)

G

FLOOR G_X

TIME (SEC.)
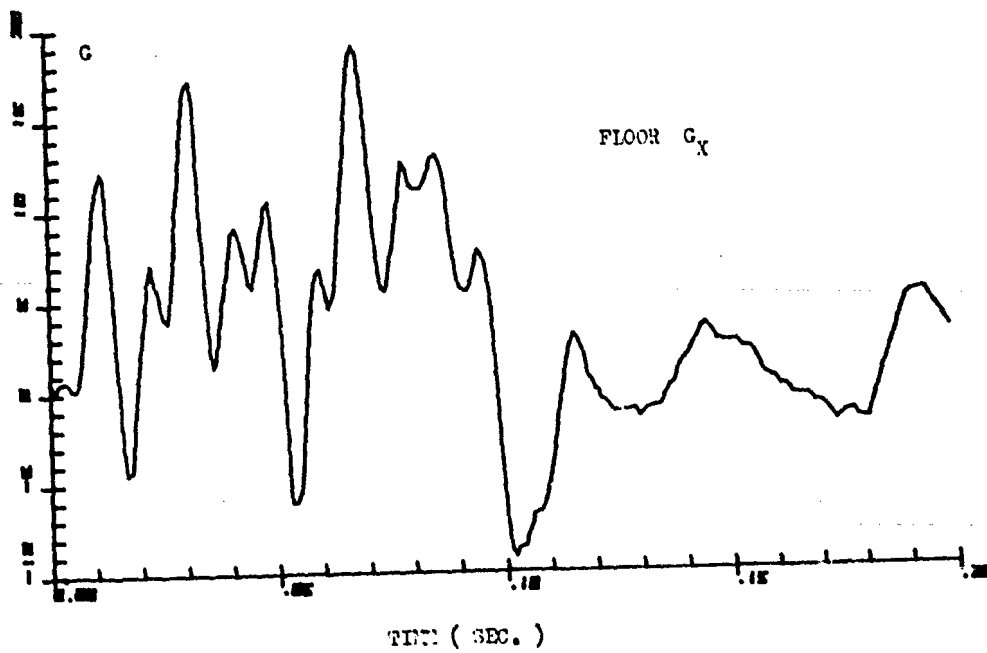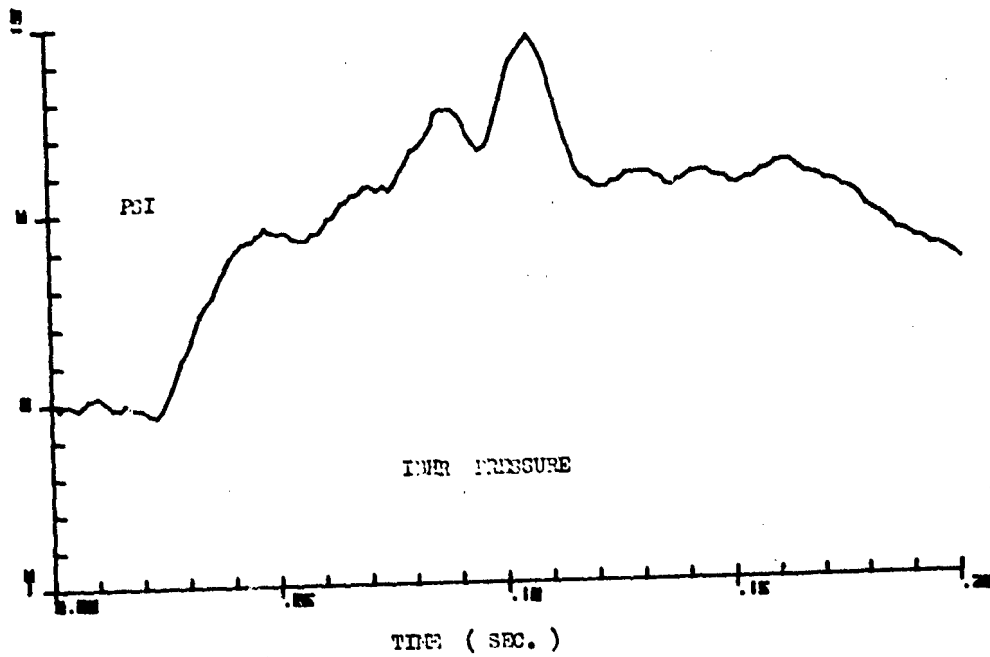
Figure 50. Aircraft horizontal acceleration and bladder pressure versus time.
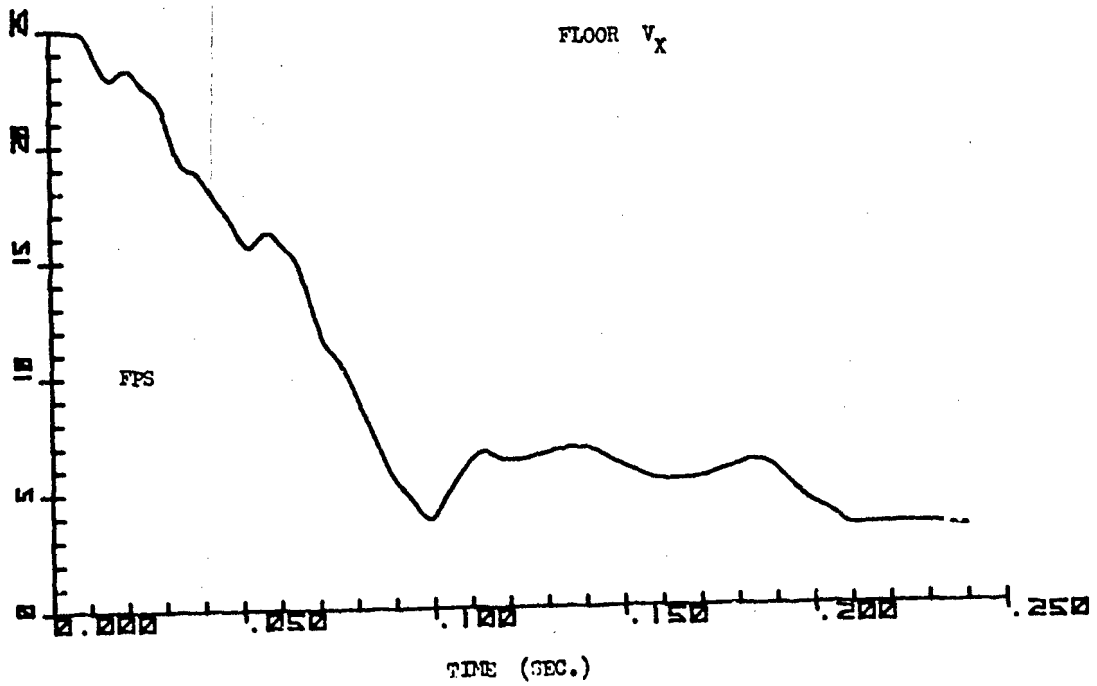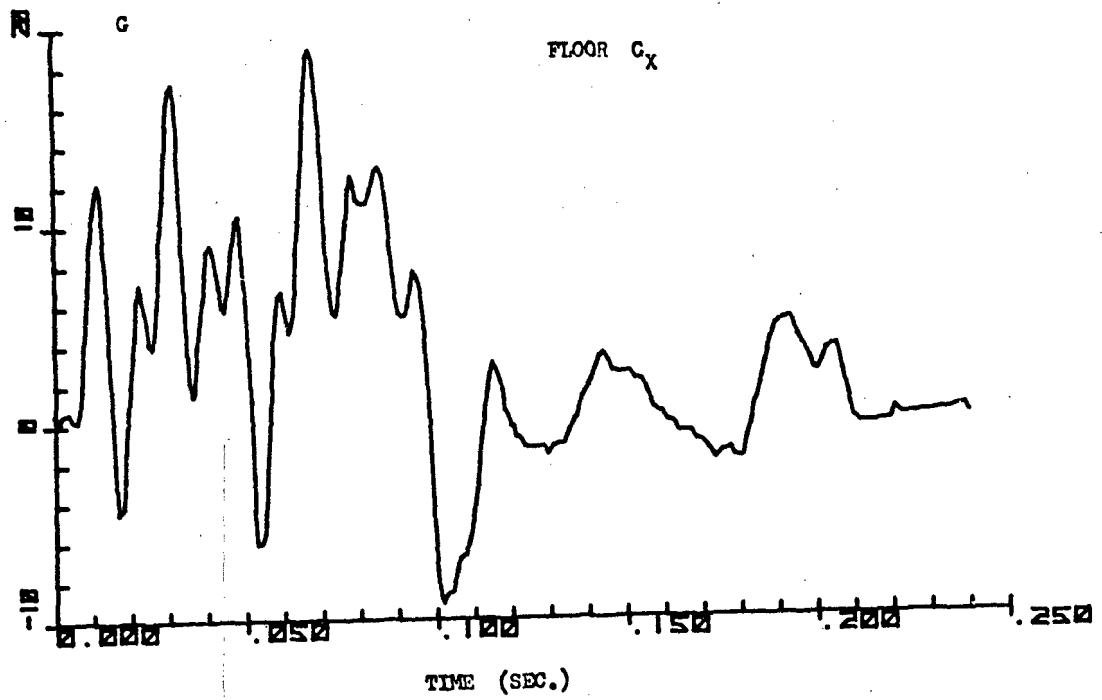
Figure 51. Aircraft horizontal acceleration and velocity versus time.

78
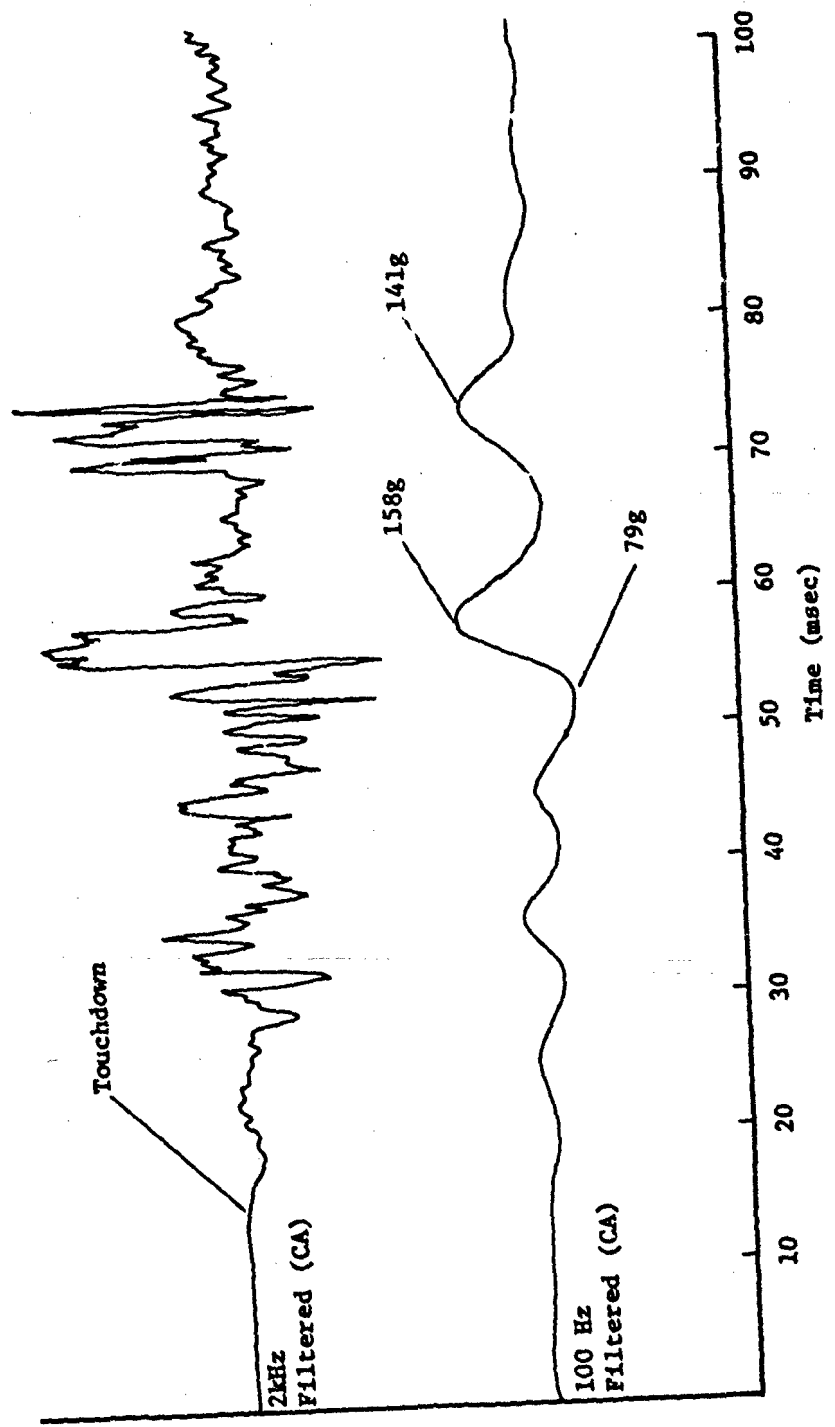
Figure 52. Aircraft vertical acceleration versus time.

79

Conclusions

T-40 demonstrated that the aircrew inflatable restraint system can function under actual crash conditions.

The crash pulse magnitude and duration obtained can be used in the development of a crash sensor for the advanced engineering model of the inflatable restraint system.

Though data permitting direct comparison with a conventional restraint was not obtained, the observed bladder inflation should result in lesser longitudinal forces being transmitted to an occupant equipped with an inflatable restraint.

APPENDIX A
INSTRUMENTATION

GENERAL

T-40 measurements were obtained using five basic type transducers: strain gages, accelerometers, load cells, displacement sensors, and pressure sensors. The locations of the transducers on the test helicopter are depicted in Figure 6. All transducers were connected to remote recording equipment via multipair and coaxial cabling. Nine recorders were employed, three of which were supplied and operated by the Army. The Army conditioning and recording equipment was positioned in a 40-foot instrumentation trailer configured to meet this project's requirements. The NASA equivalent equipment was positioned in their permanently configured drop test site control room and was operated in accordance with their usual recording procedures.

NASA and Army instrumentation technicians worked closely together in the installation and wiring of the transducers, and in sensor calibration and data acquisition.

APPLIED TECHNOLOGY LABORATORY (ARMY) RECORDING SYSTEM

The Army data recording system is graphically depicted in Figure A-1. The Army recorded data from structural strain gages, strain gage type accelerometers and load cells, and strain gage pressure and restraint belt sensors. This was accomplished using designated tape recorders O, P, and N. Recording circuits are described below.

Structural Strain Gage Recording Circuits

Thirty-four Micro-Measurements type EA-13-125AC-350/W constantan alloy 350 ohm strain gages were used in conjunction with Vishay type MDL 311218-X bridge circuit completion modules to form the transducer sense circuit (Data Channels 77 through 110). The output of each strain gage bridge was fed into an IED type CSO-340 Sub-Carrier Oscillator (SCO) and mixed in an IED type CMA 400A Mixer-Amplifier to form a 5 to 6 subcarrier frequency multiplexed signal. All 34 strain gage circuits were fed into seven SCO signal conditioners (Modules G-M) with the resulting outputs fed via individual 200-foot 52 ohm coaxial cables to the instrumentation trailer where the signals were recorded at 60 ips on a 14-channel Genisco magnetic tape recorder (Rec N), Model 10-126. A 100-kHz recording reference signal was also injected into each of the seven mixer-amplifiers to become part of the seven multiplexed signals. Recorder N also recorded IRIG A time code and supplemental voice signals. Circuit calibrations of all ATL recorded channels were accomplished on test day and consisted of circuit zeroing, plus a strain gage/bridge shunt type calibration. The selected calibration shunt resistance value was equal to 16065 μ inch/inch tension. This was equivalent to approximately 50% of the FM recording band edge. Table A-1 presents a description of recorder N functions and calibration data.

Load Cell Circuits

Two BLH SR-4 10,000-pound load cells (Channels 75 and 76) were used in conjunction with the same cargo package that was used in the March 1975 CH-47 (T-39) crash test.

This same package was used to establish comparison load impact data between T-39 and T-40. The load cell's sensor strain gage bridge output was recorded as part of the multiplex arrangement described above. Calibration consisted of bridge circuit zeroing and a resistor shunt type calibration as determined by supplied data. The selected calibration value was equal to 6,000 pounds tension. Eight PCB Model 226A Quartz Force Link type load cells (Channels 67-74) were placed in series with the rear restraint tie-downs for all four on-board cargo loads: two 3/4-ton two-wheel vehicle trailers and two simulated pallet loads. Calibration consisted of circuit balancing and then inserting a known voltage equal to a known load cell output. See Tables A-1, A-2, and A-3 for the calibration compression for a given channel. Refer to Figure A-1 for a general description of the load cell circuitry.

Pressure Sensors

Three pressure sense circuits were employed using CEC strain gage type Model 4-313 and 4-326 sensors. Two 4-313 transducers (0-200 psi), Channels 116 and 117, were installed in the lower front portion of the main fuel cells at Station 270. The third transducer (0-25 psi), Channel 115, was employed to sense pressure exerted upon an inflatable bladder which was part of the dummy pilot's restraint system. This circuit was a U. S. Naval Air Development Center (NADC) requirement and employed techniques and hardware developed by them.

Accelerometers

Two CEC Strain Gage Accelerometers, Type 4-202 (Channels 123-124), were used to sense center cockpit floor impact accelerations. The vertical sensor was a 0-250G component, while the longitudinal was 0-100G. These circuits, which were a NADC requirement, were conditioned by the Accudata Model 118 and recorded on tapes O and P.

Restraint Belt Sensors

Eight NADC-fabricated strain gage sensors were employed in conjunction with a standard flight harness plus the inflatable restraint described above. Both pilot and copilot dummies had two hip and two shoulder tension sensors installed. The strain gage output was converted and calibrated to pounds of harness pressure using NADC methods. Four sensors were converted to an FM multiplex signal (Channels 111-114) and recorded on Recorder N while the remaining four (Channels 119-122) were recorded on Recorders O and P, after being signal conditioned by an Accudata Model 118 amplifier arrangement. Calibrations were accomplished using selected shunt resistance values which produced signals equivalent to known restraint belt pressures.

82
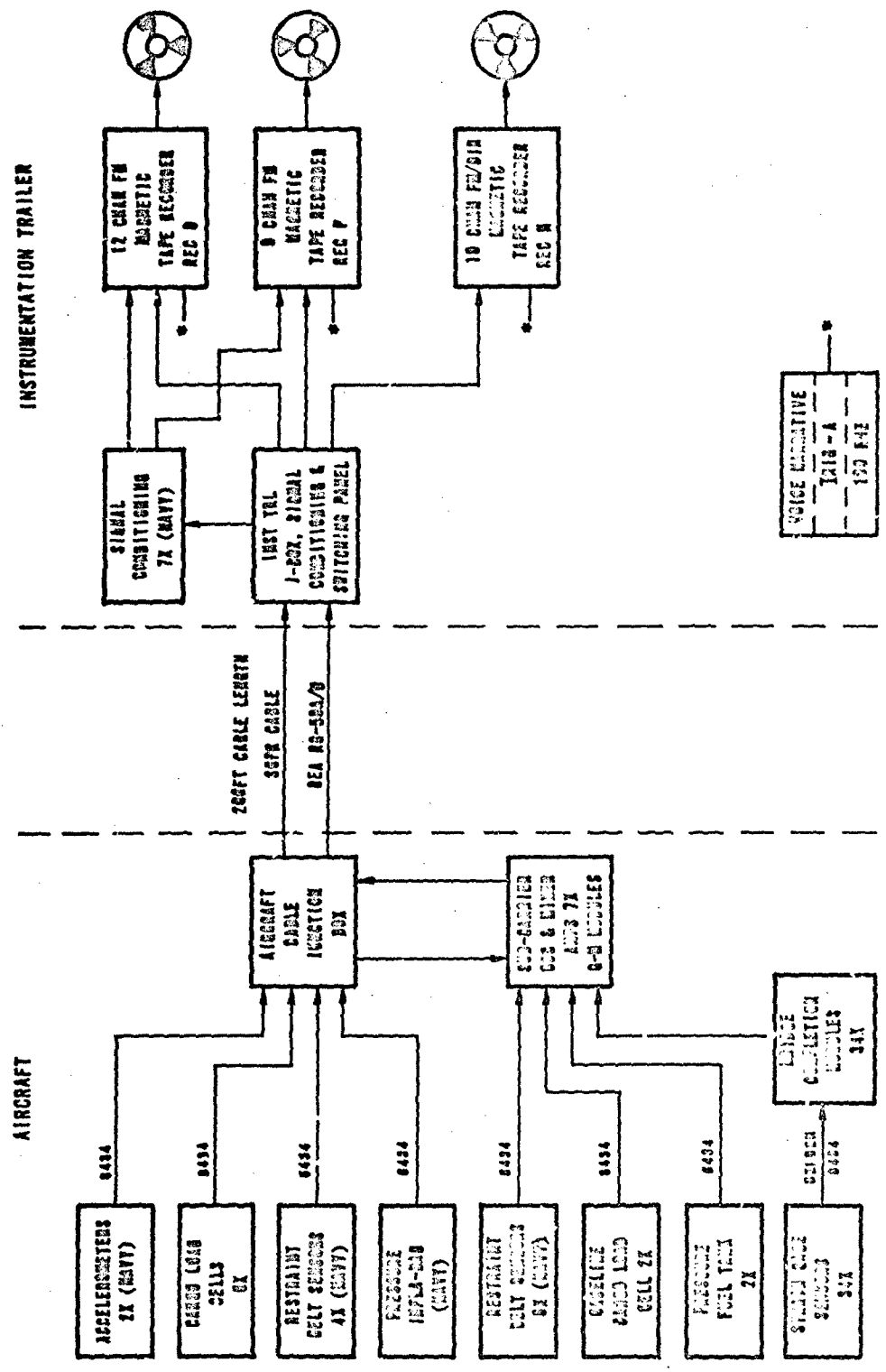
Figure A-1. Army recording system.

83

TABLE A-1. RECORDER N FUNCTIONS AND CALIBRATION DATA

TRACK	MUX DATA CHAN	DATA CHAN	TRANSDUCER	SHUNT R CAL	TAPE CAL	CAL EQUIV	+ POLARITY
1	-	-	VOICE	-	-	-	-
3	G1-G6	105-110	6 STRAIN GAGES(SG)	10KΩ	TENSION	18065$\mu\xi$	COMP
4	H1,H3 H4,H7	101-104	4SG	10KΩ	TENSION	18065$\mu\xi$	COMP
4	H5,H6	117,118	2 PRESS	25.5KΩ	INCREASE	H5-137LB H6-117LB	INCREASE
5	I1-I4	97-100	4SG	10KΩ	TENSION	18065$\mu\xi$	COMP
5	I5-I6	75,76	2 LOAD CELLS	25KΩ 50KΩ	TENSION	8000LB	TENSION
8	J1-J5	81,82 88,90	5SG	10KΩ	TENSION	18065$\mu\xi$	COMP
8	J6	111	1 RESTRANT BELT (RB)	50KΩ	COMP	1690LB	TENSION
9	K1-K5	83,84 94-96	5SG	10KΩ	TENSION	18065$\mu\xi$	COMP
9	K6	112	1RB	50KΩ	TENSION	1732LB	TENS.ON
10	L1-L5	79,80 91,93	5SG	10KΩ	TENSION	18065$\mu\xi$	COMP
10	L6	113	1RB	50KΩ	TENSION	1498LB	TENSION
11	M1-M5	77,78 85-87	5SG	10KΩ	TENSION	18065$\mu\xi$	COMP
11	M6	114	1RB	50KΩ	TENSION	1484LB	TENSION
7	-	-	IRIG-A TIME CODE			-	-
8	-	-	100K HZ REFERENCE			-	-

TABLE A-2. RECORDER O FUNCTIONS AND CALIBRATION DATA

TRACK	DATA CHAN	TRANSDUCER	TYPE CAL	CAL POLARITY	TAPE CAL DCV	CAL EQUIV	+ POLARITY
1	-	-	VOICE	-	-	-	-
2	119	RB	25KΩ	TENSION	.70	1242LB	TENSION
3	67	LC	1VDC	COMP	1.00	8174LB	COMP
4	89	LC	1VDC	COMP	1.00	8009LB	COMP
5	71	LC	1VDC	COMP	1.00	9259LB	COMP
6	73	LC	1VDC	COMP	1.00	9174LB	COMP
9	121	RB	25KΩ	TENSION	.88	1204LB	TENSION
10	122	RB	25KΩ	TENSION	.69	1226LB	TENSION
11	115	RESTRAINT PRESS	25KΩ	DECREASE	1.00	24PSIG	DECREASE
12	123	V ACCEL	25KΩ	+	1.17	207G	ACCEL DOWN (REVERSE PGU)
7	-	-	IRIG-A TIME CODE				-
8	-	-	100K HZ REFERENCE				-

TABLE A-3. RECORDER P FUNCTIONS AND CALIBRATION DATA

TRACK	DATA CHAN	TRANSDUCER	TYPE CAL	CAL POLARITY	TAPE CAL DCV	CAL EQUIV	+ POLARITY -
1	-		VOICE	-	-	-	-
2	120	LC	25KΩ	TENSION	.78	1337LB	TENSION
3	88	LC	1VDC	COMP	1.00	3091LB	COMP
4	70	LC	1VDC	COMP	1.05	8299LB	COMP
5	72	LC	1VDC	COMP	1.02	8997LB	COMP
6	74	-	1VDC	COMP	1.00	9174LB	COMP
9	124	LO ACCEL	25KΩ	+	1.10	78G	ACCEL FWD (BASE REAR)
7	-	-	IRIG-A TIME CODE				-
8	-	-	100K HZ REFERENCE				-

NASA RECORDING SYSTEM

Figure A-2 generally depicts the NASA data recording system. Two different types of transducers were recorded, piezoelectric accelerometers and extensiometers, on designated recorders A, B, C, D, E, and F.

Accelerometer Circuits

NASA recorded 62 channels of vertical, lateral, and longitudinal aircraft structural, anthropomorphic dummy and loads acceleration data using Kistler Model 818 and PCB Model 302A04 quartz type 0-1000G sensors with built-in impedance converters. The high-signal, low-impedance output (Nominal 10 mv/g) was fed through junction boxes directly into a NASA-fabricated unity gain impedance matching amplifier and ultimately into six Sangamo and Ampex 14-channel FM record magnetic tape recorders. IRIG A time code and test voice narrative were fed into each recorder. Calibrations were accomplished prior to test day by injecting a known AC RMS 1-kHz signal level at the accelerometer output (Aircraft J-Box) and setting the electronics gain as measured at and recorded by the respective magnetic tape recorder. Calibration levels were established at the 100, 200, 500, 700, and 1000G level depending on anticipated individual accelerometer G load. These calibration points were established as 100% FM record band edge. Recorders A, B, C, D, E, and F functions and calibration data are presented in Tables A-4, A-5, A-6, A-7, A-8, and A-9, respectively.

Extensiometers

Eight extensiometers (deflection/displacement sensors), six of which were electronically sensed, were fabricated, installed, and calibrated by ATL personnel. The extensiometer is basically an 8-foot 2-inch aluminum tube on which a nichrome resistance wire and wiper arm is side mounted over its length. The tube is secured to the cabin floor and the wiper arm to the fuselage exterior top. As the wire wiper traverses due to cabin floor or overhead skin movement, an electrical current change proportional to displacement is produced, allowing a time history to be recorded. In addition, a heavy rubber O-ring was positioned on the tube at the roof line to sense the peak ceiling movement manually. To facilitate calibration and obtain optimum circuit sensitivity and linearity, signal conditioning circuitry was fabricated. Calibrations were performed by creating a known deformation and measuring the resulting output voltage. Extensiometer positions are shown in Figure 6 and physical particulars are depicted in Figure A-3.

Radar Velocity Measurement

A field-portable Doppler radar system was used as a signal source to determine aircraft horizontal velocity at impact. Circuit calibration was accomplished using a tuning fork generated pulse equivalent of 20 mph. Data was recorded on Tape E.
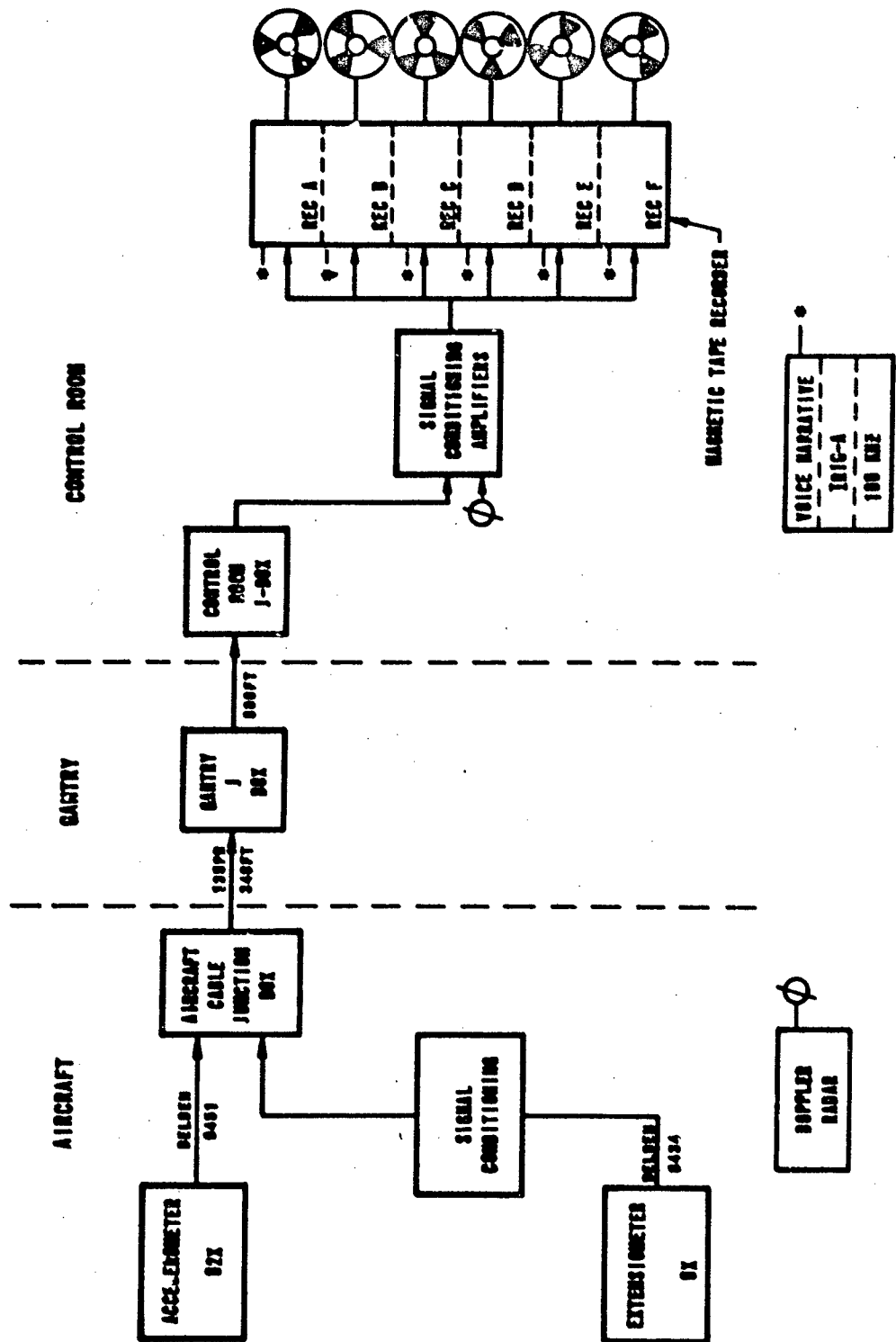
Figure A-2. NASA recording system.

88

Figure A 3. Deflection tube installation.

TABLE A-4. RECORDER A FUNCTIONS AND CALIBRATION DATA

TAPE TRACK	DATA CHAN.	AXIS	ACCELEROMETER		MAX DATA LEVEL (IN G'S)	AMP GAIN	TAPE CAL RMS	POLARITY
			S/N	SENS.				
1	81	D-1	DEFLECTION		2.5VDC = AFT	1	1.25VDC	+
2	7	LO	4805	10.04	500	1	3.55	+ (BASE FORWARD)
3	8	LA	4607	9.77	200	1	1.38	+ (BASE LEFT)
4	9	V	4609	10.06	500	1	3.57	+ (BASE DOWN)
5	16	V	1882	10.02	1000	1	7.08	+
6	29	LO	4591	9.98	500	1	3.53	+
9	30	LA	4593	10.14	200	1	1.43	+
10	31	V	4571	10.38	500	1	3.88	+
11	26	LO	4578	10.05	700	1	4.97	+
12	27	V	1886	9.85	1000	1	6.87	+
13	28	V	4583	10.07	700	1	4.98	+
7	–	–	IRIG A TIME CODE			–	1.414	–
8	–	–	100K HZ REFERENCE			–	1.414	–

TABLE A-5. RECORDER B FUNCTIONS AND CALIBRATION DATA

TAPE TRACK	DATA CHAN.	AXIS	ACCELEROMETER		MAX DATA LEVEL (IN G'S)	AMP GAIN	TAPE CAL RMS	POLARITY
			S/N	SENS.				
1	82	D-2	DEFLECTION		2.5VDC= AFT	1	1.25VDC	+
2	10	LO	4559	8.91	500	1	3.50	+
3	11	LA	4558	9.94	200	1	1.41	+
4	12	V	4553	10.05	500	1	3.55	+
5	20	LO	4551	10.05	700	1	4.97	+
6	21	V	1884	9.96	1000	1	7.04	+
9	22	V	3883	9.89	700	1	4.89	+
10	41	LO	4032	8.92	700	1	4.91	+
11	42	V	4034	10.06	700	1	4.98	+
12	43	V	4038	10.17	700	1	5.03	+
13	50	LO	4360	10.10	700	1	5.00	+
14	51	V	1904	10.08	1000	1	7.13	+
7	-	-	IRIG A TIME CODE			-	1.414	-
8	-	-	100K HZ REFERENCE			-	1.414	-

91

TABLE A-6. RECORDER C FUNCTIONS AND CALIBRATION DATA

TAPE TRACK	DATA CHAN.	AXIS	ACCELEROMETER S/N	ACCELEROMETER SENS.	MAX DATA LEVEL (IN G'S)	AMP GAIN	TAPE CAL RMS	POLARITY
1	63	D-3	DEFLECTION	DEFLECTION	2.5VDC = 8FT	1	1.25VDC	+
2	5	LO	4043	9.88	500	1	3.42	+
3	8	V	4048	10.22	700	1	5.08	+
4	32	LO	4050	10.33	500	1	3.85	+
5	33	LA	4052	10.13	200	1	1.43	+
6	34	V	4054	9.77	500	1	3.45	+
8	23	LO	4389	10.18	700	1	5.03	+
10	24	V	1885	10.14	1000	1	7.17	+
11	25	V	4070	10.00	700	1	4.90	+
12	52	LO	4077	10.11	500	1	3.57	+
13	53	LA	4298	10.21	200	1	1.44	+
14	54	V	40.78	9.77	500	1	3.46	+
7			IRIG A TIME CODE				1.414	-
8			100K HZ REFERENCE				1.414	-

TABLE A-7. RECORDER D FUNCTIONS AND CALIBRATION DATA

TAPE TRACK	DATA CHAN.	AXIS	ACCELEROMETER		MAX DATA LEVEL (IN G'S)	AGP GAIN	TAPE CAL RMS	POLARITY
			S/N	SENS.				
1	04	D-4	DEFLECTION	DEFLECTION	2.5VDC = AFT	1	1.25VDC	+
2	13	V	1006	10.03	1000	1	7.09	+
3	58	LO	4557	9.90	700	1	4.90	+
4	59	LA	4580	10.00	200	1	1.41	+
5	60	V	3605	10.23	700	1	5.07	+
6	35	LO	4041	9.97	500	1	3.52	+
9	38	LA	4352	10.19	200	1	1.44	+
10	37	V	4097	9.93	500	1	3.51	+
11	47	LO	4148	10.17	700	1	5.03	+
12	48	LA	4149	10.28	100	1	.73	+
13	40	V	1000	9.94	1000	1	7.03	+
7	-	-	IRIG A TIME CODE			-	1.414	-
8	-	-	100K HZ REFERENCE			-	1.414	-

93

TABLE A-8. RECORDER E FUNCTIONS AND CALIBRATION DATA

TAPE TRACK	DATA CHAN.	AXIS	ACCELEROMETER		MAX DATA LEVEL (IN g'S)	AMP GAIN	TAPE CAL RMS	POLARITY
			S/N	SENS.				
1	65	G-S	DEFLECTION		2.5VDC = 0FT	1	1.25VDC	+
2	14	V	1878	9.86	1000	1	6.88	+
3	38	LO	4113	8.80	500	1	3.48	+
4	39	LA	4114	10.14	200	1	1.43	+
5	40	V	4116	9.70	500	1	3.48	+
6	3	LO	4118	10.05	500	1	3.55	+
9	4	V	4119	9.76	700	1	4.83	+
10	55	LO	4145	10.05	500	1	3.55	+
11	58	LA	4139	10.13	200	1	1.43	+
12	57	V	4154	10.20	500	1	3.61	+
13	110	-	DOPPLER RADAR		-	5	20 MPH	+
7	-	-	IRIG A TIME CODE			-	1.414	-
8	-	-	100K HZ REFERENCE			-	1.414	-

94

TABLE A-9. RECORDER F FUNCTIONS AND CALIBRATION DATA

TAPE TRACK	DATA CHAN.	AXIS	ACCELEROMETER S/N	SENS.	MAX DATA LEVEL (IN G'S)	AMP GAIN	TAPE CAL RMS	POLARITY
1	86	D-8	DEFLECTION		2.5VDC= DFT	1	1.25VDC	+
2	15	V	1801	18.05	1000	1	7.07	+
3	17	L8	4158	18.32	700	1	5.11	+
4	18	V	1803	18.17	1000	1	7.10	+
5	19	V	4348	18.18	700	1	5.04	+
8	44	L8	4152	18.46	700	1	5.15	+
9	45	V	4143	18.24	700	1	5.07	+
10	48	V	4153	16.35	700	1	5.12	+
11	1	L8	4288	18.15	500	1	3.58	+
12	2	V	4381	18.13	700	1	5.01	+
13	125	L8	AC84	4.00	500	1	1.73	+
14	128	V	AC13	4.07	500	1	1.73	+
7	-	-	IRIG A TIME CODE			-	1.414	-
8	-	-	100K HZ REFERENCE			-	1.414	-

95

INTERIOR PHOTOGRAPHIC CONTROL

The circuitry used to control the test helicopter interior cameras and lights was designed and fabricated by ATL. This on-board camera/light system is shown in Figure A-4. Camera and light locations are shown in Figure 7.

DATA ACQUISITION

Procedures

All channels were calibrated as shown in Tables A-1 through A-7. A 100-kHz signal was recorded on each tape recorder for speed compensation and noise-reduction purposes. Timing information was recorded on each tape to facilitate data reduction and event occurrence definition. Also, an audio track was included on each tape recorder (edge or distinct track) to provide for tape data marking, facilitating more rapid data reduction.

Data Recording Problems

Some data was acquired on every channel. The following instrumentation malfunctions were a direct result of the crash impact.

1. Data Channels 74, 82, 86, 89, 91, 102, 116, 117: Cables severed by structural damage.

2. Data Channel 92: Cable or transducer cut or smashed (sensor and complete cable run could not be checked due to fuselage collapse).

3. Data Channels 15 and 18: Accelerometer separated from mounting pad due to epoxy bond fracture.

4. Data Channels 13, 14, 49, and 51: Accelerometer separated from mounting pad due to stripped pad threads.

5. Data Channels 31, 32, 33 and 34: Cable severed due to structural damage.

AIRCRAFT INSTRUMENTATION MOUNTING AND CABLING

All aircraft test cabling was either RG-174/J Type 50 ohm coaxial (FSN 6145-003-8237) or Belden Type 8434 four-conductor shielded (FSN 6145-011-2300) and was loosely positioned with extra slack at expected heavy stress points. All DC voltage and signal circuits used the Type 8434, and the 100-kHz plus the frequency multiplexed strain gage signals were distributed using the RG-174/J. Plastic type cable tie clamps of various lengths along with masking tape were used to suspend and secure most cabling.

The seven SCO/Bridge module (G-M) circuitry mounts consisted of two 5/32- x 4-1/2- x 11-inch aluminum plates separated by two 4-inch plastic sponge separators, all of which were secured together through four holes in the fuselage top using four 1 4-inch self-locking aircraft hardware. One plate and one sponge section were mounted on each side of the fuselage skin.
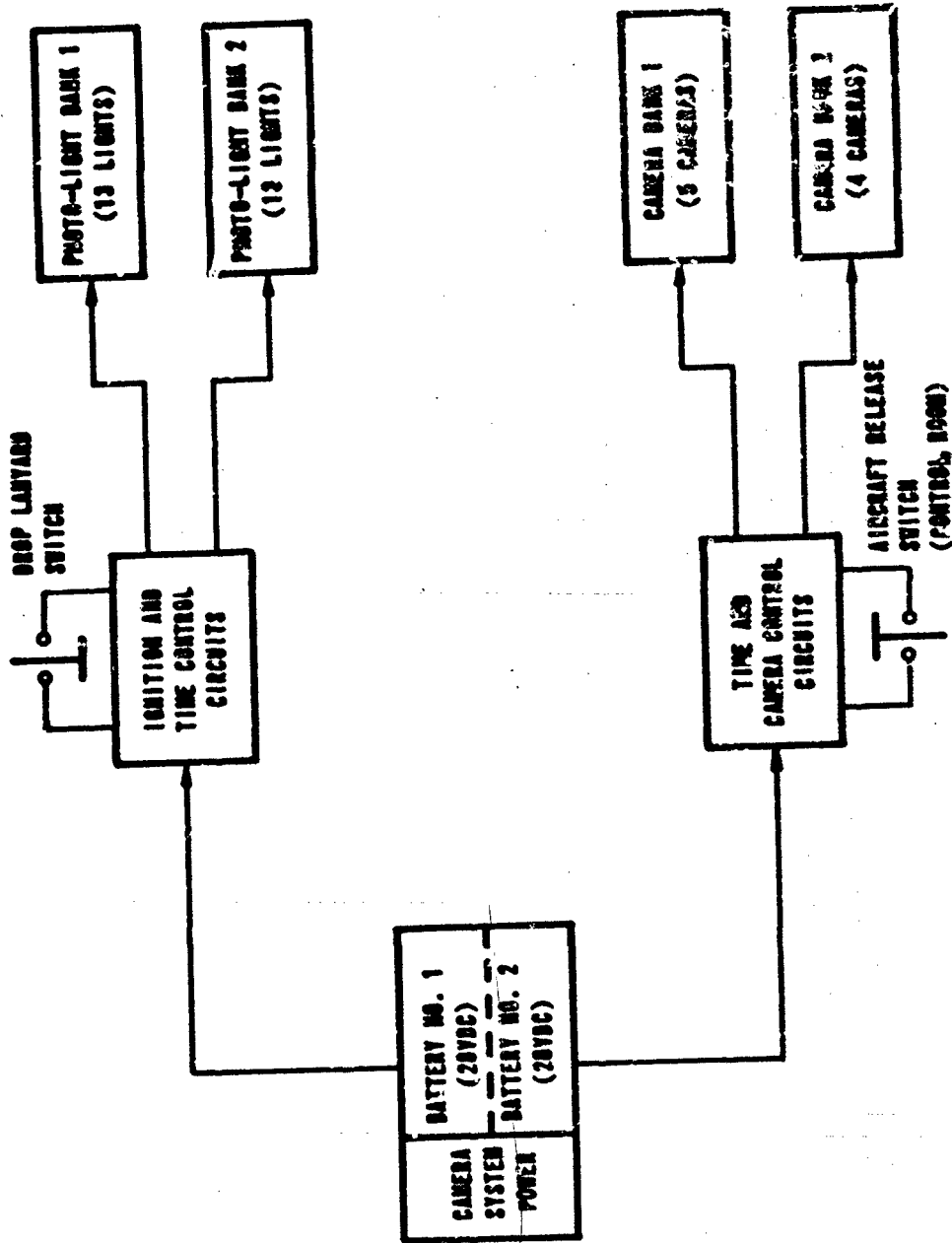
Figure A-4. On-board camera/light system.

The seven IED SCO mounts (G-M) were secured to their associated module mounts using 10-32 self-tightening aircraft type hardware. The Vishay strain gage completion modules were adhered to the module mounts using Dow Corning Silastic 732 RTV silicone adhesive (FSN-8040-865-8991). This adhesive was selected to allow undamaged module recovery upon completion of the test. The module board terminal strips were bonded using 3M Scotch-Weld Brand Epoxy Resin Structural Adhesive, Type 2216B/A (FSN 8040-145-0432).

All strain gage transducers were bonded to the aircraft structure using standard surface preparation, degreasing, plus neutralizing methods and practices as recommended by manufacturers such as Micro Measurements Inc. (MM). The MM strain gages were finger pressure adhesively bonded using Loctite Type 06 Super Bonder (Eastman 910 equivalent) and moisture protected with MM Type Gagekote 3 varnish. The sensor output was coupled to the associated bridge completion module using a Belden 8434 cable conductor.

All acelerometer mount blocks were fastened to their mounting positions by 1/4-inch or 3/8-inch hardware or adhesive bonding using 3M Scotch-Weld Epoxy Resin Structural Adhesive, Type 2216B/A. The accelerometer mounting stud bases were bonded to the mount block using the same epoxy adhesive, and the accelerometers were secured to the base using a 10-32 stud torqued to approximately 18 in.-lb. The mounting techniques are those specified by the respective accelerometer manufacturer. A Belden 8451 two-wire conductor or equivalent was used to connect the transducer to the respective J-Box.

Conventional mounting was utilized for each load cell in accordance with manufacturers' specifications and dimensions.

The camera/light control circuitry and distribution panel were prefabricated in the lab using a 1/4-inch aluminum plate as a foundation and securing all components with RTV silicone adhesive or appropriate size hardware. AWG 10, 12, 14 and 18 gage wire was used to interconnect control components and feed the light and camera loads depending on current requirements. A pre-drop system check was performed to insure proper operation and time sequencing.

The ATL and NASA aircraft cable junction boxes (J-Boxes) were mounted at Station 330 on the right and left interior sides respectively. Both J-Boxes (with covers) were constructed of 1/16-inch or 1/8-inch steel and were mounted to the aircraft skin using 3/8-inch self-locking aircraft hardware, L brackets, and exterior reinforcement washers. Required rows of terminal strips were either crew mounted using 10-32 hardware or adhered using Devcon Quick Set Epoxy Resin Adhesive, Type 5 minute. All attached cabling was firmly bonded for strength and secured at each box entrance. Connectors were conventional BNC or aeronautical MS circuit type. See Figures A-5 and A-6 for Army and NASA Junction Box positioning without covers. The aircraft-to-control room umbilical harnesses were routed through a window-mounted flexible rubber fixture. Figure A-7 shows the interior and exterior cable securing techniques. No crash impact damage was suffered by either J-Box, umbilical harness, or any of the seven module mounts or signal conditioning units mounted above the aircraft waterline.
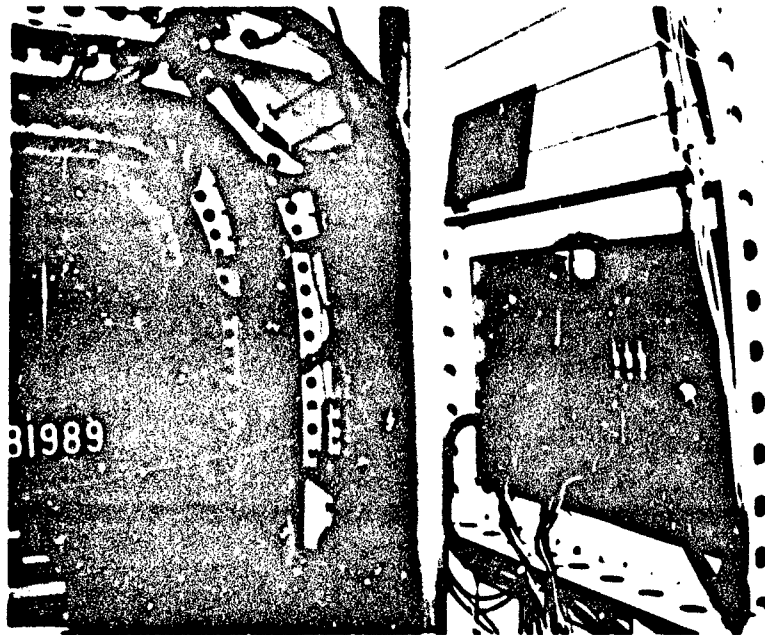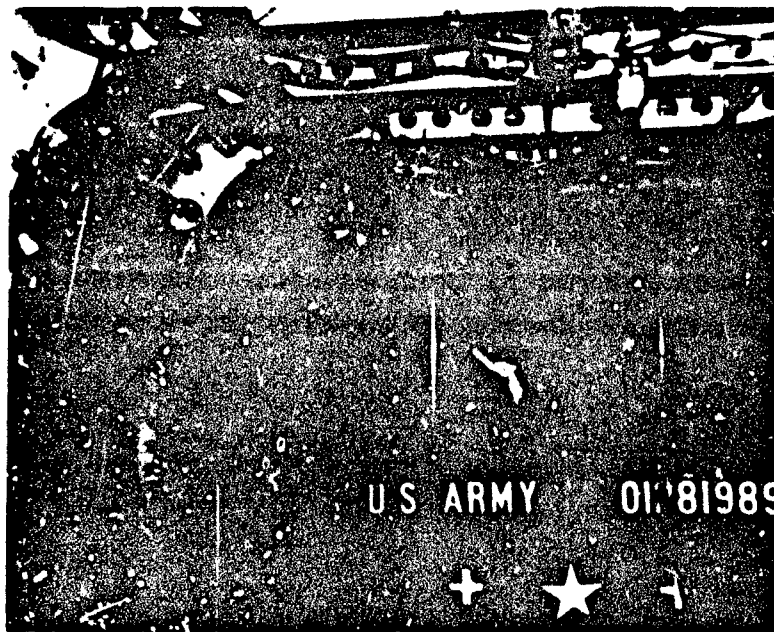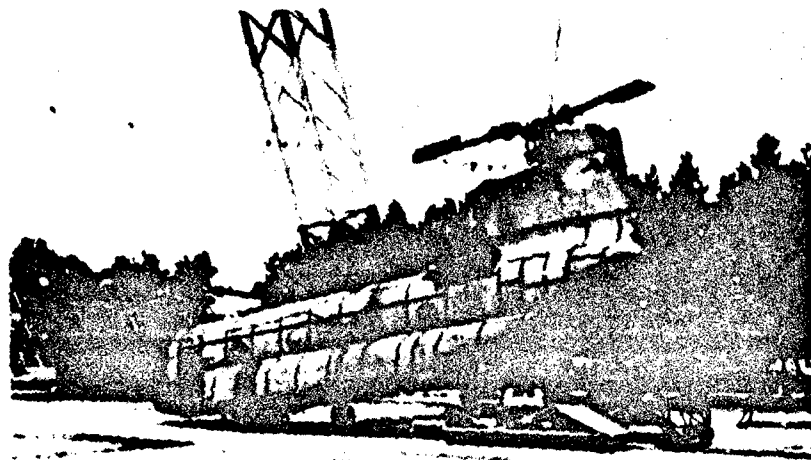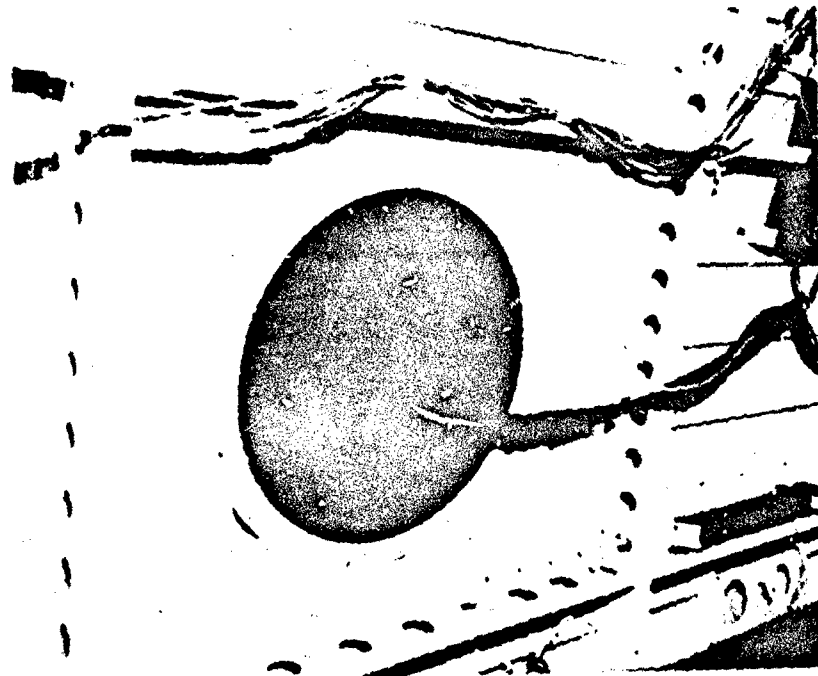
Figure A-5. Army junction box.

Figure A-6. NASA junction box.

Figure A-7. Instrumentation cabling techniques.

6500-78